DEUTSCHES ELEKTRONEN – SYNCHROTRON DESY

DESY 86-014
February 1986

EXCLUSIVE HADRON PRODUCTION IN TWO PHOTON REACTIONS

by

M. Poppe

II. Institut f. Experimentalphysik, Universität Hamburg

ISSN 0418-9833

NOTKESTRASSE 85 · 2 HAMBURG 52

To be sure that your preprints are promptly included in the
HIGH ENERGY PHYSICS INDEX,
send them to the following address (if possible by air mail):

DESY
Bibliothek
Notkestrasse 85
2 Hamburg 52
Germany

DESY 86-014
February 1986

ISSN 0418-9833

Exclusive Hadron Production in Two Photon Reactions

M. POPPE

II.Institut für Experimentalphysik der Universität Hamburg

10. December 85

ABSTRACT. This paper summarises experimental results on exclusive hadron production in two photon collisions at electron positron storage rings and attempts some interpretation. Experimental know how is described and new suggestions are made for future analyses. New model calculations on resonance form factors and pair production amplitudes are presented. The two photon vertex is decomposed such that experiments can be parameterised with the minimal number of free parameters. Selection rules for off shell photon collisions are given in addition to Yang's theorems.

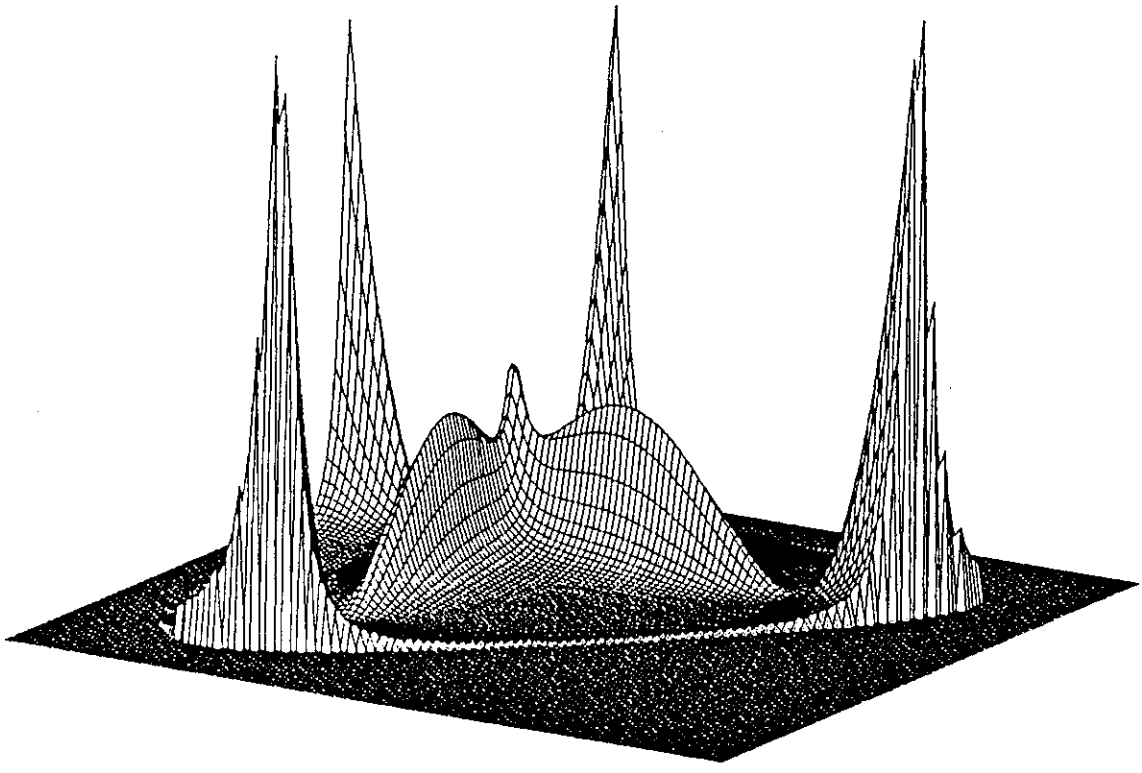

Dalitz plot of $\eta_c \to K^*\overline{K} \to K\overline{K}\pi$

Typeset by $\mathcal{A}_{\mathcal{M}}\mathcal{S}$-TEX

Contents

Introduction

This article is written for experimental high energy physicists who want to carry out two photon analyses in the future. It attempts to review the vast amount of literature which has emerged, especially since PETRA and PEP came into operation.

In principle, two photon physics can be studied with photons coming from an arbitrary source. However, in practice nearly all measurements have been carried out at e^+e^- storage rings. Unless specified otherwise, the term "two photon physics" stands for the reaction

$$e^+e^- \rightarrow e^+e^-X$$

where X is an "arbitrary" final state (c.f. fig.1.1). This article only considers exclusive hadronic final states, e.g. single resonances or hadron pairs.

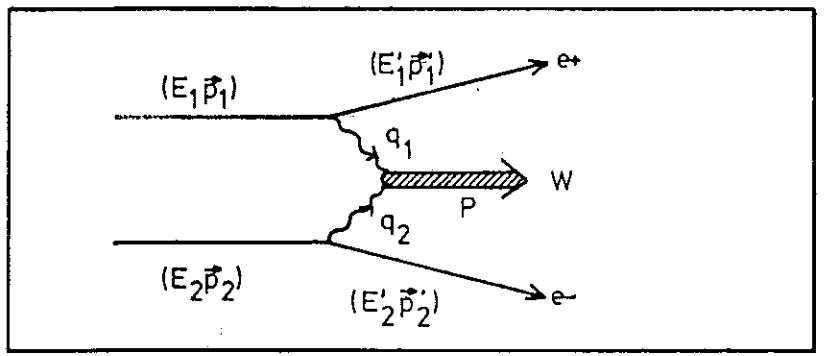

Figure 1.1: *The two photon process at e^+e^- colliders*

A great advantage of exclusive final state measurements is that in most cases, exclusive reactions can be fully described by a small number of parameters. The reaction $\gamma\gamma \rightarrow \pi^0 \rightarrow \gamma\gamma$ for example, is entirely defined through a single coupling $F_{\pi^0\gamma\gamma}$. Therefore, calculating detector acceptances without model assumptions reduces to fitting a single function to the data. Such a limitation of parameters stands in marked contrast to measurements of inclusive reactions.

The great advantage of doing two photon physics is that the initial state in these reactions is very clean. Measurements of leptonic processes up to $s = 2000\,GeV^2$ at PETRA [1] agree with the standard model and thus indicate that the initial state is pointlike. Therefore, an interpretation of the production of a state "X" in a $\gamma\gamma$ collision at an e^+e^- accellerator can be based on model assumptions about this particular final state only. In hadron scattering experiments, interpretations of the data require knowledge about a non trivial initial state in addition.

The analysis of a very short lived particle is only possible by means of a reaction, in which the quanta which *produce* the state are identical to those which *probe* it. Such an analysis *in statu nascendi* can be made with virtual photons in a $\gamma\gamma$ experiment. Therefore, two photon physics is able to measure properties of "arbitrarily" short lived particles.

However, these major advantages exact a high price. First of all, the experimental difficulties are enormous. At PETRA, for example, final state photons have to be well measured down to energies of $\sim 200\,MeV$ by shower counters which are designed to measure $20\,GeV$ electrons. Experimentally, $\gamma\gamma$ physics is nearly always the analysis of detector edge effects. In consequence, most measurements of $\gamma\gamma$ interactions have systematic errors well above 10% . In addition, the theory has to pay its price. Since, in the resonance region, the dynamics is dominated by *soft* processes, there are very few processes which can be rigorously calculated. We have thus to live with the assumption that our concepts of two photons collisions will undergo changes in the future. This implies that model independent parameterisations of the data are a necessity.

At present, a major interest of $\gamma\gamma$ physics concerns the answer to the question "do the photons resolve the hadron's structure or not?" In other words: is particle production in $\gamma\gamma$ interactions primarily the production of quark pairs or is the VDM interpretation correct that the photons turn into vector mesons before they interact? In the latter case, two photon physics would be just a continuation of fixed target hadron scattering experiments, and we would not expect great news to appear.

If on the other hand, there is evidence for a pointlike ($q\bar{q}$) coupling, $\gamma\gamma$ physics of exclusive final states may have a bright horizon:
i) "Glue balls", particles consisting of gluons only, are expected to have rather small two photon cross sections. Upper limits derived from $\gamma\gamma$ data could thus play a major role in the search for gluonium states.
ii) In certain perturbative QCD based models of pair production amplitudes (see below), the production of hadron pairs involves the exchange of a hard gluon in first order pertubation expansion. Therefore, QCD does not appear as a *correction* to a known process but as vital ingredient. Correspondingly strong is the dependence of the cross section on α_s.

Special attention will thus be dedicated to the phenomenological differences between pointlike and VDM type dynamics. Of course, such differences depend on details of the processes, and on the energies involved. The two extreme views of two photon physics, perturbative QCD and VDM, may only be two end points on the long road of our understanding of physics.

Two Ways of Looking at $\gamma\gamma$ Physics

Vector Meson Dominance

The language used for interpretation of $\gamma\gamma$ data originates in other (older) branches of

high energy physics. The first of the main developements dates back to 1960, when Sakurai [2] proposed to describe the hadronic interactions of photons as a two stage process with definite time ordering: the photon first turns into vector meson and subsequently, the meson interacts with the hadronic matter. Formally, we can account for this ordering by introducing a photon - vector (γV) meson vertex $g^{\mu\alpha}\left(\frac{m_v^2}{m_v^2-q^2}\right)\left(\frac{e}{f_v}\right)$ with e/f_v being the amplitude of finding the vector meson v in the photon (c.f. fig.(1.2)). This approach is called the vector meson dominance model (VMD). Applied to $\gamma\gamma$ physics, this gives

$$M(\gamma\gamma \to X) = \sum_{i,k}\left(\frac{e^2}{f_{v_i} f_{v_k}}\right)\frac{m_{v_i}}{m_{v_i}^2 - q_1^2}\frac{m_{v_k}}{m_{v_k}^2 - q_2^2} M(v_i v_k \to X)$$

where X is a hadronic final states and v_i are all vector mesons. The couplings (e/f_{v_i}) can be estimated from e^+e^- annihilation data [3] :

$$\sigma(e^+e^- \to X) = 4\pi\alpha \sum_i \left(\frac{e}{f_{v_i}}\right)^2 \frac{m_{v_i}^2}{s}\,\frac{m_{v_i}\Gamma_{v_i} B(v_i \to X)}{(s-m_{v_i}^2)^2 + m_{v_i}^2\Gamma_{v_i}^2}$$

giving

$$\frac{f_\rho^2}{4\pi} = 2.11 \pm 0.29 \quad \frac{f_\omega^2}{4\pi} = 18.3 \pm 1.9$$
$$\frac{f_\varphi^2}{4\pi} = 13.5 \pm 1.40 \quad \frac{f_\psi^2}{4\pi} = 11.5 \pm 1.4$$

The first application of the vector dominance model to two photon physics was one of the most successful. In 1962, Gell-Mann et al [4] calculated the π^0 width to be $7.4\,eV$, a value still in good agreement with experiment. This reaction is particularly suitable for an implementation of the VDM idea, since there is only *one* amplitude which describes the coupling between a pseudoscalar and two vectors ("VVP-coupling"). Furthermore, this coupling is gauge invariant and hence, there are no formal problems in relating the QED amplitude to hadronic ones. *In all other cases, the VDM hypothesis alone gives no unique predictions for two photon reactions.* This is so, because for all other reactions, there is more than one possible amplitude and VDM alone does not give an answer to the question which amplitude should dominate.

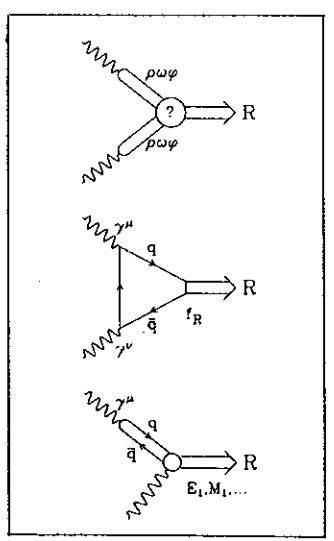

Figure 1.2: *Interpretations of resonance production in two photon collisions.*

The simplest example is that, if $T_{\mu\nu}$ is a suitable amplitude for a two photon process, so is the amplitude $T'_{\mu\nu} \equiv q_1^2 q_2^2 T_{\mu\nu}$. $T_{\mu\nu}$ may be finite for real photons, $T'_{\mu\nu}$ vanishes for on shell photons, and there is in general no rigorous argument for chosing between the two. Furthermore, there is no unique recipe for turning partial wave amplitudes into gauge invariant ones and hence, it is generally impossible to obtain the relevant amplitudes using hadron phenomenology alone. As a consequence, nearly all papers that have been published in this context make dynamic assumptions beyond the VDM idea.

In order to arrive at numerical predictions, several authors have introduced various *ad hoc* assumptions. Ginsburg and Serbo [5] for example include further vector mesons (i.e. $\rho', \rho'', ...$) and postulate a factorisation of the cross section into W and q^2 dependent terms. The q^2 terms differ from the simple vector meson propagators mainly by an estimate of the longitudinal coupling of the photons. This model is called the "*generalised vector dominance model*" (*GVDM*). Although this model is often quoted to be in good agreement with experimental data, the postulate of factorisation has yet to be tested. Alexander et al [6] have taken an entirely phenomenological approach by assuming $\sigma(\gamma\gamma) = (\sigma(\gamma p))^2/\sigma(pp)$, where σ is understood to be calculated at a certain fixed value of p^*, the c.m.s. momentum of the final state particles. They call their model the "*extended vector dominance model*, (*EVDM*)". Notice that this model tests the hypothesis "In $\gamma\gamma$ collisions, we observe the same effects as in photoproduction". Strictly speaking, however, it is not a VDM Ansatz.

Quarks and Partons

In the static quark parton model [7] , mesons are interpreted as $q\bar{q}$ bound states. Since the quarks carry charge, for a short time, the photon can form a $q\bar{q}$ pair. Because of spin and parity conservation, such a pair has the quantum numbers of a vector meson. Therefore, there is some overlap between vector mesons and photons: $<\gamma V><\sim<\gamma q(\uparrow)\bar{q}(\uparrow), L=0>\neq 0$. Thus, the quark model can give a qualitative interpretation of the successes of VDM.

In the quark model, electromagnetic transitions between mesons (i.e. $M_1 \to M_2\gamma$) are no longer necessarily two stage processes, but may be direct couplings of the photons to the charge and current distributions within the mesons. Thus, even the real photon becomes a probe for the inside of mesons with may be pointlike couplings. What really happens if two photons form a meson is subject to specific model assumptions. In particular, one can distinguish two lines of approach. The fusion mechanism can either take place in one step, i.e. the quarks annihilate directly. In this case, the radiative widths are interpreted (as in the case of positronium decays) as measures for the quark wave function at the origin in case of pseudoscalar meson decays, or as measures of the derivatives of the wave functions in case of scalar or tensor meson decays. Another Ansatz assumes a more complicated process. It may be that a better analogy are atomic photon transitions. The radiative decay of a meson would then be a two stage process: an M_1 or E_1 transition would be followed by the annihilation of the resulting $q\bar{q}$ pair into the second photon.

It is of course very tempting to mix quark and VDM arguments, i.e. take for example the tensor $\to$ vector photon ("$TV\gamma$") amplitude from the quark model and then use VDM for the $V \to \gamma$ transition. However, if we want to test experimentally, whether or not the VDM hypothesis is simply a suitable parameterisation of the unknown, or whether a γV transition actually takes place, a clear separation beween the two approximations is necessary. In the

following chapters, it will be shown that some form factor measurements can give a decisive answer.

The quark model is able to interrelate different radiative processes, but for many reactions it cannot predict the absolute scale at which the processes occur because it does not "know" how the quarks are bound together.

Until now, it has been hoped that QCD will eventually provide the answers to all questions about resonances. However, since QCD cannot yet be calculated at large distances, the large majority of measurements, which are measurements of low momentum transfer reactions, cannot be tested against QCD. In 1980, Brodsky and Lepage[8] published the first calculations of exclusive processes in $\gamma\gamma$ reactions in the framework of perturbative QCD. The basis of these (and many subsequent) calculations is the assumption of a factorisation of the full amplitude into a hard core describing the formation of $q\bar{q}$ pairs and a soft part describing the condensation of quark pairs into mesons. As far as the calculations of hadron pair amplitudes are concerned, the nicest feature of these calculations is that the gluon does not appear as a correction, but as a necessary ingredient of the first order amplitude.

Some Second Order QED at e^-e^- Machines

Storage Rings as Photon Sources

The literature on this topic is already quite sizable. Therefore, the discussion of the photon flux is kept as short as possible. The main purpose of the following section is to define the notation. More introductory chapters can be found in refs. [9-15]

The quantum mechanical description of the two photon process at storage rings is shown in fig.(1.1). The corresponding amplitude is

$$M = -e^2\bar{u}(p_1')\gamma^\mu u(p_1)\bar{v}(p_2)\gamma^\nu v(p_2')\frac{1}{q_1^2 q_2^2}T_{\mu\nu} \tag{1.1}$$

The term $T_{\mu\nu}$ contains the physics of interest. It is therefore useful to disentangle the leptonic part from the $\gamma\gamma \to$ *hadrons* vertex. The result has been given by V. M. Budnev et al [9] and others. For unpolarised beams,

$$\begin{aligned} d\sigma = \frac{\alpha^2}{16\pi^4 q_1^2 q_2^2}\sqrt{\frac{(q_1q_2)^2 - q_1^2q_2^2}{(p_1p_2)^2 - m_1^2m_2^2}}\ \Big\{ & 4\rho_1^{++}\rho_2^{++}\sigma_{TT} + 2\left|\rho_1^{+-}\rho_2^{-+}\right| \tau_{TT}cos(2\tilde{\phi}) \\ & + 2\rho_1^{++}\rho_2^{00}\sigma_{TL} + 2\rho_1^{00}\rho_2^{+-}\sigma_{LT} + \rho_1^{00}\rho_2^{00}\sigma_{LL} \\ & - 8\left|\rho_1^{+0}\rho_2^{+0}\right| \tau_{TL}cos(\tilde{\phi})\ \Big\}\frac{d^3p_1'}{E_1'}\frac{d^3p_2'}{E_2'} \end{aligned} \tag{1.2}$$

The labels $+, -, 0$ refer to the helicities of the photons in the $\gamma\gamma$ center of mass system. The

flux factors ρ^{ab} are given by

$$\begin{aligned} 2\rho_1^{++} = 2\rho_1^{--} &= \frac{1}{X}(2p_1q_2 - q_1q_2)^2 + 1 + \frac{4m}{q_1^2} \\ \rho_1^{00} &= \frac{1}{X}(2p_1q_2 - q_1q_2)^2 - 1 \\ 8\left|\rho_1^{+0}\rho_2^{+0}\right|cos(\tilde{\phi}) &= \frac{4}{X}(2p_1q_2 - q_1q_2)(2p_2q_1 - q_1q_2)C\frac{1}{\sqrt{q_1^2q_2^2}} \\ 2\left|\rho_1^{+-}\rho_2^{+-}\right|cos(2\tilde{\phi}) &= \frac{C^2}{q_1^2q_2^2} - 2(\rho_1^{++} - 1)(\rho_2^{++} - 1) \\ \left|\rho_i^{+-}\right| &= \rho_i^{+-} - 1 \\ \left|\rho_2^{a,b}(1,2)\right| &= \left|\rho_1^{a,b}(2,1)\right| \end{aligned} \tag{1.3}$$

with

$$C = -(2p_1 - q_1)(2p_2 - q_2) - \frac{1}{X}(q_1q_2)(2p_1q_2 - q_1q_2)(2p_2q_1 - q_1q_2)$$

and X is the analytic continuation of Møller's flux factor

$$X = (q_1q_2)^2 - q_1^2q_2^2$$

The angle $\tilde{\phi}$ is the angle between the electron-γ planes in the $\gamma\gamma$ center of mass system. With this convention of flux factors, the two photon cross sections σ can be expressed in terms of helicity tensors $W_{a'b',ab}$

$$\begin{aligned} \sigma_{TT} &= \frac{1}{4\sqrt{X}}(W_{--,++} + W_{--,+-}) \quad \sigma_{LL} = \frac{1}{2\sqrt{X}}W_{00,00} \\ \sigma_{TL} &= \frac{1}{2\sqrt{X}}W_{+0,-0}, \ \sigma_{LT} = \frac{1}{2\sqrt{X}}W_{0+,0-} \\ \tau_{TT} &= \frac{1}{2\sqrt{X}}W_{++,--} \\ \tau_{TL} &= \frac{1}{4\sqrt{X}}(W_{++,00} - W_{0+,-0}) \end{aligned} \tag{1.4}$$

These helicity tensors are essentially cross sections with all flux terms taken out:

$$W_{a'b',ab} = \frac{1}{2}\int d(Lips)M_{a'b'}^*M_{ab}, \quad M_{ab} = T_{\mu\nu}\epsilon_{1a}^\mu\epsilon_{2b}^\nu \tag{1.5}$$

The Lorentz invariant phase space element for a system of n particles is abbreviated in the usual manner:

$$d(Lips)_n = (2\pi)^4\,\delta^4(q_1 + q_2 - \sum_{i=1}^{n}k_i)\,\frac{1}{(2\pi)^{3n}}\,\prod_{i=1}^{n}\frac{d^3k_i}{2E_i}$$

Taking the z-direction along the momentum of the photon with label "1", the explicit form of the polarisation vectors in the two photon center of momentum system can be taken to be

$$\begin{aligned} \epsilon_{1+} &= \frac{1}{\sqrt{2}}(0,-1,-i,0),\ \epsilon_{1-} = \frac{1}{\sqrt{2}}(0,+1,-i,0),\ \epsilon_{10} = \frac{1}{\sqrt{-q_1^2}}(q_{1z},0,0,q_{10}) \\ \epsilon_{2+} &= \frac{1}{\sqrt{2}}(0,+1,-i,0),\ \epsilon_{2-} = \frac{1}{\sqrt{2}}(0,-1,-i,0),\ \epsilon_{20} = \frac{1}{\sqrt{-q_2^2}}(q_{1z},0,0,-q_{20}) \end{aligned} \tag{1.7}$$

In this frame, the photon four vectors are

$$q_1 = (\frac{q_1 q_2 + q_1^2}{W}, 0, 0, \frac{\sqrt{X}}{W}) \qquad q_2 = (\frac{q_1 q_2 + q_2^2}{W}, 0, 0, -\frac{\sqrt{X}}{W}) \tag{1.8}$$

It must be stressed that the polarisation vectors are reference frame dependent quantities. In particular, a Lorentz transformation with a finite component perpendicular to the electron beam direction leads to mappings of transverse photons onto longitudinally polarised photons and vice versa.

The way the cross section is defined here is such that at finite q^2, it has the same form as for vector mesons, but calculated at negative mass squared. However, since no possible experiment can count virtual photons, this convention is arbitrary except for the limit $q_1^2, q_2^2 \to 0$. In fact, many authors use different conventions, leading to discrepancies which are typically of the order q^2/W^2. The convention adopted here has the advantage that the $\gamma\gamma$ cross sections develop terms which are well known from other branches of high energy physics. For example, as can be seen in eq.(1.8), at fixed W, the flux factor $\sqrt{X}$ is proportional to the three momentum of the photons and it turns out that the well known $(|\vec{k}|/|\vec{k}_0|)^{2l+1}$ spin barrier factors find their spacelike counterparts in powers of $\sqrt{X}$ linking the coupling constants to the off shell $\gamma\gamma$ cross sections. With increasing $|q^2|$, these barriers become deep valleys.(!)

It must be emphasized that the way the cross section is defined here (which is identical to the conventions used by most experimental groups), the q^2 evolution of the *cross sections* is *different* from the q^2 evolution of the squared *amplitudes*. This discrepancy can fake form factor effects. Consider for example a constant amplitude for transverse photons. The cross section for the case $q_1^2 \neq 0$, $q_2^2 = 0$ would then be $\sigma_{TT} \sim \frac{1}{1-q_1^2/W^2}$, which for masses of the order $W \simeq 1\,GeV$ is numerically close to a ρ^0 pole form factor. There are many examples in the literature, where this "dummy" fall off has been misinterpreted as a vector meson dominance effect.

Restrictions on the $\gamma\gamma$ Vertex

The two photon vertex $T_{\mu\nu}$ is subject to a number of conservation laws (see also refs. [16], [17]), in particular *charge conjugation invariance*, *gauge invariance*, *Lorentz invariance* (which includes conservation of angular momentum), *Bose statistics* and conservation of *parity*.

The consequences of charge conjugation invariance are two fold. First of all, it implies that in the two photon process, only states of *positive* charge conjugation can be produced. Single ρ^0 mesons (which have negative C) in the data are thus a sign of non two photon processes or incompletely reconstructed events. A further consequence originates in the fact that the photon fusion mechanism is the *only* second order QED $e^-e^- \to e^+e^-X$ amplitude in which the final state X is linked to the leptonic system via *two* photons (see below). All other second order QED diagrams thus describe the formation of states with negative charge conjugation. Therefore, the states produced by the two photon mechanism are different from the other ones, and hence, all conservation laws that hold for the full $e^+e^- \to e^+e^-X$ process also apply to the subprocess $\gamma\gamma \to X$.

The consequences of the other symmmetry principles can be examined by expanding the amplitudes in terms of gauge invariant covariant helicity selection tensors (see appendix A). For a state of specific spin parity J^P, one then obtains for the helicity matrix elements $M_{a,b}$:

$$\begin{array}{lll}
M_{0,b}(q_1^2, q_2^2) \sim \sqrt{-q_1^2} \quad (as\, q_1^2 \to 0) & for\ \ all\ \ J^P & gauge\ \ invariance \\
M_{a,0}(q_1^2, q_2^2) \sim \sqrt{-q_2^2} \quad (as\, q_2^2 \to 0) & for\ \ all\ \ J^P & gauge\ \ invariance \\
M_{a,b}(q_1^2, q_2^2) = M_{-a,-b}(q_1^2, q_2^2) & for\ \ J^P = 0^+, 1^-, 2^+, ... & parity \\
M_{a,b}(q_1^2, q_2^2) = -M_{-a,-b}(q_1^2, q_2^2) & for\ \ J^P = 0^-, 1^+, 2^-, ... & parity \\
M_{a,b}(q_1^2, q_2^2) = (-1)^{(J-a+b)} M_{b,a}(q_2^2, q_1^2) & for\ \ all\ \ J^P & Bose\ \ symmetry \\
M_{a,b}(q_1^2, q_2^2) = \delta^{J_z}_{a-b} M_{a,b}(q_1^2, q_2^2) & with\ \ J_z \leq J & Lorentz\ \ invariance
\end{array} \tag{1.9}$$

For the implications of these conservation laws, four experimental configurations can be distinguished.

For any q_1^2, q_2^2, in the most general "double tag" configuration, one has

$$\begin{aligned}
&M_{\pm\mp}(J^P = 0^\pm, 1^\mp) = 0 \\
&M_{0\pm}(J^P = 0^\mp) = 0 \\
&M_{00}(J^P = 0^-, 1^+, 2^-, ...) = 0
\end{aligned} \tag{1.10}$$

The first two equations are a straight consequence of helicity conservation and the third one an implication of parity conservation.

For $q_1^2 = 0$, in the single tag configuration, one has in addition to eq(1.10)

$$\begin{aligned}
&M_{0,b}(J^P = anything) = 0 \\
&M_{+,b}(J^P = 0^+, 1^-, 2^-, ...) = +M_{-,b}(J^P = 0^-, ...) \\
&M_{-,b}(J^P = 0^-, 1^-, 2^-, ...) = -M_{-,b}(J^P = 0^-, ...)
\end{aligned} \tag{1.11}$$

These are consequences of gauge invariance and parity conservation.

For $q_1^2 = q_2^2 \neq 0$, in the symmetric double tag configuration, the following helicity amplitudes vanish in addition to the ones of eq.(1.10):

$$\begin{aligned}
&M_{\pm\pm}(J^P = 1^\pm, 3^\pm, 5^\pm, ...) = 0 \\
&M_{\pm\mp}(J^P = 1^-, 2^-, 3^-, ...) = 0 \\
&M_{00}(J^P = 1^-, 3^-, 5^-, ...) = 0
\end{aligned} \tag{1.12}$$

These selection rules are the result of an interplay bewteen rotational invariance, parity conservation and Bose symmetry.

For real photons $(q_1^2 = q_2^2 = 0)$, the restrictions are most severe. In this case, all selection rules stated above apply, and only a small number of amplitudes remains non zero:

$$\begin{aligned}
&M_{\pm,\mp}(J^P = 0^\pm, 2^\pm, 4^\mp, ...) \neq 0 \\
&M_{\pm,\mp}(J^P = 2^-, 3^+, 4^-, ...) \neq 0 \\
&all\ \ others\ \ vanish
\end{aligned} \tag{1.13}$$

These amplitude restrictions imply Yang's[1] theorems [16]:

$$\begin{aligned} &\sigma_{\gamma\gamma}(1^+) = \sigma_{\gamma\gamma}(1^-) = 0 \\ &\sigma_{\gamma\gamma}(J^P = 3^-, 5^-, 7^-, ...) = 0 \end{aligned} \tag{1.14}$$

and fix for a large number of states, with which helicities they are produced in the collisions of real photons:

$$\begin{aligned} J_z = 2 \quad &for \quad 3^+, 5^+, 7^+, ... \\ J_z = 0 \quad &for \quad 2^-, 4^-, 6^-, ... \end{aligned} \tag{1.15}$$

Therefore, in all cases, except for the production of $J^P = 2^+, 4^+, ...$ states, the helicities are fixed by first principles. Hence, in all other cases, the determination of the coupling of a state of known spin parity to two real photons reduces to a one parameter problem.

Determination of the Radiative Widths

In the limit $q_1^2 = q_2^2 = 0$, the formation of a single resonance by the collision of two photons is the inverse process of a radiative decay. Therefore, the two photon production cross section for a certain particle is a measure of its radiative decay width.

In order to arrive at an expression which interrelates the two photon production cross section and the radiative decay widths, we have to overcome the technical difficulty that the usual expression for the phase space of a system yields a δ distribution if evaluated for a single particle - a consequence of the fact that final state particles are commonly assumed to be stable. For wide resonances, we can overcome this problem by first considering the entire process, i.e. production *and* decay of the resonance:

$$\begin{aligned} W_{abab} &= \frac{1}{2}\int \left|\frac{M_{ab}(\gamma\gamma \to R) M_{J_z}(R \to "final")}{W^2 - M_R^2 + iM_R\Gamma_R}\right|^2 dLips_{final} \\ &= \frac{1}{2}\int |M_{ab}(\gamma\gamma \to R)|^2 \cdot \left(\frac{|M_{J_z}(R \to "final")|^2}{(W^2 - M_R^2)^2 + \Gamma_R^2 M_R^2} dLips_{final}\right) \end{aligned} \tag{1.16}$$

For the case where the resonance decays into 2 stable particles, the orthonormality of the spherical harmonics leads to a complete factorisation of the integral and we obtain a useful expression for the (total) phase space of a single particle:

$$\begin{aligned} Lips_1 &= 2\frac{M_R^2}{W}\frac{\Gamma_R}{(W^2 - M_R^2)^2 + \Gamma_R^2 M_R^2}\delta^{a-b}_{J_z(f)}\delta^{J(R)}_{J(f)} \\ \Gamma_R &\simeq \Gamma_0 \left(\frac{|\vec{k}^*(W)|}{|\vec{k}^*(M_R)|}\right)^{(2L+1)} \end{aligned} \tag{1.17}$$

where Γ_0 is the width at nominal resonance mass M_R. In this expression, the decay form factor (usually referred to as a "finite size effect" or "spin barriere penetration factor") has

[1] Some of the selection rules which are known as Yang's theorems today were given by Wheeler, Sakata, Tanikawa, Finkenstein, Steinberger and Wigner. Their works are referenced by Yang [16].

been neglected. If the total width of the resonance is two orders of magnitude smaller than its mass, such factors may be ignored; otherwise, the $(k^*)^{(2L+1)}$ factor has to be modified (c.f. appendix D).

It is useful to compare the above expression with the two photon width of a resonance[1]

$$\Gamma_{\gamma\gamma} = \frac{1}{16\pi(2J+1)M_R}\sum_{a,b}|M_{ab}|^2 \tag{1.18}$$

and the $q^2 = 0$ limit of eq.(1.4). For a particle of spin J, the result is[1]

$$\sigma_{\gamma\gamma}(q_1^2 = q_2^2 = 0) = 8\pi(2J+1)\frac{M_R}{W}\frac{\Gamma\Gamma_{\gamma\gamma}}{(W^2 - M_R^2)^2 + \Gamma_R^2 M^2} \tag{1.19}$$

This equation has interesting implications. Since the total rate is proportional to the product $\Gamma_R \times B(R \to \gamma\gamma) \times (2J+1)$, the knowledge of either pair of these quantities, together with the a $\gamma\gamma$ measurement gives information about the third. The total widths of the η and η' for example are most accurately determined by a comparison between $\gamma\gamma$ formation and resonance decay measurements.

Features of the Photon Fluxes

The full equation connecting the electron positron cross section with the various $\gamma\gamma$ cross sections is very complicated. For the simplest possible configuration, the production of a single particle with fixed mass, its evaluation already is a 3x3-4 = 5 dimensional integration. This has stimulated a large number of authors to seek for approximations (e.g. the *equivalent photon approximation*, *epa* [18]). These will not be discussed here in detail, first of all because the literature on this subject is already quite sizable, but also because the accuracy of experiments has begun to enter a domain in which current approximations are no longer valid. Roughly speaking, no published approximation should be trusted to better than 10% . A precise $\gamma\gamma$ measurement has to to be based on the full formula given in eq(1.2).

Nevertheless, the equivalent photon approximation has some lasting value. It provides us with a simple picture of two photon physics. Also, it is easy to calculate and thus provides a good tool for efficient detector design studies.

With this in mind, we shall follow for a while the key assumption of the equivalent photon approximation, the hypothesis of factorisation. Physically, this means that one can think of the interaction region as being exposed to two *independent* wide band photon beams. According to [9], each of the incoming beams has the following spectrum:

$$\frac{d^2 n_i}{d\omega_i\, dq_i^2} = \frac{\alpha}{\pi\omega_i\, q_i^2}\left(\left(1 - \frac{\omega_i}{E_b} + \frac{\omega_i^2}{2E_b^2}\right) - \left(1 - \frac{\omega_i}{E_b}\right)\frac{q_{i\,min}^2}{q_i^2}\right) \tag{1.20}$$

[1] In evaluating the phase space of a two photon system, care has to be taken of the fact that the two photons are indistinguishable, and thus, $\int d\Omega = 2\pi$.

[1] Notice that the radiative width is by definition a number, and not a function of W. Eq.(1.19) is written down under the assumption that the $\gamma\gamma$ vertex has no explicite energy dependence, i.e. $M_{ab}(W) = M_{ab}(M)$. For a large number of cases, in particulare $J^P = 0^-$ and large J meson production, it is very likely that this assumption is *not* correct. However, the energy dependence of the photon photon coupling depends on the details of the process and can thus not be implemented in this general form.

where ω_i is the photon energy in the lab. frame and $q^2_{i\,min}$ is the smallest possible invariant mass of the photon i=1,2. The total electron positron cross section then follows from

$$\sigma(e^+e^- \to e^+e^- X) = \int \sigma(\gamma\gamma \to X) \frac{d^2n_1}{d\omega_1 dq_1^2} \frac{d^2n_2}{d\omega_2 dq_2^2} d\omega_1 d\omega_2 dq_1^2 dq_2^2 \qquad (1.21)$$

Notice that measuring a total $\gamma\gamma$ cross section always means measuring a differential e^+e^- cross section. The dimensionless product $d^2n_1 d^2n_2 = d^4L_{\gamma\gamma}$ is often called the differential *photon luminosity function*.

The main features of the photon spectra are easily examined. First of all, the $1/q^2$ term from the photon propagator leads to a pole at $q^2 = 0$, which is only avoided by the kinematic constraint

$$|q^2| > |q^2_{min}| = \frac{m_e^2\omega^2}{E_b(E_b - \omega)} \qquad (1.22)$$

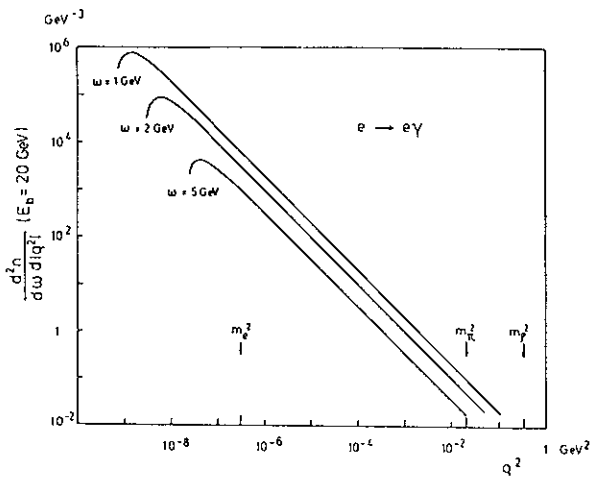

Figure 1.3: *q^2 spectrum of the photon flux from a single electron beam (from eq.1.20)*

Fig.(1.3) shows the q^2 evolution of the flux of transverse photons from 20 GeV electrons. The scale is chosen to be logarithmic, because the peak near $q^2 = 0$ is so sharp and narrow that it appears as a vertical line on more or less any linear scale. The maximum of the flux is generally more than 6 orders of magnitude (!) below the natural hadronic scale set by the ρ meson mass squared. It is thus justified to consider the large majority of two photon events as induced by real photons. However, the logarithmic scale is also misleading in the sense that it may lead to an underestimate of the fraction of photons which have large values of q^2. In fact, for some 10% of the events (the exact number depends on the final state one is measuring), form factor effects can *not* be neglected. At the current DORIS, PEP, PETRA detectors, the electrons coming from most of these events are not seen.

The energy distribution of the incoming photons resembles that of Bremsstrahlung. It

can be obtained by integrating the above flux spectrum over q^2, giving

$$\frac{dn}{d\omega} = \frac{\alpha}{\pi\omega}\left((1 - \frac{\omega}{E_b} + \frac{\omega}{2E_b^2})ln\frac{q^2_{max}}{q^2_{min}} + (1 - \frac{\omega}{E_b})(1 - \frac{q^2_{min}}{q^2_{max}})\right) \qquad (1.22)$$

This spectrum is shown in fig.(1.4). It is interesting to notice that the mass of the electron mainly enters the spectrum logarithmically (via $ln(q^2_{min})$). This has the promising consequence that proton machines may also serve as efficient photon sources.[1]

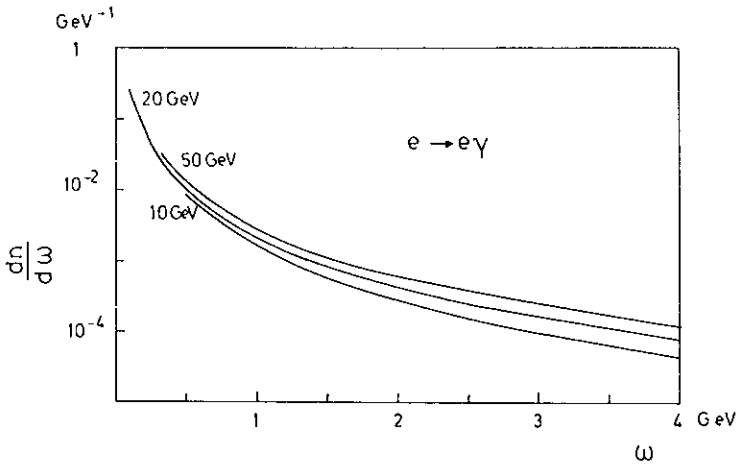

Figure 1.4: *Energy spectrum the photon flux from a single electron beam in the lab. frame (from eq.1.22)*

Other QED Processes of the same Order

The two photon fusion mechanism is not the only one contributing to the $e^-e^- \to e^+e^- X$ cross section. In addition to the $\gamma\gamma$ fusion diagram, there are three other classes of diagrams of the same order of α.(c.f.fig.(1.5)).

The Bremsstrahlung and annihilation diagrams may be considered as radiative corrections to the Bhabha process, while the conversion diagrams have no lower order relative. If the state "X_1" in the conversion diagrams shown in fig.(1.5) is an e^+e^- pair, these diagrams may simulate large q^2 two photon events. Notice that all but the $\gamma\gamma$ fusion diagram, the system X is linked to the electron lines through a single photon only, implying that it is not

[1] This may be very counter intuitive, given how very differently electrons and protons interact for example in electromagnetic calorimeters. The principle difference between virtual photon radiation and interaction with matter is that in the latter class of reactions, the proton always occurs as a propagator, leading to a $1/m_p^4$ term in the cross section, In contrast, in the case of virtual photon radiation, the proton makes external lines only.

possible to make predictions about the relative sizes of different diagrams without making specific assumptions about the ratio of 1γ to 2γ coupling constants of the system X. There is thus no way of formulating the influence of the competing processes in the form of a correction to eq.(1.2). Every final state has to be looked at individually.

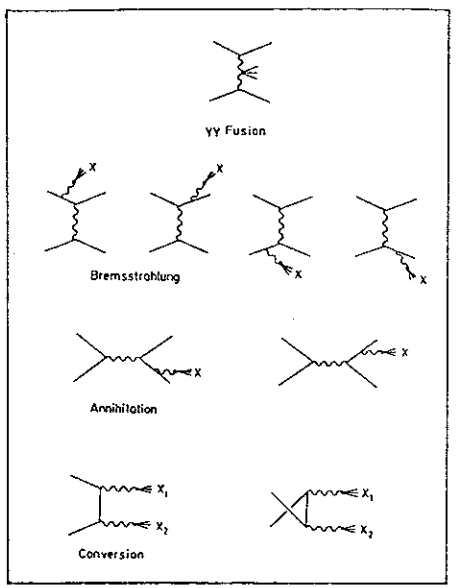

Figure 1.5: α^2 *contributions to the total* e^+e^- *cross section. The annihilation diagrams are suppressed by the photon propagators, the conversion diagrams yield high invariant masses.*

The cross section for the reaction $e^+e^- \rightarrow e^+e^-\mu^+\mu^-$ has been calculated by Behrends, Daverfeldt and Kleiss [19]. As they point out, this process not only gives a handle on the description of quark pairs, but also provides a model independent link to electron positron annihilation data. This is a result of the fact that by far the largest correction to the $\gamma\gamma$ fusion mechanism arises from the the Bremsstrahlung diagrams. Since for these diagrams, the final state "X" communicates with the electron lines via a single photon only, the differential production cross section factorises into an $e^+e^- \rightarrow e^+e^-\gamma^*$ and a $\gamma^* \rightarrow$ "X" part. For muons (c.f. appendix B), the latter is described by the function

$$f(W^2_{\mu\mu}) = \frac{\alpha}{6\pi}\frac{\beta(3-\beta^2)}{W^2_{\mu\mu}} \tag{1.23}$$

where β is the velocity of the muons in their common center of momentum frame. Because of this factorisation, one can obtain a *model independent* prediction for the Bremsstrahlung hadron production cross section by the simple replacement

$$f(W^2) \rightarrow f_{hadr.}(W^2) \equiv f(W^2)\frac{\sigma_{e^+e^-\rightarrow Hadr.}(W^2)}{\sigma_{e^+e^-\rightarrow\mu^+\mu^-}(W^2)} \tag{1.24}$$

Notice that the authors of ref. [19] have written a Monte Carlo generator for $e^+e^- \rightarrow e^+e^-\mu^+\mu^-$ in such a manner that individual diagrams can be "switched off". Therefore, by means of eq.(1.24), the tools for a simulation of Bremsstrahlungs contributions are available.

As can be seen in fig.(1.6), the total cross section for $\mu^+\mu^-$ pair creation by Bremsstrahlungs diagrams is about two orders of magnitude smaller than the cross section of the γ fusion mechanism.

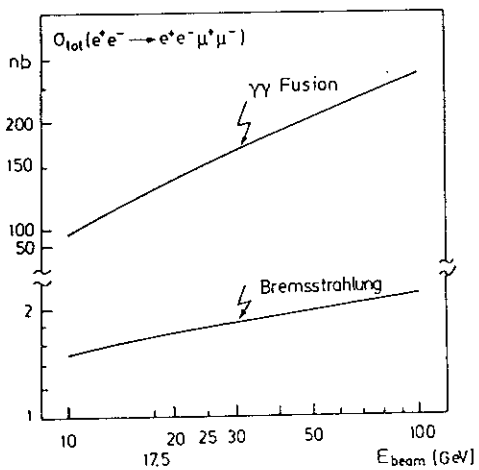

Figure 1.6: *The two largest QED contributions to the total cross section for* $e^+e^- \rightarrow e^+e^-\mu^+\mu^-$ *. The curves are interpolations of points given in ref. [19].*

For beam energies between 10 and $100GeV$, the total Bremsstrahlung cross section is only $\sigma_B = 1.06nb(E_{Beam}/GeV)^{0.155}$ (within three per cent). However, there are kinematic regions, where the Bremsstrahlung diagrams make a substantial contribution to the differential cross section. This is the case, if either or both electrons are scattered at a large angle, and the invariant mass of the $\mu^+\mu^-$ pair is close to $2m_\mu$.

The experimental evidence for contributions from non peripheral processes is still marginal (c.f. ref. [11]). The Mark J and the PLUTO collaborations have seen indications of a Bremsstrahlung contribution in $\mu^+\mu^-$ pair production, however, the available data do not yet require the presence of these amplitudes.

Ingredients for a Two Photon Analysis

Hardware

Basically, all the requirements for a good two photon detector follow from the features of the two photon flux. Two photon event detection depends critically on two main parameters:

Forward particle detection capability

trigger thresholds

In addition, particle identification may be necessary for some channels.

Since the photon spectrum roughly follows a $1/\omega$ distribution, the energies of the incoming photons are usually quite different. This leads to a large Lorentz boost from the $\gamma\gamma$ centre of momentum system to the lab. frame. As a consequence, all final state angular distributions are strongly peaked towards $cos\theta = \pm 1$, i.e. towards the beam pipe. A detector which is designed for $\gamma\gamma$ physics must be able to measure particle momenta down to the smallest possible angles. Fig.(1.7) gives an idea of the importance of small angle coverage. In this figure, the (lab.) angular distribution for muons from the reaction $\gamma\gamma \rightarrow \mu^+\mu^-$ is shown.

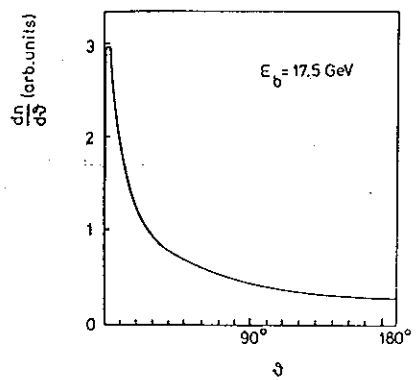

Figure 1.7: *The angular distribution of muons in the lab. frame. Notice that the number of particles per solid angle interval is* $\frac{dn}{d\Omega} = \frac{2\pi}{sin\theta}\frac{dn}{d\theta}$.

The other major feature of the photon flux is the sharp q^2 distribution which is followed by a long, slowly falling tail. Since

$$q^2 \simeq -4E_iE'sin^2(\theta/2)$$

low values of q^2 correspond to small scattering angles of the electrons. Most of the scattered electrons stay in the beam pipe. For form factor measurements however, it is crucial to measure the final state electron (this is called *tagging*). Since there may be background in the form of hard photons from other processes, an electromagnetic calorimeter may not be sufficient. In Fig.(1.8), the PLUTO detector is shown as an example of how clean tagging can be achieved by including charged particle detectors in front of the tagging shower counters.

Triggering two photon events is probably the most difficult task for a $\gamma\gamma$ detector. The reason is illustrated in fig.(1.9): beam interactions with residual atoms in the interaction region ("beam gas"). Because of the large cross section for photo production, such interactions are not only a severe background for some exclusive channels, they are also responsible for trigger rates which may easily lead to intolerable dead times. Since "beam gas events" have topologies similar to those of $\gamma\gamma$ events, a reduction of the dead time in general implies a loss of two photon events. Different collaborations have come to different hardware solutions for this problem. The TASSO and JADE detectors (c.f. figs.(1.10/1.11)) are equipped with time of flight scintillators surrounding the inner tracking chambers. The rate of false track triggers in these detectors is reduced by demanding a hit in those time of flight (TOF) modules to

which the tracks point. This is a cheap, simple and powerful technique. For track pairs with small opening angles, the JADE as also a *track*$\times$*TOF* $\times$*shower counter* trigger.

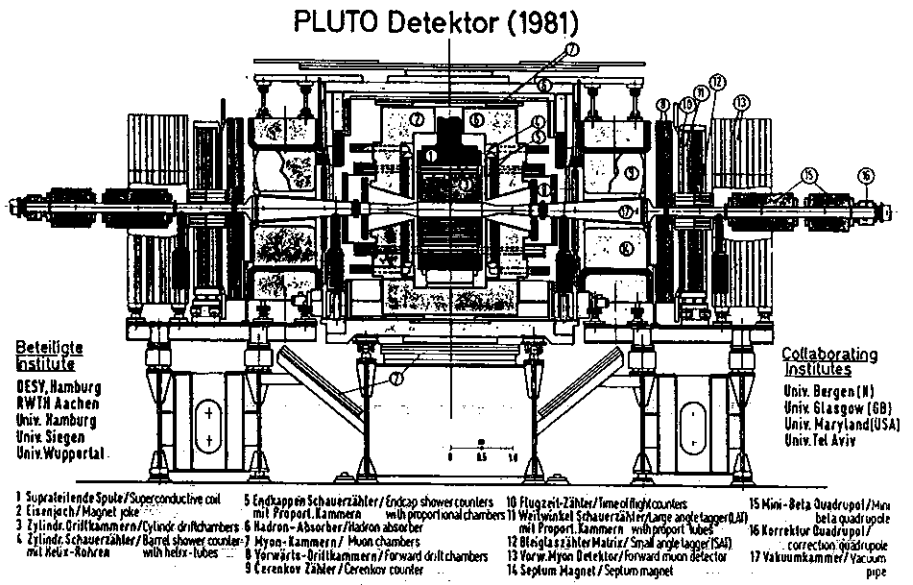

Figure 1.8: *Schematic view of the PLUTO detector, a dedicated experiment for two photon physics. The forward spectrometes strongly enhance the acceptance for two photon events and allow particle identification. The chambers in front of the shower counters enable clean tagging.*

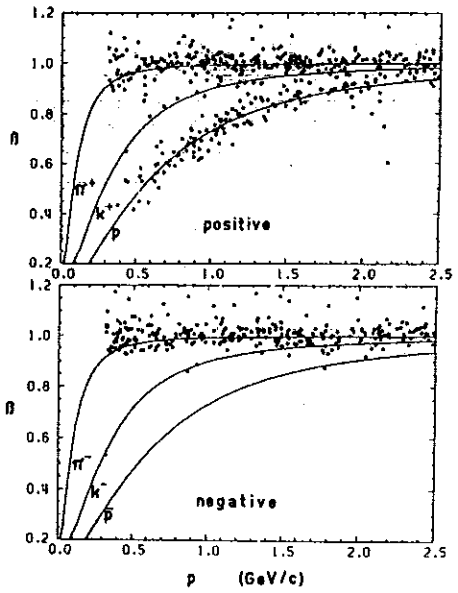

Figure 1.9: *Velocity momentum correlation for charged tracks measured in the PLUTO forward spectrometer. This sample is based on events which do not come from the interaction vertex. The excess of protons is a signature of nuclear fragments from "beam gas" interactions.*

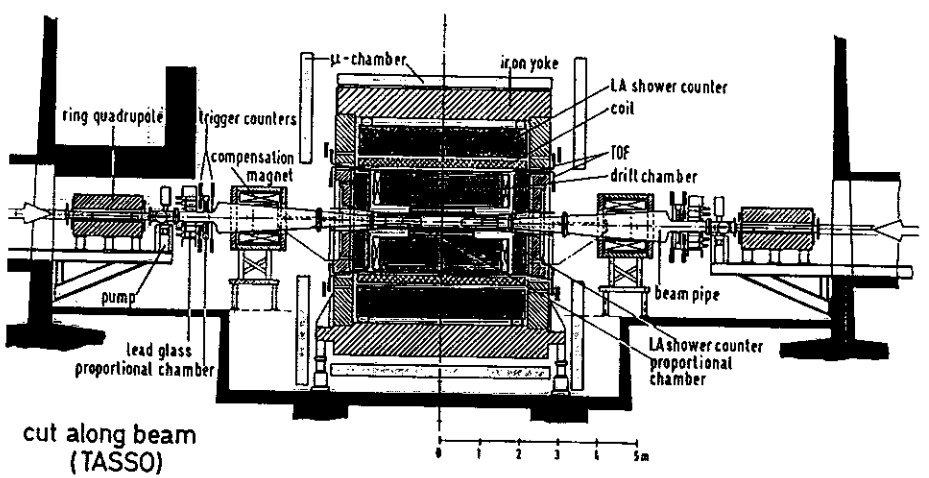

Figure 1.10: *The TASSO detector. Its large drift chamber yields good momentum resolution for charged particles.*

PLUTO and CELLO (c.f. fig.(1.12)) have taken a different approach. They reduce the number of false tracks by improving the accuracy of track recognition already at the trigger level by comparing the hits from the wire chambers with previously calculated masks. In the PLUTO detector, this is the second step in a two stage trigger (using shift register technique), whereas a large set of random access memories enables the CELLO detector to do the track recognition in one step (via parallel logic). This is the most flexible, but also the most expensive solution.

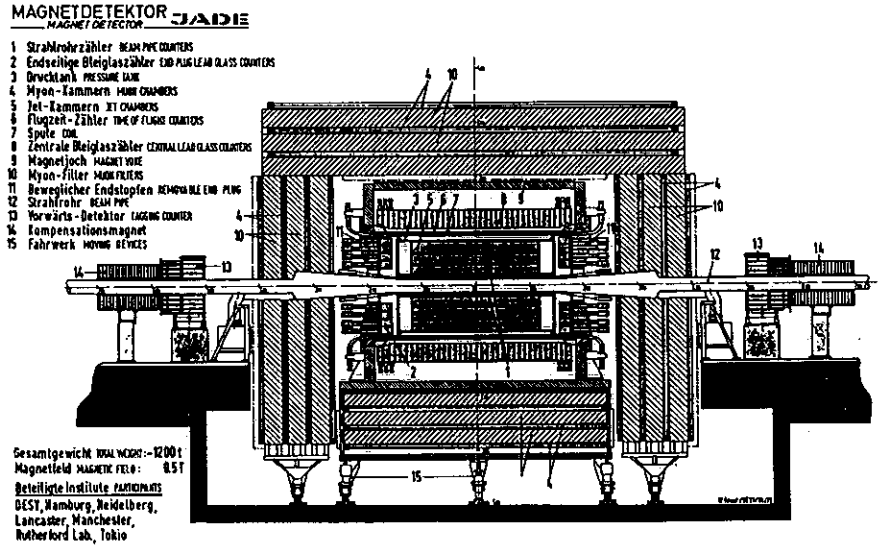

Figure 1.11: *The JADE detector. The lead glass shower counters allow accurate reconstruction of neutral final states.*

The photons coming from $\gamma\gamma$ events have small energies compared with the energies of the beam electrons, i.e. down to 100 MeV or less. Since such low energy photons can produce very short showers, it is of great help to have as little material as possible in front of the shower counters. In particular, it is preferable to have the electromagnetic calorimeter inside the magnet coil. However, the most important quantity for a shower counter in a two photon experiment is the noise equivalent, since it determines down to which energies showers can be triggered and reconstructed. BGO, NaI and lead glass are (in this order) the most suitable materials - if equipped with photo tube read out. This latter requirement may be in conflict with the demand of having the shower counters inside the coil. The Crystal Ball detector (c.f. fig.(1.13)) represents the most radical solution of this problem. It posesses no coil and only a small inner tracking chamber, thus being able to measure photons down into the $1MeV$ range. The lead glass system of the magnetic JADE detector has also proven to

be very suitable, allowing for example to record and reconstruct single η production through the decay channel $\eta \to \gamma\gamma$. For the reconstruction of exclusive final states, the granularity of the shower counters may be more important than the energy resolution since, through kinematic fits, a bad energy measurement (one variable) can be more than compensated by a good position measurement (two variables). For the triggering of entirely neutral final states, a fine segmentation of the calorimeter is important since in general, topological requirements like like acoplanarity cuts have to be implemented on the trigger level to avoid intolerable dead times from "stray" photons.

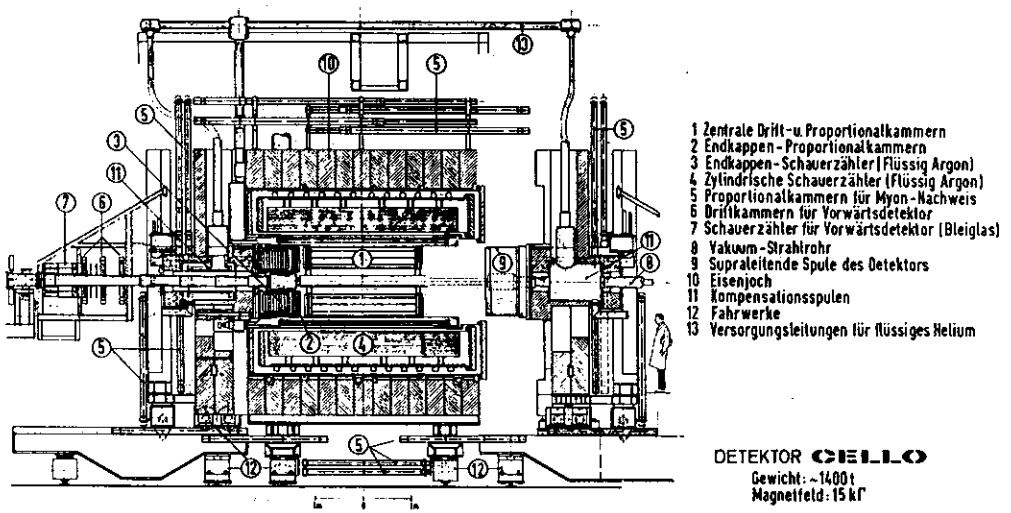

Figure 1.12: *The CELLO detector. The long inner tracking chamber gives a good acceptance over a large solid angle in the c.m.s. of the two photons.*

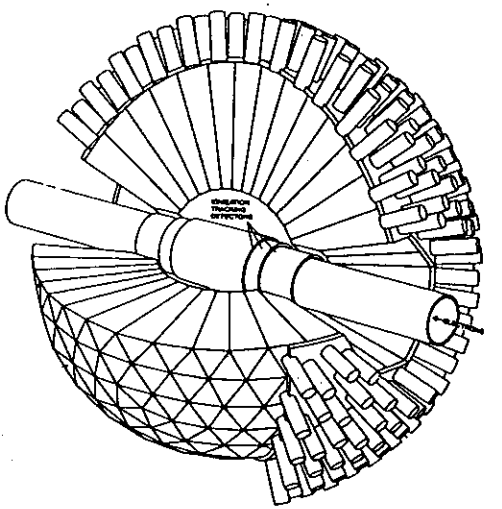

Figure 1.13: *The Crystal Ball detector, a dedicated experiment to accurately measure neutral final states.*

Software

With very few exceptions, two photon events are close to detection thresholds. This implies that the evaluation of the detection efficiency is generally very difficult. Experience shows that reliable measurements can only be obtained if the detector simulation programs are fine tuned with calibration reactions. Frequently used processes are for example

$e^+e^- \to K^0 + X$	*(track momentum resolution)*
$\gamma \to e^+e^-$	*(elm. shower resolution, efficiency)*
$e^+e^- \to e^+e^-e^+e^-$	*(elm. shower resolution, efficiency)*
$\gamma\gamma \to 4\pi^{\pm}$	*(π/e separation)*
$\sigma_{tot}(\gamma\gamma \to \mu^+\mu^-)$	*(track trigger efficiency)*

Very useful checks can be obtained from redundant measurements. Comparisons between dE/dx and TOF or energy momentum comparisons of electron samples provide simple measures of absolute efficiencies. For the intercalibration of various detector components, kinematic fits (see below) may be useful.

A similar degree of accuracy is required for the simulation of the photon photon processes. In practice, this is very difficult because the evaluation of the full $e^+e^- \to e^+e^-X$ cross section can require a seven dimensional integration (in the case of pair creation). The key technique used for such integrations is called *importance sampling*. The idea is to generate points (i.e. particle four momenta) not uniformly, but in a space which is "compressed" in those regions

where the integrand (i.e. $d\sigma/dx$) has maxima. Technically, there are many ways of achieving this. Two methods are described here.

The FORTRAN programs VEGAS by Lepage or BASIS, a further developement by S. Kawabata [20] use an entirely numerical method. The principle is shown in fig.(1.14). In the first step, a large number of points is generated uniformly in all variables. Then, the sum of the values of the integrands in each square (or "hypercube" in more than three dimensions) is compared with the average value. The program then tries to ajust the binning such that the variation of those sums over the entire domain is minimised. The bin size is reduced in regions with strong maxima. In the following steps, equal numbers of points are generated in all hypercubes (on average), followed by readjustment of the bin limits and so on.

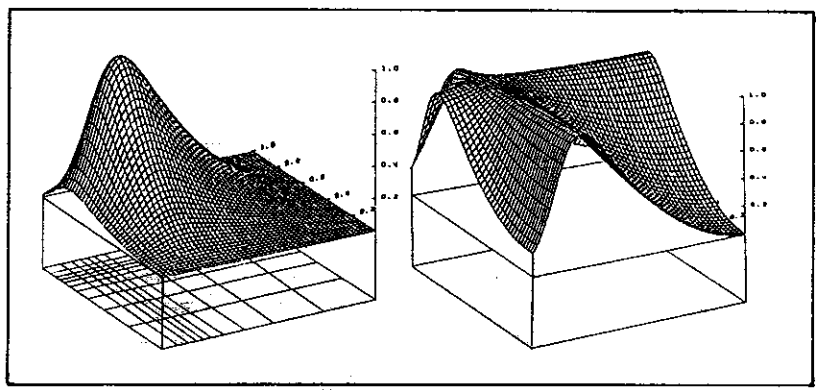

Figure 1.14: *The method of importance sampling. The numerical integration of the function on the left is very efficient, since the function factorises in the variables shown. The function on the right would not be integrated so efficiently.*

The result of such an iteration is a grid which is open in regions where the function is small, and close in regions where the function peaks. For proper normalisation, the values of the integrand have to be multiplied by the bin width (volume of the hypercube). It is easy to realise that the products $f(x) * \Delta x$ have a much smaller relative variance than $f(x)$ itself. This means that after the grid has been calculated, unbiassed event distributions can be obtained with a tolerable efficiency by the old method of first calculating the maximum M of the products $f(x) * \Delta x$ then generating points as above, and then accepting the event if the above product for this event is larger than the maximum value M, multiplied by a uniformly chosen random number between 0 and 1. This method is not a very robust one. In particular, as indicated in fig.(1.14), the algorithm becomes very inefficient if a peak occurs in several dimensions simultaneously. Given that the W and q^2 distributions are very steep in two photon physics, finding the right variables is crucial. In particular, one should aim for a set a variables, in which, by means of the Jacobian, the function becomes as flat a possible. If this cannot be achieved, then the second best choice comes from aiming for approximate factorisation. If $f(x_1, x_2) \simeq g_1(x_1) * g_2(x_2)$, the variables x_1 and x_2 are certainly better suited than for example $y_1 = x_1 + x_2$ and $y_2 = x_2 - x_1$. In the case of two photon physics, the

equivalent photon approximation offers an opportunity to find suitable variables by directly integrating the approximate formula. The third requirement for a good integration variable is that certain fixed values should coincide with the edges of the domain of integration, i.e. phase space limits or cuts. If, for example, a set of no tag events is to be generated, an integration over the scattering angle θ, or a function thereof, is more suitable than an integration over q^2, first of all, because it has no energy dependent onset, and secondly, an upper limit on θ coincides exactly with the measurement condition "no final state electron observed" (*antitag*). A much simpler integration technique can be used in case there is already a set of Monte Carlo events. Given that excellent Monte Carlo generators for the reaction $\gamma\gamma \to \mu^+\mu^-$ exist [19], it seems feasible to obtain Monte Carlo events for other processes through a simple weighting method. Suppose for example a tape with $\gamma\gamma \to \pi^+\pi^-$ events is needed. This can easily be obtained by the following algorithm. First, the maximum of the ratios $R = \frac{d\sigma(e^+e^- \to e^+e^-\pi^+\pi^-)}{d\sigma(e^+e^- \to e^+e^-\mu^+\mu^-)}$ is determined. Then, in a second step, the value of R for each individual event is compared with the product $R_{max} * (uniformly\ generated\ random\ number)$. If this product is smaller than R, the muon pairs are replaced by pion pairs of same $W^2, q_1^2, q_2^2 \ldots$ and written onto tape. Notice that for this technique it is necessary that the variables used for the weighting do *not change* their values. For the above example, the $\gamma\gamma$ c.m.s. variables W, θ, ϕ, q_1^2 and q_2^2 would be an obvious choice, since they are insensitive to the masses of the μ and π. The differential cross sections for $\mu^+\mu^-$ production are given in the appendix.

Kinematic fits are of great help in two photon physics. In addition to the usual advantages (i.e. improvement of mass resolution, background reduction, test of calibration) fits in $\gamma\gamma$ physics lead to a considerable improvement in the interpretability of the experimental results. By restricting q_1^2, q_2^2 to very small values, kinematic fits allow the accumulation of a data sample of almost real photons. The number of coupling constants determining the interaction of real photons is generally smaller than for virtual photons. Real photon collisions are thus easier to interpret. Also, the restriction to tiny q^2 values reduces the errors coming from form factor uncertainties to negligible values.

At first glance, kinematic fits seem not to be feasible for most of the $\gamma\gamma$ events. In no tag samples, six unmeasured lepton momentum components seem to overrule the four energy momentum constraints. However, the kinematics of two photon events, together with the steep q^2 dependence of the flux, leads to a solution of this problem. The latter implies that events with both photons off shell are very rare. In the more frequent case where one of the photons is almost real, ($q_2^2 \simeq 0$) the laboratory transverse momentum of the hadronic final state H can be written as

$$p_t^2(H) \simeq -q_1^2 \left\{ 1 - \frac{1}{2}\left(\frac{\omega_1}{E_1'} - \frac{\omega_2}{E_2'} \right) - \frac{E_H}{2E_b} \right\} \simeq -q_1^2$$

Thus if the hadrons are produced with modest rapidity,[1] restricting the transverse momentum of the hadrons means restricting the invariant masses of the photons. Technically, this is achieved by a little trick. It is simply pretended that the directions of the outgoing electrons are very well measured to be scattered at 0 degrees ($\pm O(1mrad)$). By this method, the energies of the final state electrons remain the only unmeasured variables. The result is a two constraint fit in which high q^2 events appear with a low χ^2 probability. Cutting on the χ^2 probability thus removes high q^2 events, together with the background from incompletely reconstructed events.

[1] large rapidity events tend to have a vanishingly small chance of detection.

Pseudoscalar Production

Introduction

The neutral members of the 0^- nonet are the $\pi^0(135\,MeV)$, $\eta(549)$, and the $\eta'(958)$. They are all very narrow resonances. In the static quark model, the observed states may be close to the pure singlet and octet states.

$$\begin{aligned} \pi^0 &= \frac{1}{\sqrt{2}}(u\bar{u} - d\bar{d}) \\ \eta \approx \eta_8 &= \frac{1}{\sqrt{6}}(u\bar{u} + d\bar{d} - 2s\bar{s}) \\ \eta' \approx \eta_1 &= \frac{1}{\sqrt{3}}(u\bar{u} + d\bar{d} - s\bar{s}) \end{aligned} \qquad (2.1.1)$$

Although the members of the pseudoscalar nonet have been known for a long time, the 0^- nonet has some interesting and to this day not understood features.

The masses for example nearly span an order of magnitude. So far, this mass splitting is only understood on rather weak phenomenological grounds. Moreover, the ways the masses are explained are highly correlated with the assumed value for the singlet octet mixing angle. Quadratic or linear mass formulae lead to mixing angles differing by as much as a factor of two. One aim of two photon experiments is therefore to test whether $SU(3)_{Fl}$ is a good symmetry for the radiative widths of the nonet members. Only if this is the case, the introduction of a mixing angle between the states η_1 and η_8 is meaningful. If $SU(3)_{Fl}$ turns out to be fulfilled, two photon experiments can determine this mixing angle and thus provide a necessary input parameter for mass splitting calculations.

The spatial structure of particles has been explored in the past mainly by single current reactions, e.g. by measurents of charge form factors. The data have been interpreted in the framework of vector meson dominance, ground state pictures and by perturbative QCD. By using the additional freedom of varying q_1^2 and q_2^2 independently, two photon physics has the opportunity to help distinguishing the various approaches. Double tag measurements may therefore be particularly fruitful in the future.

The coupling of a neutral pseudoscalar meson to two photons proceeds through a single amplitude and hence, there is only *one* form factor $F(q_1^2, q_2^2)$:

$$T_{\mu\nu} = ie_{\mu\nu\alpha\beta}q_1^\alpha q_2^\beta F(q_1^2, q_2^2) \qquad (2.1.2)$$

This form factor has the dimension of a length. A direct consequence of the form of the amplitude is that a 0^- state cannot couple to longitudinally polarised photons. The only non zero terms entering the full $e^+e^- \to e^+e^-0^-$ formula are

$$\sigma_{TT} = -\frac{1}{2}\tau_{TT} = \frac{1}{4}F^2(q_1^2, q_2^2)\frac{M^2\sqrt{X}}{W}\frac{\Gamma}{(W^2 - M^2)^2 + \Gamma^2M^2}$$

Notice the strong mass dependence which is also present in the $\gamma\gamma$ partial decay width:

$$\Gamma_{\gamma\gamma} = \frac{M_R^3F^2(0,0)}{64\pi} \qquad (2.1.4)$$

This tends to counteract the rapid variation with W of the photon flux at storage rings. In fact, measurements have shown that the cross sections for $e^+e^- \to e^+e^-$"0^-" are of similar magnitude for the three nonet members.

Measurements of $\Gamma_{\gamma\gamma}(\eta')$

The η' is the heaviest of the three neutral nonet members. Its decay products have thus comparatively large momenta. This means that the η' is the most easily seen pseudoscalar, and it has been observed in a large number of experiments. In most cases, it has been identified through its decay into $\rho^0\gamma$ (c.f. fig.(2.1.1). The published results can be seen in table (2.1.1).

$\Gamma_{\gamma\gamma}(keV)$	*Decay*	*Experiment*	*Ref.*
$5.8 \pm 1.1(\pm 1.2)$	$\rho^0\gamma$	*Mark II*	21
$5.0 \pm 0.5(\pm 0.9)$	$\rho^0\gamma$	*JADE*	22
$6.2 \pm 1.1(\pm 0.8)$	$\rho^0\gamma$	*CELLO*	23
$3.8 \pm 0.3(\pm 0.4)$	$\rho^0\gamma$	*PLUTO*	24
$5.1 \pm 0.4(\pm 0.7)$	$\rho^0\gamma$	*TASSO*	25
$3.7 \pm 1.0(\pm \ldots)$	$\eta\pi^+\pi^-$	*Mark II(prelim.)*	26
$4.2 \pm 0.3(\pm 0.6)$	$\rho^0\gamma$	*PEP49(prelim.)*	27
$4.0 \pm 1.0(\pm 0.4)$	$\gamma\gamma$	*JADE*	30

Table 2.1.1: *Measurements of* $\Gamma_{\gamma\gamma}(\eta')$

There is an indication of decrease of the average value as a function of time. The most probable reason is that the first three measurements were based on too simple η' decay models, i.e. the spin barrier factors of this $L = 1$ decay were not taken into account. This interpretation of the discrepancy is supported by the fact that both, the Mark II $\eta\pi^+\pi^-$ measurement and the JADE $\gamma\gamma$ measurement are in good agreement with the recent $\rho^0\gamma$ measurements. On the other hand, TASSO and CELLO have claimed that their result is not sensitive to the details of the η' decay [98]. At present, it seems not meaningful to evaluate a "world average" including all published values. All one can say is that the most recent and precise measurements point towards a radiative decay width of roughly 4 keV.

The correct decay matrix element for the decay $\eta' \to \pi^+\pi^-\gamma$ has a very similar form to eq.(2.1.2). Calling k_1 and k_2 the four momenta of π^+ and π^-, $P_\rho = k_1 - k_2$ the momentum of the ρ^0 and representing the outgoing photon by Q and ϵ^*, the matrix element of the η' decay can be written as

$$M(\eta' \to \pi^+\pi^-\gamma) = F_{\eta'\rho\gamma}F_{\rho\pi\pi}e_{\alpha\beta\mu\nu}\epsilon^{*\alpha}Q^\mu P_\rho^\nu \frac{m_\rho^{-2}P_\rho^\beta P_\rho^\gamma - g^{\beta\gamma}}{m_\rho^2 - P_\rho^2 + im_\rho\Gamma_\rho}(k_1 - k_2)_\gamma \qquad (2.1.5)$$

where $F_{\eta'\rho\gamma}$ and $F_{\rho\pi\pi}$ are the couplings[1] (c.f. appendix D). The "simplest" form of the decay distributions is obtained, if one uses phase space recurrence relations, giving

$$\frac{d^2\Gamma}{dm_{\pi\pi}d\Omega^*} = \frac{2F^2_{\rho\pi\pi}F^2_{\eta'\rho\gamma}}{(8\pi)^4 m^3_{\eta'}}\left(\frac{(m^2_{\eta'}-m^2_{\pi\pi})^3(m^2_{\pi\pi}-4m^2_\pi)^{3/2}}{(m^2_\rho-m^2_{\pi\pi})^2+\Gamma^2 m^2_\rho}\right)sin^2(\theta^*) \qquad (2.1.6)$$

where θ^* is the angle between the pion and the photon in the ρ^0 center of mass system and $m_{\pi\pi}$ is the invariant mass of the $\pi^+\pi^-$ system. Notice the complete factorisation into mass- and angle dependent terms. A similar expression is obtained if one uses the recipes given by Jackson [28].

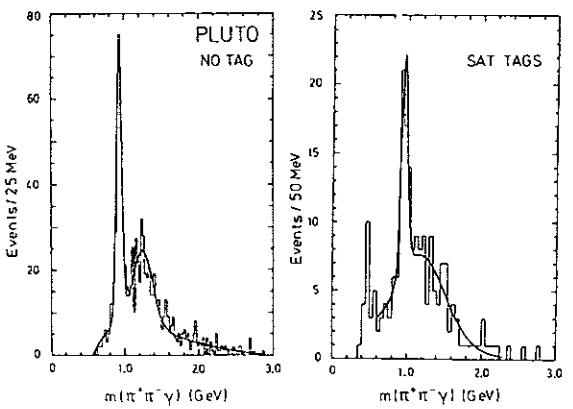

Figure 2.1.1: *These two mass spectra are the basis of an accurate determination of the radiative width of the η' and of the first measurement of a form factor in two photon physics.*

In order to settle the question of the radiative width of the η' meson, it would be very nice to see more measurements of η' production in decay modes different from $\rho^0\gamma$. The elastic reaction $\gamma\gamma \to \gamma\gamma$ seems to be the most promising one, since the Monte Carlo simulation of the two body decay of a spinless particle involving narrow resonances only requires essentially no assumptions on the decay dynamics.

Measurements of $\Gamma_{\gamma\gamma}(\eta)$

The detection of an exclusive η signal is rather difficult, not only because of the small invariant mass, but also since the η photoproduction cross section is rather high. So far, the η has only been observed in the decay mode $\eta \to \gamma\gamma$. In this channel, a "beam gas" subtraction is difficult, since in an entirely neutral final state, the interaction point is not well determined. Therefore, such analyses require single beam running. Nevertheless, three

[1] Notice that neither of these couplings are constant.

experimental groups succeeded in obtaining an exclusive η signal in quasi elastic photon photon interactions.

$\Gamma_{\gamma\gamma}(keV)$	*Decay*	*Experiment*	*Ref.*
$0.56 \pm 0.12(\pm 0.09)$	$\gamma\gamma$	*Crystal Ball*	[29]
$0.53 \pm 0.04(\pm 0.04)$	$\gamma\gamma$	*JADE*	[30]
$0.61 \pm 0.13(\pm 0.12)$	$\gamma\gamma$	*PEP49(prelim.)*	[26]
$0.58 \pm 0.04(\pm 0.08)$	$\gamma\gamma$	*Crystal Ball(prelim.)*	[112]

Table 2.1.2: *Measurements of* $\Gamma_{\gamma\gamma}(\eta)$

The three experiments are very well consistent with each other and the JADE result (c.f. fig.2.1.2)) has an impressively small systematic error. Therefore, we have reason to have confidence in those measurements.

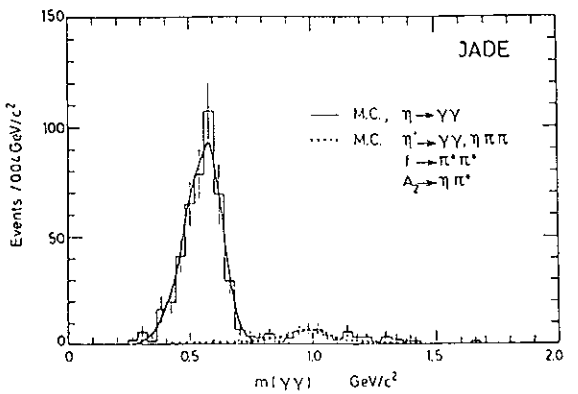

Figure 2.1.2: *The $\gamma\gamma$ invariant mass spectrum from the JADE detector gave a precise value for $\Gamma_{\gamma\gamma}(\eta)$.*

The photon photon results have resolved an old ambiguity[1] between two experiments based on the Primakov effect:

$\Gamma_{\gamma\gamma}(keV)$	*Year*	*Ref.*
1.00 ± 0.22	1967	[31]
0.342 ± 0.046	1974	[32]

It seems clear now that the true radiative width lies between the values given by these two experiments.

[1] Although the quoted widths are mutually inconsistent, the *data* of the two Primakov experiments never were. The 1967 experiment had not been accurate enough to discriminate between two possible solutions, one being consistent with the 1974 experiment, the other one being published. For this reason, the 1967 result was no longer used after 1974.

Measurements of $\Gamma_{\gamma\gamma}(\pi^0)$

The π^0 was the first meson predicted to be seen in the two photon process at storage rings (Low 1960 [33]) and the last member of the pseudoscalar nonet to be seen (Crystal Ball 1984 [34]) The requirements for a detector to measure single π^0 formation are very strong because of the small mass of the π^0 meson. If it is produced "at rest" in the laboratory frame, the two photons coming from its decay are too low in energy for a scintillator sandwich or a liquid argon calorimeter. If, on the other hand, the π^0 has a large boost -and this is the most frequent case- the finite energy resolution of the detector makes it very hard to reconstruct the invariant mass. In view of these facts, the Crystal Ball result is impressive:

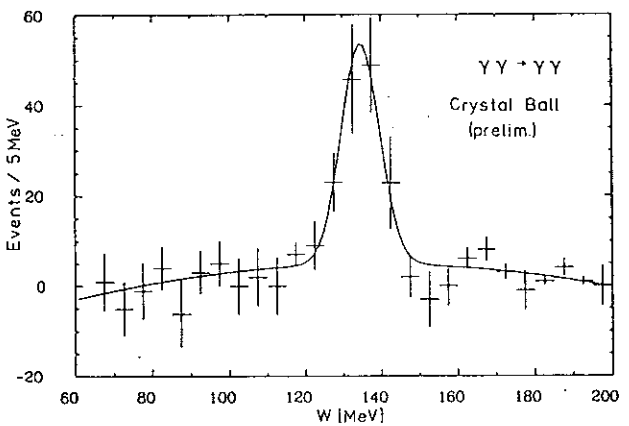

Figure 2.1.3: *The first and only observation of single π^0 production in two photon collisions (Crystal Ball, preliminary).*

$$\Gamma_{\gamma\gamma}(\pi^0) = 7 \pm 1 \pm 3\, eV \qquad Crystal\ Ball(prelim.)$$

The spectrum used for this measurement is shown in fig.(2.1.3). However, this result cannot compete with a recent direct measurement of the π^0 life time which yields [35]

$$\Gamma_{\gamma\gamma}(\pi^0) = \frac{1}{\tau} B(\pi^0 \to \gamma\gamma) = 7.25 \pm 0.18 \pm 0.11\, eV \quad NA30\,(CERN)$$

It seems unlikely that two photon experiments will ever reach this precision. On the other hand, the known techniques for direct life time measurements fail for widths in the *keV* range.

The $SU(3)_{Fl}$ Relations for Pseudoscalar Mesons

Already more than ten years ago, it was noticed that the ratios of the two photon widths can be used to measure the quark charges, provided that the masses have no influence on the quark wave functions ($\Psi_{Flavour}$). If it is assumed that the photons couple directly to the

quarks, then $F_{0^-\gamma\gamma} \sim Q^2 \Psi_{FLAVOUR}$, where Q^2 is the eigenvalue of the $(charge)^2$ operator. According to eq.(2.2.1), we then have the prediction

$$F_{\pi^0\gamma\gamma}/F_{\eta 8\gamma\gamma}/F_{\eta 1\gamma\gamma} = \frac{1}{3\sqrt{2}}/\frac{1}{3\sqrt{6}}/\frac{2}{3\sqrt{3}} \tag{2.1.7}$$

In general, one has to assume that the observed mesons are linear combinations of the singlet and the octet states.

$$\begin{aligned} \eta &= cos(\theta)\eta_8 - sin(\theta)\eta_1 \\ \eta' &= cos(\theta)\eta_1 + sin(\theta)\eta_8. \end{aligned} \tag{2.1.8}$$

This relation defines the mixing angle θ. Using eq.(2.1.4), the following relations between the radiative widths of the nonet members are obtained:

$$\begin{aligned} \Gamma_{\gamma\gamma}(\eta) &= \Gamma_{\gamma\gamma}(\pi^0)\frac{m_\eta^3}{3m_{\pi^0}^3}(\sqrt{8}sin(\theta) - cos(\theta))^2 \\ \Gamma_{\gamma\gamma}(\eta') &= \Gamma_{\gamma\gamma}(\pi^0)\frac{m_{\eta'}^3}{3m_{\pi^0}^3}(\sqrt{8}cos(\theta) + sin(\theta))^2 \end{aligned} \tag{2.1.9}$$

Furthermore, the validity of the above assumptions can be tested in a manner independent of the mixing angle, since eq.(2.1.9) also implies the *sum rule*

$$\frac{\Gamma_{\gamma\gamma}(\eta')}{m_{\eta'}^3} - \frac{\Gamma_{\gamma\gamma}(\eta)}{m_\eta^3} = 3\frac{\Gamma_{\gamma\gamma}(\pi^0)}{m_{\pi^0}^3} \tag{2.1.10}$$

It is interesting to notice that eq.(2.1.10) can also be obtained in the context of vector meson dominance. The assumptions then are that the overlap integrals $< vector|Q|0^- >$ are mass independent and that the γ to vector meson coupling constants are just as given in the Van Royen scheme [36]. Therefore, the above sum rule tests the validity of $SU(3)_{Fl}$ irrespective of the mechanism contributing to the decay.

The Experimental Status of $SU(3)_{Fl}$ for Pseudoscalar Mesons

The history of experimental tests of $SU(3)_{Fl}$ is both entertaining and admonitory:

In 1983, all two photon data agreed with the above nonet symmetry relations. Despite some experimental uncertainties,[1] the measurements even seemed to agree with the mixing angle obtained from the Gell-Mann / Okubo mass formula [37]:

$$tan^2\theta = \frac{4m_K^2 - m_\pi^2 - 3m_\eta^2}{3m_{\eta'}^2 - 4m_K^2 - m_\pi^2} \to \theta_{mass} = -11.1^0 = 0.2^0 \tag{2.1.11}$$

In 1984, the PLUTO and Mark II collaborations measured values of the radiative width of the η' below 4 keV. At this time a value of about 6.7 keV was expected from the radiative η width and π^0 life time. This not only led to controversies between the experimental groups,

[1] A careful analysis of the state of $SU(3)_{Fl}$ in 1983 can be found in ref. [61].

but also to an increase of theoretical activity. One extreme point of view was put forward by M. Chanowitz, who stated at the Brighton conference [38]: "We finally have to conclude that we cannot measure quark charges in two photon collisions." In different terms this means that $SU(3)_{Fl}$ is so badly broken for the masses that it would be naive to assume exact $SU(3)_{Fl}$ for the radiative widths. A different extreme conclusion was that the "too low" value of the radiative η' width was evidence for a gluonic component in the η' and thus provided qualitative evidence for QCD. An extensive discussion of possible gluonium admixtures, including further references, can be found in ref. [110].

In 1985, the situation reversed again. The JADE collaboration published a precise measurement of the radiative width of the η meson, leading to a considerable upward shift in the world average. Cronin et al gave a new, precise value for the π^0 life time, which is smaller than the Particle Data Group value. Together, these changes restore 0^- nonet symmetry for the radiative widths. However, the mixing angle is now $-18.4^\circ \pm 2.0^\circ$, in contradiction not only to the mass formula, but also in contradiction with old average values.

It must be stressed that there have never been inconsistencies between two photon measurements at the $\geq 2\sigma$ level. The main source of the inconsistency between the experimentally determined mixing angles is mainly due to the tiny error quoted by the 1974 Primakov effect experiment, which now appears to be wrong.

Comparison of the Measurements with Models

Successful theoretical interpretations of the radiative width of the π^0 have been given in the context of VDM and in the coloured quark model together with PCAC:[1]

$\Gamma_{\gamma\gamma}(\pi^0)/eV$	*hypothesis*	*year*	*ref*
7.4	VDM	1962	[4]
7.6	$PCAC (i.e. q\bar{q})$	1969	[39, 40]

Both values are in reasonable agreement with experiment. However, the concepts behind these calculations are completely different. Nevertheless, a fully convincing interpretation of the π^0 life time is still pending, since PCAC only holds for massless pions, and the systematic error on the VDM approach is unknown.

Since these early publications, large efforts have been made to calculate the radiative widths of the other neutral pseudo scalar mesons (c.f. table(2.1.3)). In this table, GMO stands for Gell-Mann/Okubo's mass formula, i.e. a mixing angle of -11° is assumed. As we have seen, this mixing angle is inconsistent with the measured radiative widths. However, it is interesting to notice that such a discrepancy was already predicted in 1969, when Matsuda and Oneda [41] introduced symmetry breaking effects into their calculation. A discussion of such effects, based also on data from other processes can be found in ref. [46].

Given that the data suggest the validity of $SU(3)_{Fl}$ whereas models based on explicit dynamical assumptions are not yet able to predict the absolute values of the radiative widths correctly, we are led to conclude that we see a symmetry at work, but we do not yet understand its dynamic origin. Let us thus reverse the argument and impose the validity of $SU(3)_{Fl}$ onto

[1] The first calculation of the π^0 life time was carried out by Steinberger in 1949 [117].

two extreme interpretations of two photon interactions.

$\Gamma_{\gamma\gamma}(\pi^0)/eV$	$\Gamma_{\gamma\gamma}(\eta)/keV$	$\Gamma_{\gamma\gamma}(\eta')/keV$	*input*	*ref.*
input	$0.4 - 0.6$	~ 5	GMO, *broken* $SU(3)$	[41]
input	$0.39(0.5)$	~ 6	GMO, (*broken*) $SU(3)$	[42]
13	$1.7 - 1.8$	$2.5 - 3.8$	$GMO, VDM\ SU(3)$, *h.o.*	[43]
input	0.38 ± 0.04	6.3 ± 0.7	GMO, VDM	[44]
9	0.43	7.3	$VDM \equiv QPM$	[45]
input	0.54 ± 0.05	1.16 ± 0.7	GMO, *broken* $SU(3)$	[46]
6.7	0.25	1.7	$conf.pot + QCD$	[47]

Table 2.1.3: *Predictions for the radiative widths of pseudoscalar mesons*

Let us estimate flavour symmetry breaking effects by a simple minded application of methods used in potential scattering theory. Following Blatt and Weisskopf [48], we assume that the matrix element for the two photon transition is modified[1], by an overlap integral characterised by an interaction range r and the c.m.s. photon momenta $M/2$:

$$\Gamma_{\gamma\gamma}(finite\ size\ interaction\ volume) = \Gamma_{\gamma\gamma}(naive\ SU(3)) \frac{1}{1 - (\frac{M}{2} r)^2} \qquad (2.1.12)$$

Since the data indicate the validity of the naive $SU(3)_{Fl}$ relation to within 10 %, we have to conclude that the interaction takes place within a volume of $r \lesssim 0.13\, fm$ for the η'. This value is surprisingly small, given that in hadronic decays of resonances, a scale of roughly $1\, fm$ has repeatedly been observed to govern deviations from $L = 1$ Breit Wigner amplitudes. However, it may be that a factor like the one given in eq.(2.1.12) is present, but the decay dynamics is such that the product $M \cdot r$ is roughly constant.

In the framework of VDM, the discrepancy between the mixing angle obtained from the Gell-Mann/Okubo mass formula and the one obtained from measurements of radiative widths is difficult to interpret. By introducing a limited range for the VVP transition, it is possible, to reproduce the observed ratio of $\Gamma_{\gamma\gamma}(\eta')/\Gamma_{\gamma\gamma}(\pi^0)$, keeping a mixing angle of -11°, however at the price of getting the completely wrong prediction of $\Gamma_{\gamma\gamma} \simeq 0.34\, keV$ for the radiative width of the η. At the moment, is seems that we have to live with this discrepancy, since we have no handle to decide between the validity of VDM or GMO.

If we interpret mesons as bound states of two massive (i.e. $m_q \simeq \frac{1}{2}M$) quarks, the radiative widths can be calculated according to the positronium decay formula $\Gamma_{\gamma\gamma}(M) \sim |\Psi(0)|^2/M^2$ where $\Psi(r)$ is the radial wave function. Since the data indicate $\Gamma_{\gamma\gamma}(M) \sim M^3$, a mass dependence of about $\Psi(0)^2 \sim M^5$ is a required ingredient for such models. For a binding potential of the form $V \sim r^\nu$, Quigg and Rosner [49] calculated the mass dependence of the wave function at the origin to be $|\Psi(0)|^2 \sim M^{3/(2+\nu)}$. Hence the potential should be

[1] This modification of the $SU(3)$ relations may be surprising. However, it must be stressed that the introduction of damping terms at some level is a *necessity* for the VDM hypothesis. If such terms were not included, amplitudes corresponding to large L transitions, like $\gamma\gamma \to h(2040)$, would have amplitudes *growing* monotonically with q^2.

$V \sim \frac{1}{r^{7/3}}$ to be consistent with the data. This result does not look very promising. However, it is not a real problem for the quark parton model. To illustrate why difficulties in describing the light mesons as bound states of massive quarks are to be expected, let us try a little exercise; let us "put" two non relativistic quarks into a cube of volume $(a = 1fm)^3$. Each of them will then have a ground state momentum of $< p >= \sqrt{3}\pi/a = 600\,MeV$. If we compare this number with the mass of the pion, we have no choice but to conclude that the non relativistic Ansatz is so problematical for the light mesons that discrepancies with the data are no surprise. This of course also implies that the discrepancy between the data and non relativistic potential models does *not* mean that those models are altogether wrong. It just means that such models should only be applied for heavy systems, i.e. from charmonium onwards.

If we want to understand the radiative decays of the pseudoscalar mesons as photon quark interactions, we need relativistic calculations. Unfortunately, the fully relativistic $PCAC$ approach neglects the mass of the π^0. The data however suggest its validity even for the η' - but what does this mean? In 1979, Philippov [50] discussed deviations from exact $SU(3)_{FI}$ in the framework of QCD with additional phenomenological input. His calculation, which describes the masses of the pseudoscalar mesons well, yields effective mixing angles of

$$\theta_\eta = -17.67^\circ \pm 0.54^\circ \qquad \theta_{\eta'} = -20.8^\circ \pm 0.14^\circ$$

Together with the measured width of the π^0 meson, these angles correspond to values of $0.53\,keV$ and $4.6\,keV$ for the radiative widths of the η and η' meson respectively. These values are in good agreement with the measured values. Although radiative widths cannot be rigorously calculated in QCD, it thus appears that QCD points into the right direction.

Observation of η_c Production

In 1985, the PLUTO Collaboration [51] found an η_c signal (fig.(2.1.4)) of 10 events in the reaction

$$\gamma\gamma \rightarrow K_s^0 K^\pm \pi^\mp$$

from an integrated luminosity of $42\,pb^{-1}$ only. This experimental achievement is a proof of the statement that in many cases, refined analysis techniques can overcome apparent statistical limitations. In this particular case, it was the excellent K^0 identification by means of secondary vertex reconstruction which enabled the measurement.

The calculation of the radiative widths from a $K\bar{K}\pi$ signal is difficult, since little is known experimentally about the dynamics of the η_c decay. A simple three body phase space decay[1] may not be a good enough description, since preliminary spectra obtained by the MarkIII Collaboration [115] from J/ψ decays indicate a sizeable contribution of the chain decay

$$\eta_c \rightarrow K^*(1430)\bar{K} \rightarrow (K\pi)\bar{K}$$

The matrix element of such a decay chain involves two $L = 2$ couplings and, using the

[1] Such simple decays have been assumed in all previous experimental upper limits on η_c production. These limits should therefore be treated with some caution.

formulae given in the appendix, can be written as

$$M(\eta_c \rightarrow K\bar{K}\pi) = F_{\eta_c K^*\pi} F_{K^*K\pi} \left\{ \left(\frac{1}{k_{12}^2}(k_{12}\cdot k_{12-3})(k_{12}\cdot k_{1-2}) - (k_{12-3}\cdot k_{1-2}) \right)^2 \right.$$
$$\left. - \frac{1}{3}\left(\frac{1}{k_{12}^2}(k_{12}\cdot k_{12-3})^2 - k_{12-3}^2 \right)\left(\frac{1}{k_{12}^2}(k_{12}\cdot k_{1-2})^2 - k_{1-2}^2 \right) \right\} \frac{1}{k_{12}^2 - M_{K^*}^2 + iM_{K^*}\Gamma_{K^*}} \tag{2.1.13}$$

In this formula, k_1 is the momentum of the kaon coming from the K^* decay, k_2 the pion momentum, and k_3 is the momentum of the kaon produced at the primary η_c vertex. The indices are short hand notations of differences and sums, for example is $k_{12-3} \equiv k_1 + k_2 - k_3$.

Since the K^* is an iso spinor, the $K^+K^0\pi^-$ decay can proceed either through $\bar{K}^{*0}$ or K^{*-}. Because of isospin invariance, the interference is constructive, i.e.

$$M(\eta_c \rightarrow K^+K^0\pi^-) = M(\eta_c \rightarrow (K^{*0} \rightarrow K^+\pi^-)K^0) + M(\eta_c \rightarrow (K^{*-} \rightarrow K^0\pi^-)K^+)$$

and the amplitudes are equal in magnitude.[1] The corresponding Dalitz plot distribution is so beautiful that is has been put onto the front page.

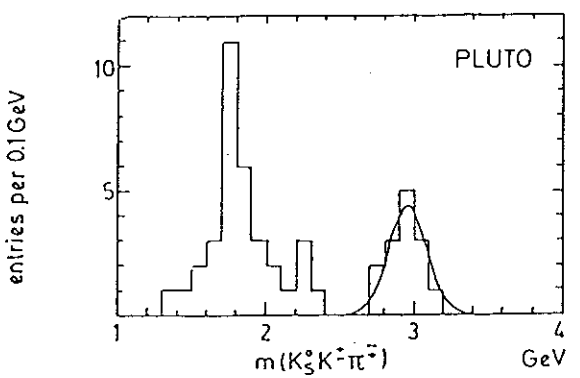

Figure 2.1.4: *The first evidence for η_c formation in two photon interactions.*

In the PLUTO analysis, it turned out that because of the fact that the $K\bar{K}\pi$ final state was detected far above the trigger thresholds, the final result was quite independent of the assumed decay dynamics. The systematic error on the experimental result

$$\Gamma_{\gamma\gamma}(\eta_c) \cdot B(\eta_c \rightarrow K_s^0 K^\pm \pi^\mp) = 0.5^{+0.2}_{-0.15} \pm 0.1 keV \qquad PLUTO$$

includes the uncertainty on the fraction of intermediate $K^*(1430)$ production. Since the branching ratios of the η_c are still subject to considerable experimental uncertainties (c.f. ref. [51]), we are not yet in the position to turn this measurement into an accurate number for the radiative width of the η_c. For the same reason, a direct comparison with most of the

[1] By simply adding the two amplitudes, we have neglected final state interactions.

previously calculated upper limits has to be postponed to a time when the decay rates of the η_c are accurately measured.

$\Gamma_{\gamma\gamma}(\eta_c)B(\eta_c \to X)$	$Cl.$	$Channel X$	$Experiment$	$Ref.$
$< 4.2\,keV$	95%	$\pi^+\pi^-\pi^0\pi^0$	$JADE$	[61]
$< 2.3\,keV$	95%	$\pi^+\pi^-$	$JADE$	[61]
$< 0.32\,keV$	95%	$p\bar{p}$	$TASSO$	[104]
$< 27\,keV$	95%	$K\overline{K}\pi^0$	$TASSO$	[61]
$< 0.7\,keV$	95%	$2\pi^+2\pi^-$	$TASSO$	[61]
$< 4.4\,keV$	95%	$K\overline{K}\pi$	$TASSO$	[114]

Table 2.1.4: *Upper limits for η_c production*

Notice that the TASSO Collaboration assumes $B(\eta_c \to K\overline{K}\pi) = 3B(\eta_c \to K^0_s K^\pm\pi^\mp)$. The directly comparable upper limits by TASSO are thus consistent with the PLUTO result.

The q^2 Dependence of Pseudoscalar Production

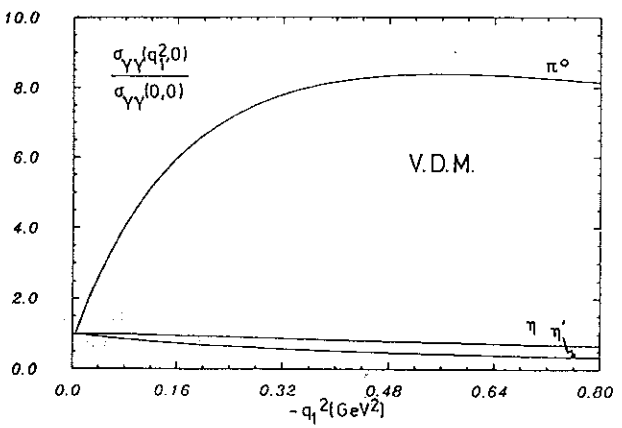

Figure 2.1.5: *The VDM prediction for the off shell cross section for the production of pseudoscalar mesons. One of the photons is real (see text).*

The antisymmetric coupling for $\gamma\gamma \to 0^-$ has drastic implications for the q^2 evolution of the cross section. The $\sqrt{X}$ term in the cross section should be understood as $X/\sqrt{X}$ where the denominator comes from the flux factor and the numerator is the same factor which gives rise to the $(|\vec{k}^*|/|\vec{k}^*_0|)^{2L}$ spin barrier factor in hadronic decays. However, in contrast to these decay factor, whose range of accessibility is limited by the total width Γ, the "initial state barrier" $\sqrt{X}$ can take any value. For single tag events, eq.(2.1.3) implies that at resonance mass, $\sigma(q_1^2,0) \sim F^2(q_1^2,0)\cdot(1-\frac{q_1^2}{M^2})$. Thus, apart from form factor effects, the cross section grows

with q_1^2 ! It is interesting to notice that the scale of this "natural" grows of the cross section is set by the mass of the meson - quite in contrast to form factor effects which, to the extent that they have been measured so far, seem to be governed by the ρ^0 meson mass squared. This scale difference implies a non trivial shape of the off shell cross section, particularly for the light mesons. If, for example, it is assumed that $F(q_1^2,0) = (1-q_1^2/m_\rho^2)^{-1}$, the cross sections for π^0 η and η' production should evolve as shown in fig.(2.1.5). Notice that a simple ρ^0 pole form factor leads to a quite pronounced maximum of the π^0 production cross section at finite q^2.

A Measurement of the η' Form Factor

The "natural" growth of the basic amplitude helps experimental determinations of the cross section by increasing the cross section. The PLUTO collaboration [24] found an η' signal in the reaction $e^+e^- \to e^\pm(seen)e^\mp(not\ seen)\pi^+\pi^-\gamma$ in the region $0.2 < |q_1^2| < 1.0\,GeV^2$. A sample of 35 ± 9 events was obtained from an integrated luminosity of $25\ pb^{-1}$ at PETRA and turned into the form factor measurement shown in fig.(2.1.6). At the admittedly poor level of statistics, a simple ρ^0 pole form factor seems to describe the data well.

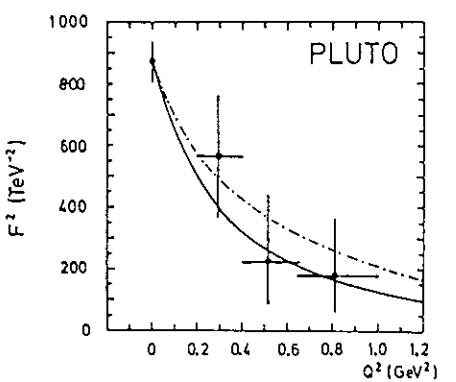

Figure 2.1.6: *The first measurement of the $\eta'\gamma\gamma$ transition form factor. The solid line is a simple ρ^0 pole. The dashed line is the prediction of the finite size model with $r = 1fm$.*

But there is also an indication of a deviation from VDM [24]: "*Using the ρ^0 pole for both photons and taking our no tag measurement for normalisation, we expect 0.8 ± 0.2 events in the sample with both electrons in the tagging range. In the data, we find four double tagged η' events with an estimated background of less than 0.3 events.*"

Predictions for Pseudoscalar Form Factors

A simple vector meson dominance prediction for the q_1^2, q_2^2 dependence of the form factor

is:

$$F_{0^-\gamma\gamma} = const.\left(F^2_{\rho\gamma}\frac{<0^-|\rho\rho>}{(1-q_1^2/m_\rho^2)(1-q_2^2/m_\rho^2)} + F_{\rho\gamma}F_{\omega\gamma}\frac{<0^-|\rho\omega>}{(1-q_1^2/m_\rho^2)(1-q_2^2/m_\omega^2)} + ...\right)$$
$$\simeq \frac{F(0,0)}{(1-q_1^2/m_\rho^2)(1-q_2^2/m_\rho^2)} \qquad (2.1.14)$$

As we have seen, this formula is consistent with the single tag data. We could thus stop here and declare VDM to be "in good shape". However, VDM is not the only possible explanation of the data.

For the sake of the argument, let us try an alternative interpretation of the form factor. Let us assume that what has been observed in the data is a reflection of the fact that the interactions which are responsible for meson formation in two photon recations take place in a finite size volume. This assumption leads to a substantially different prediction for double tag events than VDM. Whereas in the context of VDM, the form factor factorises in good approximation into $F(q_1^2, q_2^2) = F(q_1^2) \cdot F(q_2^2)$, the interpretation of the form factor as a measure of the spatial extent may give a non factorising prediction. If we interpret the transition form factor as a finite size effect, it seems natural to assume that the *wave lengths* of the photons should be the significant variables,[1] rather than q_1^2 and q_2^2. Since these are always equal in the meson c.m.s, this particular interpretation of the form factor can be formulated as a *scaling law*:

$$F(q_1^2, q_2^2) = F\left(\frac{X}{W^2}\right) = F\left(\frac{(q_1\cdot q_2)^2 - q_1^2 q_2^2}{W^2}\right) \qquad (2.1.15)$$

and hence, the double tag cross section is entirely determined by the single tag cross section. It would be a particularly interesting situation, if eq.(2.1.14) described well single tag data and eq.(2.1.15) was fulfilled simultaneously. This could be taken as an indication of VDM being a suitable parametrisation of finite size effects. On the other hand, an experimental observation of approximate factorisation of the form factor would point towards a literal interpretation of vector meson dominance.

If we guess the form factor from the $L = 1$ spin barriere suppression formula of Blatt and Weisskopf [48] as an alternative interpretation of the η' form factor we obtain

$$F^2(q_1^2, q_2^2) = F^2(0,0)\,\frac{1+\frac{r^2}{4}W^2}{1+r^2\frac{X}{W^2}} \qquad r \simeq 1fm \pm 20\% \qquad (2.1.16)$$

As can be seen in fig.(2.1.6), this formula reproduces the data as well as the VDM hypothesis. Moreover, the indication in the PLUTO data that VDM underestimates the double tag cross section finds its natural explanation.

It may be interesting to notice that for the reaction $\gamma\gamma \to \pi^0$, the numerical differences between the two interpretations of the η' form factor are drastic. The two approaches lead to single tag cross sections differing by about an order of magnitude for $-q^2 \simeq 0.6GeV^2$.

[1] The wave lengths of a particle is of course a frame dependent quantity, however, in the case of two photon physics, the $\gamma\gamma$ c.m.s. system seems to be a quite natural frame to choose.

Moreover, the breakdown of factorisation is clearly visible in the q_1^2, q_2^2 evolution of the form factor in the finite size model (fig.(2.1.7)).

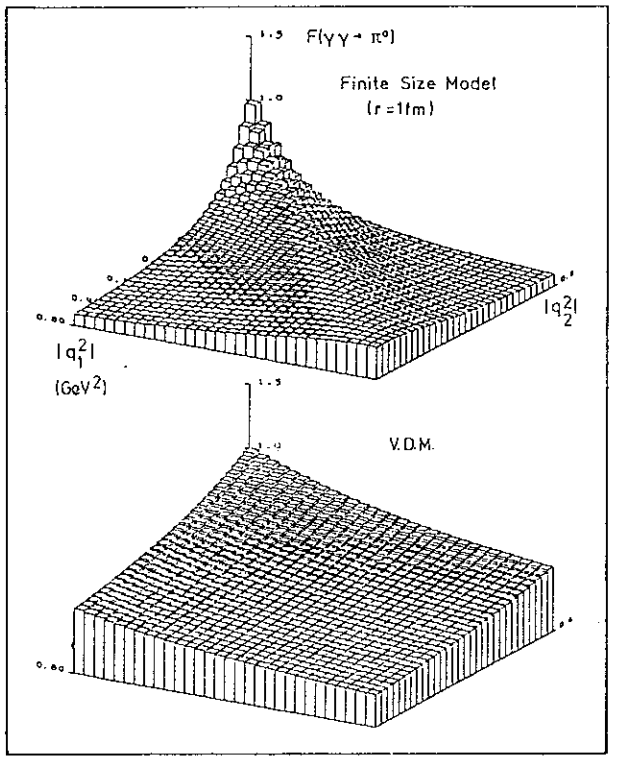

Figure 2.1.7: *Two predictions for the $\gamma\gamma\pi^0$ transition form factor in the region $|q_1^2|, |q_2^2| < 0.6GeV^2$, normalised to the point $q_1^2 = q_2^2 = 0$. The dissimilarity emphassizes the need for double tag measurements.*

In the quark-parton model, the form factor measures an integral over the so called "*parton distribution function*", $\phi(x)$, which has little q^2 dependence in the high q^2 region [17].

$$F(q_1^2, q_2^2) \to \frac{2}{(q_2-q_1)^2}\widehat{f}(\xi), \quad \widehat{f}(\xi) = \int_0^1 \frac{\phi(x)}{1+(2x-1)\xi}dx \qquad (2.1.17)$$

where $\xi = 2(q_2^2 - q_1^2)/(q_2 - q_1)^2$. The $(q_2 - q_1)^{-2}$ is simply the quark propagator between the two photons. The shape of $\phi(x)$ is unknown, but its integral has to obey the normalisation $3\int \phi(x)dx = f_{0^-}$, where f_{0^-} is the decay constant. For the π, this constant is determined from the weak decay of the π^+. For the η and η', one has to estimate this constant either

from measurements of $\Gamma_{\gamma\gamma}$ according to eq(2.1.4), or in the context of $SU(3)$, giving

$$\widehat{f}_{\eta'}(\xi)/\widehat{f}_{\eta}(\xi)/\widehat{f}_{\pi^0}(\xi) = \left(\sqrt{\frac{8}{3}}cos\theta + \sqrt{\frac{1}{3}}sin\theta\right) / \left(\sqrt{\frac{1}{3}}cos\theta - \sqrt{\frac{8}{3}}sin\theta\right) /1 \qquad (2.1.18)$$

For single meson production, the quark model prediction is identical with the QCD expectation. Moreover, it has been argued [8] that the shape of ϕ is calculable in perturbative QCD, provided that q^2 is large enough: $\phi(x) \to 2f_\pi x(1-x)$. However, at present it is completely unknown from which q^2 onwards this parton distribution function gives a reasonnable estimate its true shape.

Finally, it should be pointed out that it is in the double tag case that QCD corrections are best understood. Novikov et al [119] have shown that for large $q_1^2 = q_2^2$, the uncertainties coming from the fact that $\phi(x)$ is not known have very little impact on the rate. They obtain

$$F_\pi \to \frac{2}{3}\left\{\frac{1}{-q^2}(1 - \frac{5\alpha_s(q^2)}{6\pi}) - \frac{8\delta^2}{9q^4}\right\} \qquad (2.1.19)$$

where the higher twist term δ turns out to quite small: $\delta^2 = 0.18GeV^2$. Measuring the double tag cross section would thus provide an excellent test of QCD. However, an integrated luminosity of $1fb^{-1}$ might be needed to perform such a test.

How one could test QCD with $O(100\,pb^{-1})$ has been pointed out by Brodsky and Lepage [8]. They noticed that in first order perturbative QCD[1], the same integral as in eq.(2.1.17) appears in the cross section for $\gamma\gamma \to \pi^+\pi^-$. However, the latter process requires at least one gluon. The ratio $\sigma(\pi^-\pi^-)/\sigma(\pi^0)$ is therefore a measure of α_s.

[1] However, *only* in first order.

Of course, testing QCD is not the only motivation to investigate the channel $\gamma\gamma \to \pi^+\pi^-$. The $f(1280)$, the $S^*(980)$ and the $\epsilon(1300)$ all decay into pion pairs, and the f' has been seen on a large K^+K^- background. For the determination of the two photon widths of these particles, some understanding of the underlying continuum is thus vital.

It turns out that, in the resonance region, one has to deal with $\pi^+\pi^-$ pairs lying in a kinematic domain for which neither QED nor perturbative QCD can be expected to give an adequate description of the data. The resulting uncertainty is reflected in the range of analysis methods of the many experiments which have analysed the $\gamma\gamma$ coupling of the f^0. However, the available data now span the energy region from nearly threshold up to 3.5 GeV. Taking these data as a guideline, it is in fact possible to get an at least numerically satisfying description of the process. We shall start at $W_{\gamma\gamma} = 2m_\pi$ where QED is the obvious candidate theory to compare the data with.

The QED Born Term

The Born amplitude for the pair production of spin zero particles i.e. $\pi^+\pi^-$ is

$$T_{\mu\nu} = e^2\left\{\frac{(2k_1 - q_1)_\mu(2k_2 - q_2)_\nu}{t - m^2} + \frac{(2k_2 - q_1)_\mu(2k_1 - q_2)_{1\nu}}{u - m^2} - 2g_{\mu\nu}\right\} \qquad (2.2.1)$$

where k_1 and k_2 are the four momenta of the π^+ and π^- and t and u are the usual Mandelstam variables $t = (q_1 - k_1)^2$, $u = (q_1 - k_2)^2$. The term $g_{\mu\nu}$ comes from the "sea gull" graph which is absent in the case of lepton pair creation. The helicity amplitudes are then

$$\begin{aligned}
M_{--} &= e^2\left(\frac{\beta^2W^2cos^2\theta}{2(t - m_\pi^2)} + \frac{\beta^2W^2cos^2\theta}{2(u - m_\pi^2)} - 1\right)\\
M_{-+} &= -\frac{e^2}{2}e^{2i\phi}\beta^2cos^2\theta W^2\left(\frac{1}{t - m_\pi^2} + \frac{1}{u - m_\pi^2}\right)\\
M_{00} &= 2e^2\sqrt{q_1^2q_2^2}\left(\frac{q_1q_2 - W^2\beta^2cos^2\theta}{(q_1q_2)^2 - X\beta^2cos^2\theta}\right)\\
M_{+0} &= \sqrt{2}e^2e^{i\phi}W\sqrt{-q_2^2}\beta^2cos^2\theta\left(\frac{q_1^2 + q_1q_2}{(q_1q_2)^2 - X\beta^2cos^2\theta}\right)\\
M_{0+} &= \sqrt{2}e^2e^{-i\phi}W\sqrt{-q_1^2}\beta^2cos^2\theta\left(\frac{q_2^2 + q_1q_2}{(q_1q_2)^2 - X\beta^2cos^2\theta}\right)
\end{aligned} \qquad (2.2.2)$$

where the angles θ and ϕ are given by $\vec{k_1} = |\vec{k}|(sin\theta cos\phi, sin\theta sin\phi, cos\theta)$. Using eq. (1.4) and

(1.5), we get the following cross sections:

$$\frac{d\sigma_{TT}}{d\Omega} = \frac{\alpha^2\beta}{16\sqrt{X}}\left\{\left(\frac{\beta^2W^2cos^2\theta}{2(t-m_\pi^2)} + \frac{\beta^2W^2cos^2\theta}{2(u-m_\pi^2)} - 1\right)^2 + \left(\beta^2cos^2\theta W^2\left(\frac{1}{2(t-m_\pi^2)} + \frac{1}{2(u-m_\pi^2)}\right)\right)^2\right\}$$

$$\frac{d\sigma_{TL}}{d\Omega} = \frac{\alpha^2\beta}{4\sqrt{X}}(-q_1^2)W^2\beta^4\cos^4\theta\left(\frac{q_1^2 - q_1q_2}{(q_1q_2)^2 - X\beta^2cos^2\theta}\right)^2 \qquad (2.2.3)$$

$$\frac{d\sigma_{LL}}{d\Omega} = \frac{\alpha^2\beta}{2\sqrt{X}}q_1^2q_2^2\left(\frac{q_1q_2 - W^2\beta^2cos^2\theta}{(q_1q_2)^2 - X\beta^2cos^2\theta}\right)^2$$

For real photons, the cross section simplifies to

$$\frac{d\sigma}{d\Omega} = \frac{\alpha^2\beta}{2W^2}\frac{(1-\beta^2)^2 + \beta^4sin^4(\theta)}{(1-\beta^2cos^2(\theta))^2} \qquad (2.2.4)$$

β being the velocity of the pions in their center of momentum system.

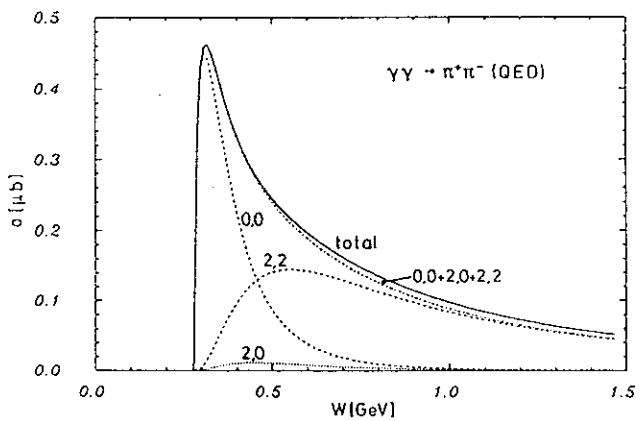

Figure 2.2.1: *This partial wave decomposition of the Born term cross section for $\gamma\gamma \to \pi^+\pi^-$ shows that the resonance region is dominated by $Y_L^m = Y_2^2$.*

For $q_1^2 \simeq q_2^2 \simeq 0$, the reaction $\gamma\gamma \to \pi\pi$ is particularly suitable for a partial wave analysis because rotational invariance implies that many partial waves *have* to be zero, i.e. all partial waves with total spin $J = 1$ or with helicities different from $J_z = 0, \pm 2$ vanish. The completeness relation can thus be written in the form

$$M_{++} = r_{0,0}Y_{0,0} + r_{2,0}Y_{2,0} + \ldots$$
$$M_{+-} = r_{2,2}Y_{2,2} + r_{3,2}Y_{3,2} + \ldots \qquad (2.2.5)$$

with $r_{J,J_z} = \int Y_{J,J_z}M_{a,b}\delta^{J_z}_{a-b}d\Omega$. The orthonormality of the spherical harmonics gives then

$$\sigma_{\gamma\gamma}(J,J_z) = \frac{\beta}{128\pi^2W^2}\mid r_{J,J_z}\mid^2 \qquad (2.2.6)$$

We can take the Born term as a guide to which partial waves have to be included in a fit to the data in order to get a satisfactory description of the process. Taking the amplitudes $M_{++} = 2e^2(1-\beta^2)/(1-\beta^2cos^2\theta)$ and $M_{+-} = 2e^2\beta^2e^{2i\phi}sin^2\theta/(1-\beta^2cos^2\theta)$, the result is

$$r_{00} = e^2\sqrt{4\pi}\frac{1-\beta^2}{\beta}ln\left(\frac{1+\beta}{1-\beta}\right)$$
$$r_{20} = e^2\sqrt{5\pi}(1-\beta^2)\left\{\frac{3-\beta^2}{\beta^3}ln\left(\frac{1+\beta}{1-\beta}\right) - \frac{6}{\beta^2}\right\} \qquad (2.2.7)$$
$$r_{22} = e^2\sqrt{15\pi/2}\left\{\frac{(1-\beta^2)^2}{\beta^3}ln\left(\frac{1+\beta}{1-\beta}\right) + \frac{2}{\beta^2}\left(\frac{5}{3}\beta^2 - 1\right)\right\}$$

As can be seen in fig.(2.2.1), these spin amplitudes nearly saturate the Born cross section in the resonance region. This is useful to know when the interference with direct channels is to be estimated (see chapter on tensor and scalar resonances). In particular, eq.(2.2.7.) shows that the interference between the $\pi^+\pi^-$ continuum and a tensor meson produced with helicity $J_z = \pm 2$ should be very large, while the interference between the continuum and a scalar resonance, or a tensor meson produced with helicity 0 should be small.

A Measurement of low W $\pi^+\pi^-$ Production

Measurements of low energy $\pi^+\pi^-$ pairs produced in $\gamma\gamma$ collisions are very difficult. With solenoid detectors, it is virtually impossible to trigger such events. The number of events from the reactions $\gamma\gamma \to e^+e^-$ and $\gamma\gamma \to \mu^+\mu^-$ greatly exceeds the number of $\pi^+\pi^-$ pairs and, because of the small transverse momenta of the particles produced, are difficult to identify in a central detector. Time projection chambers have the potential of particle identification in the required momentum range. However, corresponding cross sections have not yet been published.

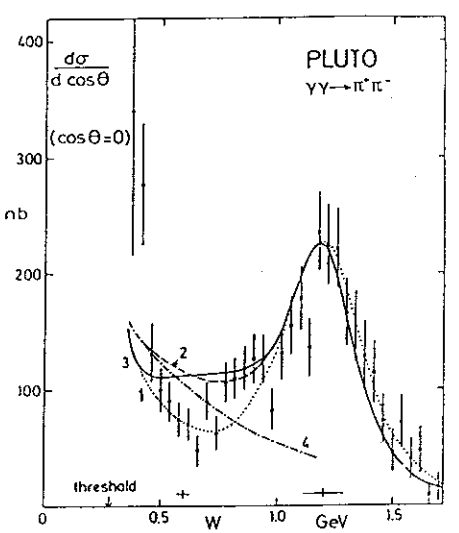

Figure 2.2.2: *A measurement of low energy pion pairs. Curve 4 is the Born term contribution alone, curve 3 is the Mennessier Model fitted to an f Breit Wigner amplitude, curve 2 is the Born term added coherently to an f amplitude. Curve 1 is the finite size pion model added to an f Breit Wigner amplitude.*

An alternative approach is particle identification in a forward spectrometer, since selecting events in which the two tracks have a small angle with the beam direction is equivalent to selecting events which have a small invariant mass, but not such small energies in the lab. frame. Because of this kinematic relation, the electron and muon identification of the PLUTO forward spectrometer [52] could be used to identify lepton pairs on an event by event basis and thus obtain a rather clean $\pi^+\pi^-$ sample[1]. Since the acceptance for these events has its maximum for pions produced at 90° in the $\gamma\gamma$ c.m.s., the observed rate is a measure of the differential cross section at $cos\theta^* = 0$.

The data are shown in fig.(2.2.2). Despite the experimental uncertainty of $\sim 20\%$ on the overall normalisation, it is clear that the Born term does not give an accurate description of the data.

Final State Interactions

The QED amplitude cannot accout for the fact that the π meson is a stronly interacting particle. By means of Watson's theorem [78], the influence of the strong interaction is related to $\pi^-\pi^-$ phase shifts as measured in hadronic interactions. Watson showed that under certain conditions, the full amplitude for the production of a pair of strongly interacting particles can be split into a "primary" amplitude and a "final state interaction" amplitude. If we follow the published literature and assume that the primary interaction *is* the Born amplitude, then measurements of $\pi^-\pi^-$ phase shifts can be turned into an absolute prediction for the process $\gamma\gamma \rightarrow \pi^+\pi^-$. Since the early 1970's, this line of approach has be further developed by the introduction of correlations between different hadronic channels ("coupled channel analyses", c.f. [53]). In such models, transitions of the type $\pi^+\pi^- \rightarrow K^+K^-$ are assumed. Particularly interesting are the terms involving neutral mesons, since they lead for example to a finite cross section for $\gamma\gamma \rightarrow \pi^0\pi^0$, a process which is absent in lowest order QED.

The calculation based on the most recent $\pi\pi$ phase shifts is the one by Mennessier [54]. His result, fitted to an f meson Breit Wigner amplitude is shown in fig.(2.2.2). The model predicts the correct magnitude of the cross section, however, in detail it is not compatible with the data. The PLUTO collaboration pointed out that the discrepancy arround $W = 600MeV$ cannot possibly be explained by the destructive interference due to a (hypothetical) meson. Therefore, it appears that the final state interaction approach is alone not sufficient to describe the process in the measured energy range- at least if future experiments confirm the observations of the PLUTO collaboration.

Theoretically, two points need further investigation. Firstly, it is not clear, whether or not the QED Born term gives a good estimate of the "true" primary amplitude. Since pions are not pointlike, at some energy, QED will overestimate this amplitude. Secondly, final state interaction models rely on the applicability of Watson's theorem. However, this theorem can only be applied easily, if inelastic contributions are small. This restriction becomes problematic beyond the four pion threshold $W = 560\,MeV$. We shall see later that the cross section for $\gamma\gamma \rightarrow 2\pi^+2\pi^-$ exceeds the non resonant pion pair production cross section at energies of $\sim 1\,GeV$. Therefore, the disagreement of the data with the calculation by Mennessier arround $600MeV$ may not be too surprising. It simply reminds us of the fact

[1] In the low W region, K^+K^- pairs of similar event topology are rare compared to the number of $\pi^+\pi^-$ events, because the kaons are heavier and thus produced by a smaller "number" of photons.

that for pion pairs, the method "QED + final state interactions" is only applicable within a rather small region in W.

If we want to understand, or at least describe the production of pion pairs in the *entire* resonance region, we need a new approach. In the following, we shall therefore attempt to incorporate the spatial extension of the pion pair already at the level of the primary amplitude.

The Finite Size Model

Before going into the details of this model it must be pointed out that, given our limited understanding of the strong interaction at large distances, it is not yet possible to implement the structure of the π meson in a fully convincing manner. The following attempt to parameterise the $\gamma\gamma \rightarrow \pi^+\pi^-$ continuum in the resonance region is therefore largely based on analogy arguments, however keeping close track of the basic constraints involved.

We start from the three Born term diagrams shown in fig.(2.2.3), but take the couplings of the photons to be non pointlike. We do so by multiplying the pole terms (e.g. $\frac{1}{t-m^2}$) by a function $F(t-m^2)$. The motivaton for this particular choice of variables is two fold: at $t = m^2$, the pion is on shell and hence, finite size effects should disappear. This provides the convenient normalisation $F(0) = 1$. Also, $t - m^2$ has the same dimension as for example q^2 in the reaction $e^-\pi^- \rightarrow e^-\pi^-$. Therefore, we tentatively idenify this function F with the measured electrical form factor of the pion, F_π, which is the best experimental information we have about the structure of the pion so far.

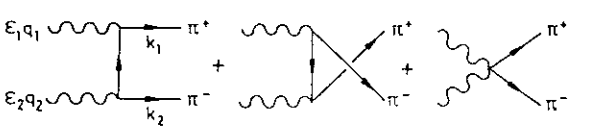

Figure 2.3.2: *The Born term matrix elements for non resonant pion pair production*

To be specific, we assume

$$\begin{array}{lll} & \frac{1}{q^2} \rightarrow \frac{1}{q^2}F_\pi(q^2) & from \quad e^-\pi^- \rightarrow e^-\pi^- \\ gives & \frac{1}{t-m_\pi^2} \rightarrow \frac{1}{t-m_\pi^2}F_\pi(t-m_\pi^2) & for \quad \gamma\gamma \rightarrow \pi^+\pi^- \\ and & \frac{1}{u-m_\pi^2} \rightarrow \frac{1}{u-m_\pi^2}F_\pi(u-m_\pi^2) & for \quad \gamma\gamma \rightarrow \pi^+\pi^- \end{array} \qquad (2.2.8)$$

where for the pion form factor, we take the measurement [55] $F_\pi^2(q^2) = (1 - < r^2 > q^2/6)^{-2}$ with $< r^2 >= 0.43 \pm 0.01\,fm^2$. This equation specifies two of the three QED diagrams. The "sea-gull" term in eq(2.2.1) follows now from gauge invariance, since gauge invariance implies that only such modifications of a full amplitude are allowed which can be written in the form[1]

$$T_{\mu\nu} = G(t,u)\sum_i T^i_{\mu\nu}(= all\ diagrams) \qquad (2.2.9)$$

[1] For the case of pion pair production, this can easily be verified. Starting from the most general form of the

The explicit form of G can conveniently be obtained by calculating a matrix element which has no contribution from the sea gull term (i.e. M_{+-}) and imposing the result on all matrix elements by means of eq(2.2.9): The result is the explicit form of the finite size model for *real* photons.

$$M_{a,b}(finite\,size) = G(t,u)M_{a,b}(QED)$$
$$G(t,u) = -\frac{1}{s}\left\{\frac{t-m_\pi^2}{1-\frac{u-m_\pi^2}{x_0^2}} + \frac{u-m_\pi^2}{1-\frac{t-m_\pi^2}{x_0^2}}\right\} \qquad (2.2.10)$$

were x_0 is the scale set by the pion form factor. Expressed in units of energy, $x_0 \simeq m_\rho$.

As can be seen in fig.(2.2.2), this Ansatz gives a good description of the low lying $\pi^+\pi^-$ continuum. Let us thus try to extend the model to a prediction for the cross section for virtual photons.

The simplest possibility is to take

$$G_1(t,u,q_1^2,q_2^2) = G(t,u)$$

The motivation for this is that at fixed $W_{\gamma\gamma}$ and fixed production angle, one has $|t-m_\pi^2| \sim |u-m_\pi^2| \sim (q_1q_2)$ which rises with q_1^2 for $q_2^2 = 0$. Thus, a suppression of the propagators leads to a suppression of the off shell cross sections beyond the QED fall off.

Two other possibilities arise from either assuming factorisation

$$G_2(t,u,q_1^2,q_2^2) = G(t,u)\left(\frac{1}{1-q_1^2/x_0^2}\right)\left(\frac{1}{1-q_2^2/x_0^2}\right)$$

or from the esthetically more pleasing search for a function G_3, such that

$$G_3(t,u,q_1^2,q_2^2)M_{+-}(QED) = \frac{1}{1-\frac{q_1^2+q_2^2+t-m^2}{x_0^2}}M_{+-}(t-channel,QED) + (\text{"}t\to u\text{"}) \qquad (2.2.11)$$

---

modification,

$$T_{\mu\nu} \sim f(t,u,q_1^2,q_2^2)\frac{(2k_1-q_1)_\mu(2k_2-q_2)_\nu}{t-m_\pi^2} + f(u,t,q_2^2,q_1^2)\frac{(2k_2-q_1)_\mu(2k_1-q_2)_\nu}{u-m_\pi^2} + g(t,u,q_1^2,q_2^2)\,2g_{\mu\nu}$$

where the functions multiplying the u and t channel diagrams have to be identical, but evaluated with exchanged arguments by virtue of Bose Statistics, the requirement of gauge invariance leads to the constraint

$$(2k_2-q_2)_\nu\left\{f(t,u,q_1^2,q_2^2) - g(t,u,q_1^2,q_2^2)\right\}$$
$$+(2k_1-q_2)_\nu\left\{f(u,t,q_2^2,q_1^2) - g(t,u,q_1^2,q_2^2)\right\} = 0$$

and thus

$$f(t,u,q_1^2,q_2^2) = g(t,u,q_1^2,q_2^2)$$
$$f(u,t,q_2^2,q_1^2) = g(t,u,q_1^2,q_2^2)$$

which implies the above statement.

This Ansatz, which may not be correct in detail, since it neglects $\pi\pi$ phase shifts and thus implicitely violates Whatson's theorem, is the most consequent extension of eq.(2.2.8), since it implies that it does not matter in which direction the amplitude is taken away from the point where all particles are on mass shell.

G_3 is of such a form that the inherent scale which determines the cross section fall off for all agruments is identical. In a factorisation Ansatz, one still has the option of taking different scales for the q^2 evolution and for the t,u fall off. This would leave too much freedom. G_1 is no satisfying solution either, since at fixed t it has no longer any q^2 dependence. Thus, the most symmetric solution is also the most promising one, and the finite size model for all q_1^2, q_2^2 reads

$$M_{ab}(finite\,size) = G_3(t,u,q_1^2,q_2^2)M_{ab}(QED)$$
$$G_3(t,u,q_1^2,q_2^2) = \frac{x_0^2}{t+u-2m_\pi^2}\left(\frac{u-m_\pi^2}{x_0^2+m_\pi^2-t-q_1^2-q_2^2} + \frac{t-m_\pi^2}{x_0^2+m_\pi^2-u-q_1^2-q_2^2}\right) \qquad (2.2.12)$$

It is hoped that this will be a useful tool for the determination of the f and f' form factors by providing a sensible parameterisation of the background.

Measurements of large W Meson Pairs

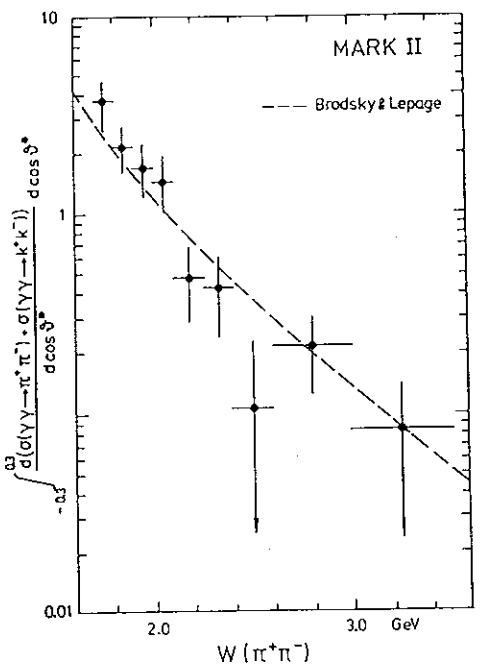

Figure 2.2.4: *A preliminary measurement of hadron pairs at large momentum transfer. The agreement with the QCD based model of Brodsky and Lepage is impressive.*

For the large W region, there are now data as well as predictions. As far as the interpretation

of the data is concerned, some caution is required because in the existing data particle identification is limited to the discrimination between leptons and hadrons. This implies that some model input for the pions to kaons ratio is necessary for the data analysis. Still, the cross section can be parameterised in such a manner that the data are numerically insensitive to the assumed π to K ratio.

The PLUTO collaboration [56] noticed that the differential cross section $d\sigma/d|\vec{k}^*|$, where $|\vec{k}^*|$ is the centre of mass momentum of the hadrons is quite insensitive to mass assumptions. This is because the difference $\Delta k^{*2} = k^{*2}(\pi's\, assumed) - k^{*2}(K's\, assumed)$ is $\Delta k^{*2} = (|\vec{k}_1| - |\vec{k}_2|)^2(m_k^2 - m_\pi^2)/(4|\vec{k}_1||\vec{k}_2|) + O\left(\frac{m_K^4}{k^4}\right)$ where $\vec{k}_1$ and $\vec{k}_2$ are the lab 3-momenta of the hadrons. Since the triggers prefer events with $|\vec{k}_1| \sim |\vec{k}_2|$, Δk^{*2} is tiny. In the same approximation, one obtains $\Delta W^2 = (|\vec{k}_1|^2+|\vec{k}_2|^2)(m_k^2-m_\pi^2)/(4|\vec{k}_1||\vec{k}_2|)+O\left(\frac{m_K^4}{k^4}\right)$. Therefore, $\sigma(W)$ is a much more model dependent quantity than $\sigma(|\vec{k}^*|)$. The result of the PLUTO measurement, which spans the range $1GeV < k^* < 2GeV$, can be summarised as follows: The cross section $\frac{d\sigma}{d\Omega}(\gamma\gamma \to \pi^+\pi^- + K^-K^-)_{\theta^*=90^0}$ is far below the Born term expectation. Above $k^* = 1.2GeV$, it agrees qualitatively with the first order QCD calculation of Brodsky and Lepage [8].

The Mark-II collaboration did a similar analysis with a sixfold statistics [57]. $240pb^{-1}$ enabled a quantitative test of the theory up to invariant masses $W_{\pi\pi} = 3.5GeV$ (see fig.(2.2.4)). Since the data agree so well with the QCD calculation, the assumptions and results of this calculation shall be described in brief.

QCD Expectations

For both deep inelastic lepton nucleon scattering, and high s e^+e^- annihilation, it has been found that the full amplitudes factorise into quark production amplitudes (i.e. $T(\nu_\mu p \to \mu q\, qq), T(e^+e^- \to q\bar{q})$) and thereof independent fragmentation functions $\Phi(q\bar{q} \to hadrons)$. Brodsky and Lepage have argued that a similar factorisation might also work for exclusive $\gamma\gamma$ channels: the photons first produce a four quark system which then "condensates" into two mesons. If we call $T^H_{\mu\nu}$ the amplitude for the production of two quark pairs and Φ the amplitude for finding the meson as a $q\bar{q}$ state, then

$$T_{\mu\nu}(\pi^+\pi^-) = \int_0^1\int_0^1 \Phi^*_{\pi^+}(x_1,\widetilde{Q_1})\Phi^*_{\pi^-}(x_2,\widetilde{Q_2})T^H_{\mu\nu}(x_1,x_2,W_{\gamma\gamma},\theta^*)dx_1dx_2 \qquad (2.2.13)$$

In an energy regime where quark masses can be neglected as well as meson masses, x_i and $(1-x_i)$ are the fractional longitudinal momenta of the quarks in the meson and $\widetilde{Q}_i$ is the minimum transverse quark momentum occurring in the process, $\widetilde{Q}_i = min(x_i,(1-x_i))W_{\gamma\gamma}|sin\theta^*|$. Within this model, Φ is the same amplitude which also governs the q^2 evolution of the single pseudoscalar production cross section (c.f. eq.(2.1.17)).

In first order perturbative QCD, the hard scattering amplitude $T^H_{\mu\nu}$ gives the following

matrix elements for two quark pairs with opposite spins:

$$\begin{aligned}
M_{++}(\gamma\gamma \to 2(q\bar{q})) &= \frac{16\pi\alpha_s}{3s}\frac{32\pi\alpha}{x_1(1-x_1)x_2(1-x_2)}\left(\frac{(e_2-e_1)^2a}{1-cos^2\theta}\right)\\
M_{+-}(\gamma\gamma \to 2(q\bar{q})) &= \frac{16\pi\alpha_s}{3s}\frac{32\pi\alpha}{x_1(1-x_1)x_2(1-x_2)}\left(\frac{(e_2-e_1)^2(1-a)}{1-cos^2\theta}\right.\\
&\left. + \frac{e_1e_2a(x_1(1-x_1)+x_2(1-x_2))}{a^2-b^2cos^2\theta} + \frac{(e_1^2-e_2^2)(x_1-x_2)}{2}\right)
\end{aligned} \qquad (2.2.14)$$

where $a\,(b) = (1-x_1)(1-x_2) + (-)x_1x_2$. The cross sections follow, if specific assumptions are made about Φ and α_s. Imposing $\Phi(x) = \Phi(1-x)$ and $\int \alpha_s\Phi^*dx \simeq \alpha_s\int\Phi^*dx$ gives

$$\begin{aligned}
M_{++}(\gamma\gamma \to \pi^+\pi^-) &= \frac{256\pi^2\alpha\alpha_s}{3s}I_1\left(\frac{<(e_1-e_2)^2>}{1-cos^2\theta}\right)\\
M_{+-}(\gamma\gamma \to \pi^+\pi^-) &= \frac{256\pi^2\alpha\alpha_s}{3s}I_1\left(\frac{<(e_1-e_2)^2>}{1-cos^2\theta} - 2<e_1e_2>I_2\right)\\
I_1 &= \int_0^1\int_0^1 \frac{\Phi^*_{\pi^+}\Phi^*_{\pi^-}}{x_1(1-x_1)x_2(1-x_2)}dx_1dx_2\\
I_2 &= \frac{1}{I_1}\int_0^1\int_0^1 \frac{\Phi^*_{\pi^+}\Phi^*_{\pi^-}}{x_1(1-x_1)x_2(1-x_2)}\frac{b^2}{a^2-b^2cos^2\theta}dx_1dx_2
\end{aligned} \qquad (2.2.15)$$

From the last set of equations, explicit cross sections can be derived by choosing a certain function Φ and evaluating the integrals. Brodsky and Lepage argue that

$$\Phi(x,\widetilde{Q^2}) \underset{\widetilde{Q}^2\to\infty}{\to} \sqrt{3}f_\pi x(1-x)$$

and so, at high energies, everything but α_s is known and the cross section becomes

$$\frac{d\sigma}{d\Omega} \to \frac{1}{s^3}\left(\frac{32\pi\alpha\alpha_s f_\pi^2}{sin^2\theta}\right)^2 \qquad (2.2.16)$$

Theoretically, it is not at all clear above which energy this prediction is valid. First of all, Brodsky and Lepage calculate that the evolution of the parton distribution amplitude Φ to the form $x(1-x)$ is very slow (logarithmic). Secondly, even if one calculates the $\gamma\gamma \to \pi^+\pi^-$ amplitude *at* a a certain value of $W_{\gamma\gamma}$ and $sin^2\theta$, one implicitly averages α_s over the $\tilde{Q}^2$ range from 0 to $\frac{1}{2}p_t$. Formally, this means that the hard scattering amplitude is integrated over a range where it is *soft*, i.e. not calculable in perturbative QCD. However this range decreases to the extent the product $W \cdot sin\theta$ increases. Being aware of these difficulties, Brodsky and Lepage chose a rather large value of $\alpha_s = 0.9$ for their absolute prediction of the cross section. The question then remains whether it makes sense to use a first order perturbative calculation in currently available energy domains.

A Nice Coincidence

In this light, the Mark II and PLUTO data are surprisingly well described by Brodsky and Lepage's calculation. However, it could well be that the agreement is merely the result of a numerical coincidence. For illustration, let us make a little Gedankenexperiment. Let us assume that experimental Physics had proven QCD to be wrong and only the two photon experts had not noticed yet. Let us also assume that a new "correct" theory of strong interactions had led to a similar formalism as discussed under "finite size effects". From eq.(2.2.10) we see that a two photon experimentalist, having measured a cross section of $\frac{d\sigma}{d\Omega}(\gamma\gamma \to \pi^+\pi^-)|_{90^o} \simeq 2\alpha^2 m_\rho^4/s^3$, would take the QCD prediction and first of all notice that the predicted $1/s^3$ fall off of the cross section is well reproduced by the data. He would then proceed to calculate the strong coupling constant as $\alpha_s = \sqrt{2m_\rho^2/(32\pi f_\pi^2)} = 0.96$. If his measurement was made at $p_t \simeq 2GeV$, he would argue that $\alpha_s \simeq 4\pi/(9ln\frac{0.25GeV^2}{\lambda^2})$ and publish a value of $\lambda = 240MeV$...

This numerical coincidence has a fortunate consequence for the parameterisation of the $\pi^+\pi^-$ continuum in the resonance region. It means that the model given in eq's (2.2.8) and (2.2.12) *does* provide a good handle on the interference effects, since it asymptotically coincides with Brodsky and Lepage's calculation and thus with the available high momentum transfer data.

However, K^+K^- pair production has not been considered. The ratio between pion and kaon pairs can easily be a nontrivial function of the available energy, since in the resonance region, we witness an interplay between kinematic and dynamical terms. The kinematics, i.e. flux and phase space factors clearly prefer pions, whereas there are indications that the dynamics prefers kaons at high energies.

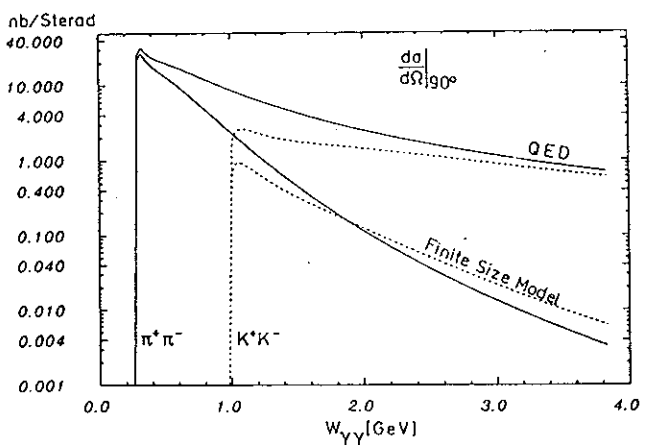

Figure 2.2.5: *Two calculations of the differential cross section for meson pair production at 90°. In QED, this cross section is equal for pions and kaons as $W \to \infty$. In the finite size model, kaons dominate beyond $W \simeq 2\,GeV$.*

The Born term Ansatz predicts the $\pi^+\pi^-$ cross section to be larger than the K^+K^- cross section throughout, as can be seen in eq.(2.3.5). The finite size model gives a similar behaviour for small center of mass energies. However, since the form factor of the K^- meson [58] has been measured to give a slower fall off than the pion form factor, i.e. $F_K = (1 + \frac{1}{6}q^2 < r^2 >)$ with $< r^2 >= 0.28 \pm 0.05 fm^2$, kaons are expected to dominate as the energy increases. Fig.(2.2.5) shows the expected cross sections at 90° production angle.

In the QCD calculation of Brodsky and Lepage, the cross section ratio between pions and kaons is simply f_K^4/f_π^4, which gives about a factor of 2 in favour of the kaons.

After this manuscript was nearly completed, the PEP49 collaboration showed the first preliminary measurement of K^+K^- pairs over a wide range of W (c.f. ref.[27]). Fig.(2.2.6) shows that for large energies, the data are consistent with the QCD model of Brodsky and Lepage as well as with the finite size model. In the resonance region, however, the QCD calculation predicts a too large cross, since it leaves no room for the known resonances in this channel. In particular the f' "peak", which is clearly visible in the data, cannot be accomodated in addition to the non resonant amplitude.

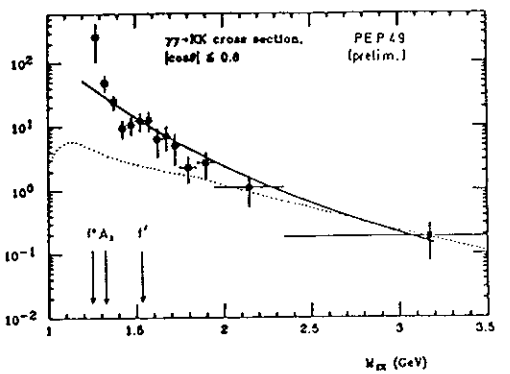

Figure 2.2.6: *A preliminary measurement of K^+K^- pairs. The solid line is the QCD prediction of ref [8]. The prediction of the finite size model (dotted line) leaves room for resonances (c.f. Fig.(2.2.5)).*

Summing up all measurements of charged pseudoscalar pair production, it appears that the simple finite size model offers an opportunity to consistently describe the non resonant amplitudes from threshold, through the entire resonance region, up to the higest values of W measured. It is therefore a key ingredient for the experimental determination of resonance parameters for states which decay into $\pi^+\pi^-$ and K^+K^- pairs.

Scalar Resonances

Introduction

The 0^+ states $\delta(980)$, $S^*(980)$ and $\epsilon(1300)$ are altogether not very well understood, and for many years, their existence was disputed. Experimentally, we know comparatively little about these states. The best measured 0^+ resonance, the S^*, has been seen in $\pi\pi(78 \pm 3\%)$ and $K\bar{K}(22 \pm 3\%)$ final states. The δ has only been observed in the final states $K\bar{K}$ and $\pi^0\eta$, but with unknown branching ratios. The ϵ is said to decay into pion pairs predominantly. However, the current value for its width of $200 \rightarrow 600 MeV$ not only indicates a lack of experimental understanding of this state, but also implies that the detection of an $\epsilon(1300)$ signal without phase shift analysis is close to impossible.

Most puzzling are the small widths of the S^* and the δ. There is no a priori reason why they should not decay through the strong interaction - nevertheless, $\Gamma(S^*) = 33 \pm 6 MeV$ and $\Gamma(\delta) = 54 \pm 7 MeV$. Hence interpretations of the known scalar resonances in terms of conventional $q\bar{q}$ pairs should be viewed with suspicion. In particular, the $SU(3)_{Fl}$ relations (c.f. ref. [59])

$$\begin{aligned} S^* &= S_1 sin(\theta) + S_8 cos(\theta) \\ \epsilon &= S_1 cos(\theta) - S_8 sin(\theta) \end{aligned} \tag{2.3.1}$$

where the mixing angle could be taken from the mass formula

$$4M_\kappa^2 = M_\delta^2 + 3(M_S^2 . cos^2(\theta) - M_\epsilon^2 sin^2(\theta)) \tag{2.3.2}$$

are subject to considerable uncertainty. Given the poor state of theory *and* experiment for scalar resonances, two photon physics has the opportunity to make a substantial contribution to our understanding of these states.

The two photon formation of scalar resonances can be parameterised in terms of two form factors. Using the helicity projection operators introduced in appendix A, we can construct the amplitudes such that one of the two form factors only enters the cross section, if both photons are off mass shell:

$$T_{\mu\nu} = F_{TT0} G_{\mu\nu} + F_{LL} L_{\mu\nu} \tag{2.3.3}$$

In the absence of interference effects, one obtains the following cross sections:

$$\begin{aligned} \sigma_{TT} &= \frac{\tau_{TT}}{2} = \frac{1}{4} F_{TT0} \frac{M^2}{W\sqrt{X}} \frac{\Gamma}{(W^2 - M^2)^2 + \Gamma^2 M^2} \\ \sigma_{LL} &= \frac{1}{2} F_{LL} \frac{M^2 X q_1^2 q_2^2}{(q_1 q_2) W \sqrt{X}} \frac{\Gamma}{(W^2 - M^2)^2 + \Gamma^2 M^2} \\ \sigma_{LT} &= \sigma_{TL} = 0 \end{aligned} \tag{2.3.4}$$

where, at least for the ϵ, Γ has to be taken as a variable. Because of time invariance, both form factors are real valued functions at $W = M$. Notice that no tag and single tag data can be parameterised in terms of a single transition form factor. This coupling is related to the $\gamma\gamma$ width via

$$F_{TT0}^2(0,0) = 16\pi M \Gamma_{\gamma\gamma} \tag{2.3.5}$$

Upper Limits for $\gamma\gamma \rightarrow S^*$

The Crystal Ball [60] and the JADE [61] Collaborations searched for an S^* signal in the reaction

$$\gamma\gamma \rightarrow \pi^0\pi^0 \rightarrow 4\gamma.$$

No signal was found and thus, the results so far are only upper limits:

$\Gamma_{\gamma\gamma}(S^*)$	*Channel*	*Experiment*	*Ref.*
$< 0.8 keV$	$\pi^0\pi^0$	*Crystal Ball*	[60]
$< 0.8 keV$	$\pi^0\pi^0$	$JADE(prelim.)$	[61]

Table 2.3.1: *Upper Limits on* $\Gamma_{\gamma\gamma}(S^*)$

A comparison with currently available predictions shows that e^+e^- experiments are on the brink of making conclusive statements about the models (see below).

Observation of δ Formation

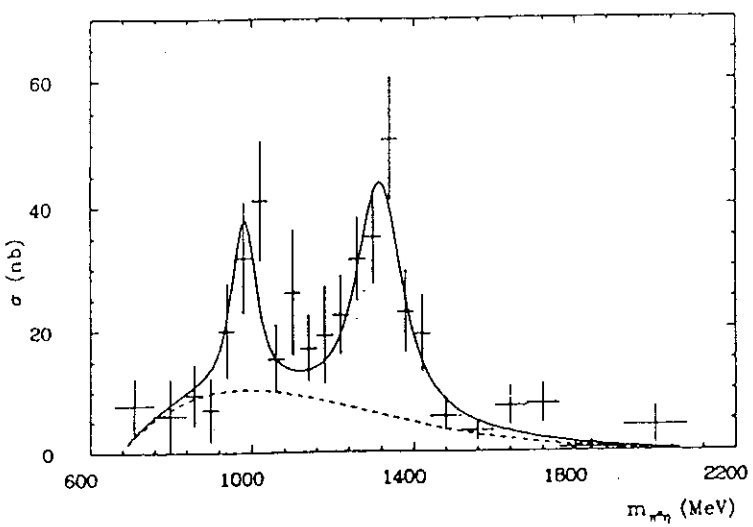

Figure 2.3.1: *A measurement of* $\gamma\gamma \rightarrow \pi^0\eta$. *These data are the first indication of scalar resonance formation in two photon collisions. The peaks are attributed to the* δ *and the* A_2 *resonances (Crystal Ball).*

The Crystal Ball Collaboration [62] analysed the reaction

$$\gamma\gamma \to \pi^0\eta \to 4\gamma.$$

From an integrated luminosity of $110pb^{-1}$, at $E_b \simeq 5GeV$ in DORIS II, the mass spectrum shown in fig.(2.3.1) was obtained. The data are well described by a superposition of a smooth background plus the Breit Wigner curves for the δ and the A_2. However, the statistical significance of the δ signal is not yet too impressive:

$$\Gamma_{\gamma\gamma}(\delta) \cdot Br(\delta \to \pi^0\eta) = 0.19 \pm 0.07^{+0.10}_{-0.07} keV \quad (Crystal\ Ball)$$

Since the branching ratios of the δ are not yet known these data cannot be used for a comparison with models.

Interference of 0^+ States with the $\pi^+\pi^-$ Continuum

For most detectors, the acceptances for charged pions is much better than for π^0 mesons, where good energy resolution of the shower counters is required. However, the interpretation of the data is harder because of the large non resonant $\pi^+\pi^-$ continuum (c.f. fig.(2.3.2)).

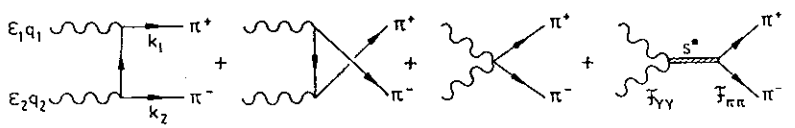

Figure 2.3.2: *The matrix element for pion pair production including resonant and non resonant contributions*

Before we can calculate this interference, we need the full $\gamma\gamma \to 0^+ \to \pi^+\pi^-$ amplitude. The $0^+\pi\pi$ matrix element is just the corresponding form factor, since there are no spins involved in the decay: $M(0^+ \to \pi\pi) = F_{0^+\pi\pi}$ leads to the normalisation

$$\Gamma(0^+ \to \pi^+\pi^-) = \frac{F^2_{0^+\pi\pi}}{16\pi M_{0^+}}\sqrt{1 - 4\frac{m_\pi^2}{M^2_{0^+}}} \tag{2.3.6}$$

For the collision of transversely polarised photons, the interference with a continuum of pions with finite radius can then be written of the form

$$\frac{d\sigma}{d\Omega} = \frac{\beta}{(16\pi)^2\sqrt{X}}\left(|M(non-res.)|^2 + |M(res.)|^2 + "Interference"\right) \tag{2.3.7}$$

the nonresonant term is given in eq.(2.4.10) of the discussion of the radiative width of the f meson, leaving[1]

$$|M(res.)|^2 = \frac{(F_{TT0}F_{0^+\pi\pi})^2}{(W^2 - M^2_{0^+})^2 + \Gamma^2 M^2_{0^+}}$$

$$"Interference" = 8\pi\alpha G(t,u,q_1^2,q_2^2)F_{TT0}F_{0^+\pi\pi}\frac{W^2 - M^2_{0^+}}{(W^2 - M^2_{0^+})^2 + \Gamma^2 M^2} \tag{2.3.8}$$

$$* \left(\frac{\beta^2 cos^2\theta}{2(t - m_\pi^2)} + \frac{\beta^2 cos^2\theta}{2(u - m_\pi^2)} + 1\right)$$

where $G(t,u,q_1^2,q_2^2)$ accounts for the finite size of the pion in the non resonant amplitude. Whether or not the product of the resonance coupling constants is positive is an open question. Given the large width of the $\epsilon(1300)$ it is also quite possible that the coupling $F_{0^-\pi\pi}$ has some explicit energy dependence (c.f. appendix D).

$SU(3)_{Fl}$ Relations for Scalar Mesons

It would be of great interest to see, whether the 0^+ nonet obeys a sum rule similar to the 0^- nonet since, in this case, different models lead to different sum rules.

The basic amplitude for the radiative decay of a scalar resonance has the characteristic features of an $L = 0$ transition: the form factor for transversely polarised photons has the dimension of an energy and the basic amplitude has no explicit energy dependence (in striking contrast to pseudoscalar mesons!). Given that all hadronic decays we know are dominated by the lowest possible L transitions, the prediction for the $SU(3)_{Fl}$ relations in the structureless VMD model is

$$\Gamma_{\gamma\gamma}(\epsilon) = \Gamma_{\gamma\gamma}(\delta)\frac{m_\epsilon}{3m_\epsilon}(\sqrt{8}cos(\theta) - sin(\theta))^2$$
$$\Gamma_{\gamma\gamma}(S^*) = \Gamma_{\gamma\gamma}(\delta)\frac{m_\epsilon}{3m_{S^*}}(\sqrt{8}sin(\theta) + cos(\theta))^2 \tag{2.3.9}$$

with the corresponding sum rule

$$\Gamma_{\gamma\gamma}(S^*)m_{S^*} + \Gamma_{\gamma\gamma}(\epsilon)m_\epsilon = 3\Gamma_{\gamma\gamma}(\delta)m_\delta \tag{2.3.10}$$

If we assume that the photons resolve the structure of the scalar mesons, we obtain a different set of $SU(3)_{Fl}$ equations. In the static quark parton model, the radiative decay is in first order due to the electric dipole moment of a $q\bar{q}$ bound state. Thus, if the dipole moments obey $SU(3)_{Fl}$ on purely dimensional grounds, one would expect

$$\Gamma_{\gamma\gamma}(\epsilon) = \Gamma_{\gamma\gamma}(\delta)\frac{m_\epsilon^3}{3m_\epsilon^3}(\sqrt{8}cos(\theta) - sin(\theta))^2$$
$$\Gamma_{\gamma\gamma}(S^*) = \Gamma_{\gamma\gamma}(\delta)\frac{m_{S^*}^3}{3m_\epsilon^3}(\sqrt{8}sin(\theta) - cos(\theta))^2 \tag{2.3.11}$$

with the corresponding sum rule

$$\frac{\Gamma_{\gamma\gamma}(S^*)}{m^3_{S^*}} + \frac{\Gamma_{\gamma\gamma}(\epsilon)}{m^3_\epsilon} = \frac{3\Gamma_{\gamma\gamma}(\delta)}{m^3_\delta} \tag{2.3.12}$$

[1] Here, we assume that the non resonant amplitude is entirely real, since according to Watson [78], final state interactions become unimportant as $\beta \to 1$.

Thus, *provided that it is correct to consider the known* 0^+ *resonances as* $q\bar{q}$ *states*, the way the mass enters the $SU(3)_{Fl}$ relations is sensitive to the mechanism responsible for the decays.

It seems that the second set of $SU(3)_{Fl}$ equations makes more sense than the first because the photons coming from the decay of a $1\,GeV$ object have a wavelength of $\sim 0.4\,fm$ and should thus be able to resolve the meson's structure.

Predictions for the Radiative Widths

Predictions for the radiative decay rates of scalar resonances have been made in the framework of (non relativistic) oscillator potential models and VDM:

$\Gamma_{\gamma\gamma}(S^*)$	$\Gamma_{\gamma\gamma}(\delta)$	$\Gamma_{\gamma\gamma}(\epsilon(1300))$	*Input*	*Ref.*
–	$3.7MeV^2/\Gamma(\delta \to \pi\eta)$	$1.5MeV^2/\Gamma(\epsilon \to \pi\pi$	VDM	[63]
–	$2.5 - 3.8keV$	–	$q\bar{q}$ *oscillator*	[43]
–	$< 0.37keV$	$< 0.38keV$	$SU(6), VDM$	[64]
–	$550 \pm 270keV$	–	VDM	[65]
$A \cdot 12.8keV$	$4.8keV$	$B \cdot 8.4keV$	$q\bar{q}$ *oscillator*	[46]

$$A = (sin\theta - \frac{1}{\sqrt{8}}cos\theta) \quad B = (sin\theta - \frac{1}{\sqrt{2}}cos\theta)$$

Table 2.3.2: *Predictions for the radiative widths of scalar mesons*

From table(2.3.2), two things can be derived: 1) The differences between the model calculations are large enough to be distinguish by experiments in the near future. 2)Models with similar theoretical assumptions come to final results differing by substantial factors. Thus, it will be experimentally easy to differentiate between certain calculations, however, the present state of the theories does not allow a conceptual distinction.

Given the rather poor state of the experimental literature, it is evident that we are not yet in the position to differentiate between the model calculations.

There are no serious quantitative predictions for the radiative decays of 0^+ resonances in the framework of $K\bar{K}$ or $q\bar{q}q\bar{q}$ models [66]. Qualitatively, one would expect that such models predict rather small radiative widths, compared to the conventional approaches.

The q^2 Dependence of Scalar Meson Formation

We have seen that the experimental evidence for 0^+ states in $\gamma\gamma$ collisions is quite limited. Therefore, a discussion of the q^2 dependence of their cross sections may seem unnecessary. However, if we extrapolate the vast experimental progress in $\gamma\gamma$ physics by a few years, and if we think of the large luminosity now delivered by DORIS-II and PEP, there should be no doubt that in the medium term future, tagged 0^+ resonances will appear in the experimental literature.

Since the basic amplitude for scalar formation has no explicit energy dependence, the cross section can be expected to be rapidly falling. Eq.(2.3.4) implies that, on resonance mass, it evolves with q_1^2 like $\sigma_{TT}(q_1^2,0) \sim (F^T(q_1^2,0))^2 \cdot \frac{1}{1-q_1^2/M^2}$. Thus, even in the absence of form factor effects, the cross section falls with q_1^2.

There is only one paper which tries to calculate the q^2 evolution of scalar meson formation on a quantitative basis[1] In the framework of the non relativistic quark model, Krasemann and Vermaseren [67] give a tensor which, contracted with the transverse photon polarisation vector, gives the following shape of the $(++)$ amplitude:

$$M_{++}(q_1^2 q_2^2) \sim \frac{W^2((q_2 - q_1^2)^2 - 4q_1q_2)) - (q_2^2 - q_1^2)^2}{(q_1q_2)^2} \tag{2.3.13}$$

The authors prediction for the q^2 dependence of scalar formation is based on the quark model and the observation of a striking feature of the covariant amplitude for an VVS $(L = 0)$ coupling (see appendix D). Consider the $q_1^2 \to 0$ limit for such an amplitude:

$$A_{\mu\nu}(q_1, q_2) = g_{\mu\nu} - \frac{q_{2\mu}q_{1\nu}}{q_1 \cdot q_2 - \sqrt{q_1^2 q_2^2}} \to g_{\mu\nu} - \frac{q_{2\mu}q_{1\nu}}{q_1 \cdot q_2} \tag{2.3.14}$$

The latter tensor is gauge invariant *and* simultaneously the covariant formulation of an E_1 transition between a scalar ($\uparrow\uparrow$ $L, L_z = 1, -1$) and a vector ($\uparrow\uparrow$ $L = 0$). Since photons have a large overlap with spin aligned $q\bar{q}$ pairs of zero relative orbital angular momentum, the above amplitude connects the final state scalar with the largest hadronic component of the photon. We can thus assume that at least in the low q^2 regime, this amplitude dominates[2].

Having established the form of the covariant amplitude, we can proceed to calculate the form factor. For the case, where one photon is real, this is trivial, because of the exact identity of an E_1 and an $L = 0$ amplitude at $q_1^2 = 0$. For the latter, it is well known that finite size effects cancel to first order. We can just assume the form factor to be constant. The prediction is then

$$\begin{aligned} T^{\mu\nu} &= g_{\mu\nu} - \frac{q_{2\mu}q_{1\nu}}{q_1 \cdot q_2} \\ \to M_{++}(q_1^2, q_2^2) &= M_{++}(0.0) \\ M_{00}(q_1^2, q_2^2) &= 2M_{++}(0.0)\frac{\sqrt{q_1^2 q_2^2}}{W^2 - q_1^2 - q_2^2} \end{aligned} \tag{2.3.15}$$

The resulting helicity amplitudes are finite throughout. This *a posteriori* confirms that the use of the E_1 amplitude without further form factors is meaningful.

The q^2 independence of the transverse helicity amplitude is in marked contrast to what would be expected in the context of VDM, where an additional $\frac{1}{1-q^2/m_\rho^2}$ term would enter the amplitude.

[1] In ref [17], asymptotic power laws are given, however, it is not specified which kinematic configuration is referred to.

[2] For large values of momentum transfer, higher order transitions may become important.

Introduction

The three neutral tensor mesons $f(1270)$, $A_2(1320)$ and $f'(1525)$ have all been seen in $\gamma\gamma$ reactions. The tensor meson nonet has the nice feature that it seems to be ideally mixed. The f' resonance has only been firmly established in the $K\overline{K}$ final state. Accepted data yield an upper limit of $B(f' \to \pi^+\pi^-) < 0.013(95\%cl.)$. This implies that for SU(3) considerations of the $\gamma\gamma$ couplings, the mixing angle needs not necessarily be taken as a variable. In other words, the quark representation

$$\begin{aligned} f &= \frac{1}{\sqrt{2}}(u\bar{u} + d\bar{d}) \\ A_2 &= \frac{1}{\sqrt{2}}(u\bar{u} - d\bar{d}) \\ f' &= (s\bar{s}) \end{aligned} \tag{2.4.1}$$

is a good starting point for further considerations. For the tensor mesons, such a well founded framework is necessary, given the many parameters which enter their $\gamma\gamma$ coupling.

The formal description of tensor meson formation in two photon reactions is rather complicated because the most general amplitude involves five couplings (form factors). Only one paper [17] deals with this problem in all generality. However, from an experimentalists point of view, the result cannot be considered satisfactory.[1] The amplitudes relevant for no tag and single tag data can more suitably be written as (c.f. appendix A)

$$\begin{aligned} T_{\mu\nu} = \Big\{ & F_{TT0}\, G_{\mu\nu}\Delta_\alpha\Delta_\beta + F_{TT2} G_{\mu\alpha} G_{\nu\beta} \\ & + F_{TL}\left(G_{\mu\alpha}Q_{2\nu} - Q_{1\mu}G_{\nu\alpha}\right)\Delta_\beta \\ & + F'_{TL}(q_2^2 - q_1^2)\left\{G_{\mu\alpha}Q_{2\nu} + Q_{1\mu}G_{\nu\alpha}\right\}\Delta_\beta \Big\} E^{\cdot\alpha\beta} \end{aligned} \tag{2.4.2}$$

These form factors of eq.(2.4.2) have a straight forward experimental interpretation: F_{TT0} and F_{TT2} measure the rate of helicity zero and two respectively.[2] They are only sensitive to transversely polarised photons. The effective form factor

$$F_{TL}^{eff.} \equiv F_{TL} + (q_1^2 - q_2^2)F'_{TL} \tag{2.4.3}$$

which measures the rate of $J_z = \pm 1$ formation, only contributes if at least one photon is off mass shell. Notice that the amplitudes for helicity $J_z = +1$ and $J_z = -1$ have to be equal in magnitude for either $q_1^2 = q_2^2$ or $q_2^2 = 0$. If we restrict one of the photons to be real, the cross sections can be written as

$$\begin{aligned} \sigma_{TT}(J_z = 2) &= \frac{(F_{TT2})^2}{4\sqrt{X}} \frac{M^2}{W} \frac{\Gamma}{(W^2 - M^2)^2 + \Gamma^2 M^2} \\ \sigma_{TT}(J_z = 0) &= \frac{1}{2}\tau_{TT} = \frac{8(F_{TT0})^2}{3\sqrt{X}} \frac{X^2 M^2}{W^5} \frac{\Gamma}{(W^2 - M^2)^2 + \Gamma^2 M^2} \\ \sigma_{TL}(J_z = 1) &= \frac{(F_{TL}^{eff.})^2}{W^5}(-q_2^2)\sqrt{X}M^2 \frac{\Gamma}{(W^2 - M^2)^2 + \Gamma^2 M^2} \end{aligned} \tag{2.4.4}$$

Only two of the form factors enter the partial width:

$$\Gamma_{\gamma\gamma} = \frac{(F_{TT2})^2}{80\pi M} + \frac{(F_{TT0})^2 M^3}{120\pi} \tag{2.4.5}$$

and thus, for an analysis of "no tag" data, $F_{TL}^{eff.}$ may be ignored. However, the assumed ratio of F_{TT2}/F_{TT0} can have a large impact on the final result. Fortunately, what ever way one looks at tensor meson formation from a theoretical point of view, one ends up with a very small contribution from F_{TT0}. In particular, if the tensor meson is considered to be a non relativistic bound state [67], and the decay proceeds through direct annihilation of the quarks, the amplitude M_{--} vanishes for on shell photons. If the tensor meson is produced by some VDM mechanism, one would expect the $L = 0$ amplitude to dominate as well. Finite energy sum rules [69,70] give a very similar result: $M_{--} \gg M_{++}$. Thus, if an experiment is not able to measure the helicity amplitudes separately, the assumption of $J_z = \pm 2$ is the obvious one. However, in the static quark model (see below), a sizeable contribution of the $J_z = 0$ amplitude is also possible. Assuming that the E_1 transition dominates, one gets $\Gamma_{\gamma\gamma}(J_z = 0) = \frac{1}{6}\Gamma_{\gamma\gamma}(J_z = 2)$.

Measurements of $\Gamma_{\gamma\gamma}(A_2)$

The formation of the A_2 meson in two photon reactions was first observed by the Crystal Ball collaboration in the decay channel $A_2 \to \eta\pi^0 \to 4\gamma$. The dominant decay mode $A_2 \to \rho^\pm\pi^\mp$ was subsequently analysed by $PETRA$ experiments. The results are shown in table(2.4.1):

$\Gamma_{\gamma\gamma}(keV)$	*Experiment*	*chan.*	*Ref.*
$0.77 \pm 0.18(\pm 0.27)$	*Crystal Ball*	$\eta\pi^0$	[71]
$0.81 \pm 0.19(\pm 0.27)$	*CELLO*	$\rho\pi$	[72]
$0.84 \pm 0.07(\pm 0.15)$	*JADE(prelim.)*	$\rho\pi$	[61]
$1.06 \pm 0.18(\pm 0.19)$	*PLUTO*	$\rho\pi$	[73]
$1.14 \pm 0.20(\pm 0.26)$	*Crystal. Ball*	$\eta\pi^0$	[62]

Table 2.4.1: *Measurements of* $\Gamma_{\gamma\gamma}(A_2)$

The channel $\eta\pi^0$ is the ideal one to study the helicity composition of the A_2 formation, since it is rather clean and the η and the π^0 have both no spin so that their angular distribution

[1] First of all, the problem of avoiding $1/q^2$ type singularities is overcome by giving the basis tensors dimensions up to the sixth power of energy. This leads to artificial mass shifts of the resonances. Secondly, each of the form factors contributes to so many helicity amplitudes that an experimental analysis in terms of the given form factors would be a mess.

[2] The form factors defined here are *not* dimensionless. Different dimensions for different couplings are well known in classical electrodynamics (c.f. dipole, quadrupole etc. transitions).

with respect to the $\gamma\gamma$ axis should show the characteristic $sin^4\theta$ term if the the A_2 is produced dominantly with helicity $J_z = \pm 2$. On the other hand, the two photon width determined through this channel crucially depends on the assumptions on the helicity because of the strong centering of the detector acceptance near $cos\theta = 0$. The Crystal Ball collaboration [62] collected enough statistics at DORIS II to disentangle the $J_z = 2$ and $J_z = 0$ amplitudes, obtaining

$$\sigma(J_z = 2) = 0.81 \pm 0.22\,\sigma(tot) \quad (Crystal\ Ball)$$

The reaction $A_2 \to \rho^{\pm}\pi^{\mp}$ is much harder to analyse because the large widths of the ρ makes the interference terms between the ρ^+ and the ρ^- decay non negligible. The modelling of this decay is particularly hard, because of the spin barriere and phase space correlations between the two wide mesons A_2 and ρ. The easiest way of implementing such factors correctly is to consider the entire process in one piece, i.e. write

$$|M(\gamma\gamma \to \pi^-\pi^-\pi^0)|^2 = |M(\gamma\gamma \to A_2)BW(A_2)\{M(A_2 \to \rho^-\pi^-)M(\rho^+ \to \pi^+\pi^0)BW(\rho^+) + M(A_2 \to \rho^-\pi^-)M(\rho^- \to \pi^-\pi^0)BW(\rho^-)\}|^2 \tag{2.4.6}$$

The A_2 decay matrix element, i.e. the term in curly brackets above can be written covariantly in terms of the momenta $k_1(\pi^+)$, $k_2(\pi^0)$ and $k_3(\pi^-)$:

$$M = iE^{\alpha\beta}k^{\alpha}_{12-3}\,e_{\mu\nu\beta\gamma}\,k^{\mu}_3 k^{\nu}_{12}k^{\gamma}_{1-2}\,BW(1,2) + \text{"1} \to 3\text{"} \tag{2.4.7}$$

Here, as in other chapters, the indices of a vector denote its parents, for example is $k_{12-3} = k_1 - k_2 - k_3$. Since the matrix element is covariant, one can calculate the helicity amplitudes in a common frame. In the $\gamma\gamma$ c.m.s. they are

$$\begin{aligned}
\xi M_{--} &= \frac{W}{4}|\vec{k}_{12-3}|^2|\vec{k}_{1-2}|sin\theta_{12-3}e^{i\phi_{12-3}}BW(1,2)\\
&\cdot\{cos\theta_{12-3}sin\theta_{1-2}e^{i\phi_{1-2}} - sin\theta_{12-3}cos\theta_{1-2}e^{i\phi_{12-3}}\}\\
&- \frac{W}{4}|\vec{k}_{32-1}|^2|\vec{k}_{3-2}|sin\theta_{32-1}e^{i\phi_{32-1}}BW(3,2)\\
&\cdot\{cos\theta_{32-1}sin\theta_{3-2}e^{i\phi_{3-2}} - sin\theta_{32-1}cos\theta_{3-2}e^{i\phi_{32-1}}\}\\
\xi M_{-0} &= \frac{W}{4}|\vec{k}_{12-3}|^2|\vec{k}_{1-2}|\{isin^2\theta_{12-3}sin\theta_{1-2}sin(\phi_{12-3} - \phi_{1-2})e^{i\phi_{12-3}}\\
&- cos\theta_{12-3}(cos\theta_{12-3}sin\theta_{1-2}e^{i\phi_{1-2}} - sin\theta_{12-3}cos\theta_{1-2}e^{i\phi_{12-3}})\}BW(1,2)\\
&- \frac{W}{4}|\vec{k}_{32-1}|^2|\vec{k}_{3-2}|\{isin^2\theta_{32-1}sin\theta_{3-2}sin(\phi_{32-1} - \phi_{3-2})e^{i\phi_{32-1}}\\
&- cos\theta_{32-1}(cos\theta_{32-1}sin\theta_{3-2}e^{i\phi_{3-2}} - sin\theta_{32-1}cos\theta_{3-2}e^{i\phi_{32-1}})\}BW(3,2)\\
\xi M_{--} &= \frac{3W}{2\sqrt{6}}|\vec{k}_{12-3}|^2|\vec{k}_{1-2}|sin\theta_{12-3}cos\theta_{12-3}sin\theta_{1-2}sin(\phi_{12-3} - \phi_{1-2})BW(1,2)\\
&- \frac{3W}{2\sqrt{6}}|\vec{k}_{32-1}|^2|\vec{k}_{3-2}|sin\theta_{32-1}cos\theta_{32-1}sin\theta_{3-2}sin(\phi_{32-1} - \phi_{3-2})BW(3,2)
\end{aligned} \tag{2.4.8}$$

ξ being the inverse of the couplings involved: $\xi = (F_{A_2\rho^-\pi^-}F_{\rho^-\pi^-\pi^0})^{-1}$. It can be seen from the characteristic $|\vec{k}|$ factors that this is an $L = 2$ transition, as required by the intrinsic

parities involved. Thus, the couplings and consequently the widths in the Breit Wigner functions have to be taken variable (c.f. appendix D).

The interference terms resulting from eq.(2.4.8) makes all angular distributions more isotropic. This implies that the $\gamma\gamma$ widths obtained from an analysis of the $\rho\pi$ final state has only little dependence on the assumptions about the A_2 helicity (usually less than detector specific systematic errors.).

Nevertheless, a full Dalitz Plot analysis (c.f. fig.(2.4.1)) gave a non trivial result [73]

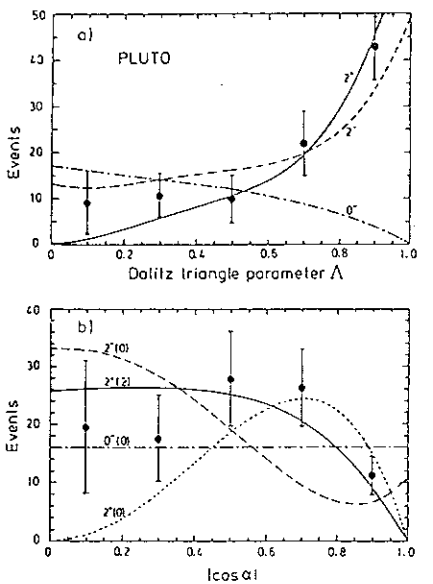

Figure 2.4.1: *The Dalitz plot analysis of the reaction $\gamma\gamma \to \pi^+\pi^-\pi^0$ confirms the interpretation of the data as A_2 formation and indicates the expected dominance of helicity 2 production.*

$$\sigma(J_z = 2) = 0.62 \pm 0.39\,\sigma(tot) \quad (PLUTO)$$

This is consistent with the Crystal Ball result but, for the reasons stated above, not as accurate.

Measurements of $\Gamma_{\gamma\gamma}(f)$

The f meson has been seen by most of the experiments doing two photon physics. No other state has been analysed in as many different ways as the f. The Crystal Ball collaboration, for example [71], studied the reaction $\gamma\gamma \to \pi^0\pi^0$ and measured a radiative width of

$$\Gamma_{\gamma\gamma}(f) = 2.7 \pm 0.2 \pm 0.6keV \quad (J_z \equiv 2) \quad Crystal\ Ball$$
$$\Gamma_{\gamma\gamma}(f) = 2.9^{+0.6}_{-0.4} \pm 0.6keV \quad (J_z\,fitted)$$

Furthermore, the helicity of the f meson could be determined to be

$$\sigma(J_z = 0)/\sigma(J_z = 2) = 0.12 \pm 0.39 \quad Crystal\ Ball$$

All other published experiments are based on analyses of the $\pi^+\pi^-$ final state. The wide range of analysis methods is a reflection of the uncertainty about the structure of the non resonant $\pi^+\pi^-$ continuum under the f meson.

The parameterisation of the $\pi^+\pi^-$ continuum in the resonance region poses problems since, with increasing energy, the Born term approximation becomes less reliable. Further complications arise from other direct channels, in particular the scalar mesons $S^*(980)$ and $\epsilon(1300)$, which may contribute to the observed cross sections. How large is the error introduced by the uncertainty about the structure of the $\pi^+\pi^-$ continuum? The published values of $\Gamma_{\gamma\gamma}(f)$ give an *a posteriori* estimate, since most collaborations have done the analysis in different ways, the only common assumption being that the f is produced with helicity $J_z = \pm 2$. Theoretically, this seems to be what everybody expects, however this assumption has a large impact on the final results, as can be seen in fig(2.4.2), where the centre of mass decay distributions are superimposed onto a "typical" acceptance curve for a solenoid detector. One can easily see that assuming $J_z = 0$ rather than 2 leads to an increase of the "measured" cross section by some 30 per cent.

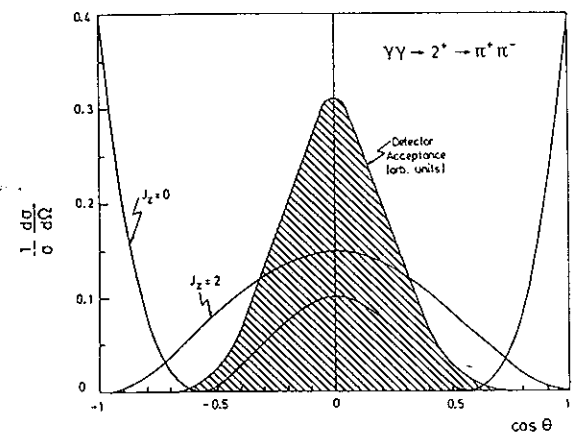

Figure 2.4.2: *The angular distribution of pion pairs from the decay of a tensor resonance, assuming helicity* 0 *and* ± 2 *respectively. The comparison with a "typical" detector acceptance (shaded area) stresses the importance of the knowledge of the helicity.*

$\Gamma_{\gamma\gamma}(keV)$	*Experiment*	*continuum*	*Ref.*
$2.30 \pm 0.50(\pm 0.35)$	*PLUTO*	*none*	[74]
$3.60 \pm 0.30(\pm 0.50)$	*Mark II*	*Born, coherent*	[75]
$3.20 \pm 0.20(\pm 0.60)$	*TASSO*	*incoherent fit*	[76]
$2.50 \pm 0.10(\pm 0.50)$	*CELLO*	*Mennessier Model*	[77]
$2.85 \pm 0.25(\pm 0.50)$	*PLUTO*	*Mennessier Model*	[51]
$2.70 \pm 0.05(\pm 0.20)$	*DELCO*	*Born, coherent*	[79]
$2.39 \pm 0.06(\pm 0.30)$	*PEP49(prelim.)*	*Born, phase fit*	[80]
$2.52 \pm 0.13(\pm 0.38)$	*Mark II*	*Born/QCD, ph.fit*	[81]

Table 2.4.2: *Measurements of* $\Gamma_{\gamma\gamma}(f)$ *in* $\gamma\gamma \to \pi^+\pi^-$

As can be seen from this table, the purely experimental uncertainties are at present still

larger than possible systematic mass shifts due to the different assumptions on the underlying continuum. It is interesting to notice that those collaborations who have analysed f formation in terms of models with explicit assumptions on the size and phase of the $\pi^+\pi^-$ continuum, i.e. Born Amplitude or Mennessier Model, all get values for the f mass, which are consistent with its nominal value, as can for example been seen in fig.(2.4.3). On the other hand, this is in clear contradiction with the PLUTO result on the low lying continuum, which is not well described by either of these models.

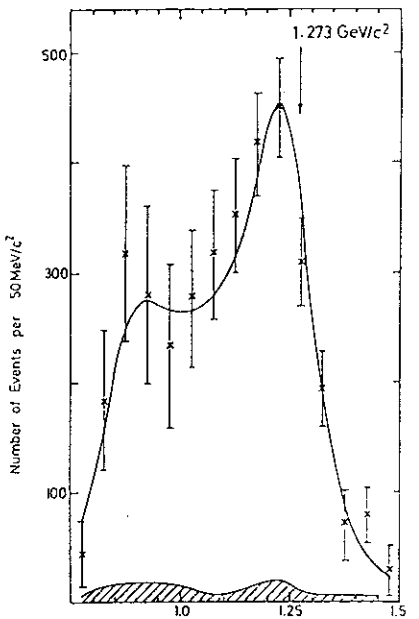

Figure 2.4.3: *This analysis of* $\pi^+\pi^-$ *pairs in the* f *region was the first one taking into account the interference of the* f *with the nonresonant continuum. The curve is the Mennessier model.*

There is a possible explanation for this discrepancy: the shift of the f peak is determined by both, the average amplitude *and* the fall off of the nonresonant amplitude with $W_{\gamma\gamma}$. Roughly speaking, a fast falling small background can lead to the same mass shift as a slowly varying large background. It is quite likely that the apparently good description of the $\pi^+\pi^-$ cross section in the f region is the result of such a compensation. This in turn would imply that all current experiments *underestimate* the two photon width of the f, since they overestimate the background. Also, it should not be forgotten that most analyses approximate the M^2/W term in the single particle phase space by M, leading to an upwards shift of the f mass in the Monte Carlo and hence to a downwards shift of the "measured" f mass, which is again compensated by assuming a too large background. Last, not least, although the scalar resonances do not interfer with the f, all three of them lead to fast falling event backgrounds, the δ and the S^* because of finite momentum (detector-) effects, and the ϵ since its large widths allows it to "move" below the f mass. It must be stressed that a flat angular distribution below the f would be a strong indication for the presence of a scalar resonance!

It would be nice to see a partial wave analysis, in particular in view of the fact that so

many partial waves vanish because of helicity conservation (c.f. eq 2.2.5). Another alternative - which may be more realistic because of the small detector acceptances beyond $cos\theta^* \simeq 0.3$- would be to use the finite size pion Ansatz for the calculation of the continuum and its interference.

Interference of the f with the $\pi^+\pi^-$ Continuum

For the calculation of the interference between the finite size pion continuum and the f, we first need the covariant expression for the decay matrix element. The standard form

$$\begin{aligned} M_{J_z}(f \to \pi^+\pi^-) &= F_{f\pi\pi} E^{\mu\nu}_{J_z}(k_2 - k_1)_\mu (k_2 - k_1)_\nu \\ \to \Gamma_{\pi\pi} &= \frac{M_f^3 F_{f\pi\pi}^2}{120\pi}\beta^5 \end{aligned} \tag{2.4.9}$$

leads to the following products of spherical harmonics and Clebsch Gordan coefficients:

$$\begin{aligned} M_2 &= \frac{1}{2}F_{f\pi\pi}\beta^2 W^2 sin^2\theta e^{2i\phi} \\ M_1 &= -F_{f\pi\pi}\beta^2 W^2 sin\theta cos\theta e^{i\phi} \\ M_0 &= \frac{1}{\sqrt{6}}F_{f\pi\pi}\beta^2 W^2(3cos^2\theta - 1) \end{aligned} \tag{2.4.10}$$

and the transverse cross section can now be written as

$$\frac{d\sigma}{d\Omega} = \frac{\beta}{(16\pi)^2\sqrt{X}}\left(|M(non-res.)|^2 + |M(res.)|^2 + "INF"\right)$$

$$\begin{aligned} |M(non-res.)|^2 &= 16\pi^2\alpha^2 G^2(t,u,q_1^2,q_2^2)\left(\frac{\beta^2W^2cos^2\theta}{2(t-m_\pi^2)} + \frac{\beta^2W^2cos^2\theta}{2(u-m_\pi^2)} + 1\right)^2 \\ &+ 8\pi^2\alpha^2 G^2(t,u,q_1^2,q_2^2)\beta^4W^4cos^4\theta\left(\frac{1}{t-m_\pi^2} + \frac{1}{u-m_\pi^2}\right)^2 \\ |M(res.)|^2 &= \frac{1}{4}(F_{TT2}F_{f\pi\pi})^2\beta^4W^4sin^4\theta\frac{1}{(W^2-M^2)^2+\Gamma^2M^2} \\ &+ \frac{16}{9}(F_{TT0}F_{f\pi\pi})^2\beta^4X^2(3cos^2\theta-1)^2\frac{1}{(W^2-M^2)^2+\Gamma^2M^2} \\ "INF" &= -2\pi\alpha G(t,u,q_1^2,q_2^2)F_{TT2}F_{f\pi\pi}\beta^4W^4sin^2\theta cos^2\theta \\ &\cdot\left(\frac{1}{t-m_\pi^2} + \frac{1}{u-m_\pi^2}\right)\frac{W^2-M^2}{(W^2-M^2)^2+\Gamma^2M^2} \\ &+ \frac{32}{3}\pi\alpha F_{TT0}F_{f\pi\pi}G(t,u,q_1^2,q_2^2)X\beta^2(3cos^2\theta-1) \\ &\cdot\left(\frac{\beta^2W^2cos^2\theta}{2(t-m_\pi^2)} + \frac{\beta^2W^2cos^2\theta}{2(u-m_\pi^2)} + 1\right)\frac{W^2-M^2}{(W^2-M^2)^2+\Gamma^2M^2} \end{aligned} \tag{2.4.11}$$

If we assume that the non resonant amplitude is entirely real, the entire dynamics is reflected in four unknown functions: $G(t,u,q_1^2,q_2^2)$ describes the non pointlike structure of the pion in the non resonant amplitude ($G = 1 \to$ QED). An estimate on how G could look like is

given in the chapter of pseudoscalar pair production. For the purpose of determining the f parameters for the collision of quasi real photons, our knowledge can be regarded as sufficient. The fact that the interference is constructive below the nominal resonance mass indicates that the product $(F_{TT2}F_{f\pi\pi})$ must be negative (it has to be real).

A Measurement of $\Gamma_{\gamma\gamma}(f')$

The f' seems to decay nearly exclusively into kaon pairs; 50 % into K^+K^-, 25 % into $K_s^0K_s^0$ and $K_l^0K_l^0$ respectively[1] It has only been seen by the TASSO collaboration [82] giving a radiative width of

$$\Gamma_{\gamma\gamma}(f') \simeq \Gamma_{\gamma\gamma}(f') \times B(f' \to K\overline{K}) = 0.11 \pm 0.02 = 0.04keV \quad (TASSO)$$

The corresponding invariant mass spectra are shown in fig.(2.4.4). The fact that there is only one measurement so far, and that this measurement is only two standard deviations away from 0 is already a hint towards severe difficulties in the analysis of $K\overline{K}$ final states. In the charged decay channel, one can only hope to find it by means of particle identification. The rate of f' events is so small compared with the QED channels $\mu^+\mu^-$ and e^+e^- that by means of statistical subtractions one would never recover the signal from behind the statistical error bars. Good particle identification is thus necessary. For the case of neutral kaons, this means positive identification of secondary vertices (from the in flight decays) or excellent momentum resolution.

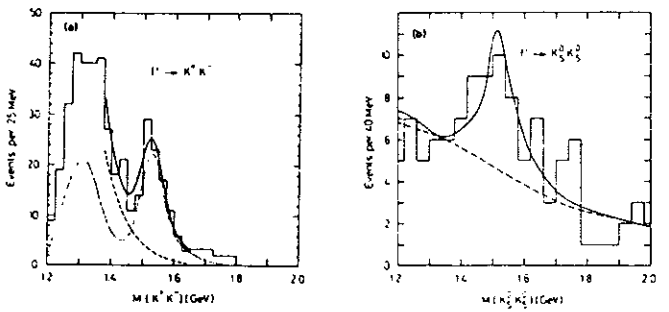

Figure 2.4.4: *These two mass spectra from the TASSO detector are the basis of the first, and so far only measurement of $\Gamma_{\gamma\gamma}(f')$. The solid lines are the final fits, the dashed lines are background estimates.*

[1] the decay into $K_l^0K_s^0$ violates CP and occurs only at a negligible rate.

Interference Patterns in $K\bar{K}$ Final States

The two other tensor mesons decay into kaon pairs as well. Since all of them are fairly wide objects, they do not only interfer with the non resonant K^+K^- continuum, but also with each other, and all the interference terms turn out to be non negligible. Fortunately, as pointed out by Lipkin [83], the signs of the interference terms follow from rather weak assumptions, the Zweig rule and (approximate) $SU(3)_{Fl}$ symmetry of the strong interaction. Arguing as demonstrated in fig.(2.4.5), which is a pictorial representation of Lipkin's arguments, one gets

$$\begin{aligned} &< f|K^+K^- > = + < A_2|K^+K^- > = < f'|K^+K^- > /\sqrt{2} \\ &= < f|K^0\bar{K}^0 > = - < A_2|K^0\bar{K}^0 > = < f'|K^0\bar{K}^0 > /\sqrt{2} \end{aligned} \tag{2.4.12}$$

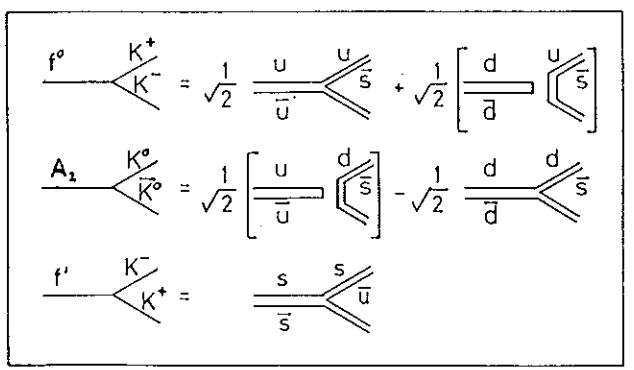

Figure 2.4.5: *Three examples of tensor meson decays into kaon pairs. The amplitudes in brackets are small according to the Zweig rule.*

The fact that $SU(3)_{Fl}$ is not exact may alter the relative strengths of the amplitudes, however, it can never change the signs. Thus, the direct channel contribution in K^+K^- production is the sum

$$|M_{a,b}(res)|^2 = \left| \sum_{R=f,A_2,f'} \frac{M_{a,b}(\gamma\gamma \to R) M_{J_z=a-b}(R \to K^+K^-)}{W^2 - M_R^2 + iM_R\Gamma_R} \right|^2 \tag{2.4.13}$$

with all coupling constants having the same sign. For the case of $K^0\bar{K}^0$ production, the A_2 contribution has a minus sign relative to the others. The explicit form of eq.(2.4.13) follows from eq.(A-8). Another consequence of the above reasonning is that one expects the interference between the tensor mesons and the underlying K^+K^- continuum to have the same sign as the $f - \pi^+\pi^-$ interference. This interference is of the same form as in eq.(2.4.10), just that "INF" now becomes a sum over the three tensor mesons.

$SU(3)_{Fl}$ Relations for Tensor Mesons

Since there is more than one coupling involved in the radiative decay of tensor mesons $SU(3)_{Fl}$ cannot give a unique prediction. In plain terms: Using the ratios of the values for the radiative widths of tensor mesons alone, *one cannot test* $SU(3)_{Fl}$. *However*, from other measurements involving tensor mesons, i.e. hadronic decays, it is known that $SU(3)_{Fl}$ is a good symmetry for this nonet. Let us thus reverse the argument and impose the validity of $SU(3)_{Fl}$ as well as ideal mixing onto different approaches - and try thus to get some insight into the dynamics.

In the context of VDM, one would expect that tensor meson formation proceeds through the lowest possible order of angular momentum. Although an $L = 0$ tensor vector vector coupling is not gauge invariant, there is *one* amplitude which has the characteristic features of an $L = 0$ transition: $T_{\mu\nu}^{TT2}$ is structureless, produces thus no spin barriere. and has the dimension of energy. In contrast, $T_{\mu\nu}^{TT0}$ has the characteristic features of an $L = 2$ transition.[1] Thus, assuming that radiative decays behave like hadronic ones, one gets

$$\begin{aligned} &\Gamma_{\gamma\gamma}(f, J_z = 2) \cdot M_f / \Gamma_{\gamma\gamma}(A_2, J_z = 2) \cdot M_{A_2} \cdot \Gamma_{\gamma\gamma}(f', J_z = 2) \cdot M_{f'} = 25/9/2 \\ &\quad \textit{dominating} \quad \textit{over} \\ &\frac{\Gamma_{\gamma\gamma}(f, J_z = 0)}{M_f^3} / \frac{\Gamma_{\gamma\gamma}(A_2, J_z = 0)}{M_{A_2}^3} / \frac{\Gamma_{\gamma\gamma}(f', J_z = 0)}{M_{f'}^3} = 25/9/2 \end{aligned} \tag{2.4.14}$$

The purely electromagnetic interactions which take place between neutral systems are reflections of their internal charge and current distributions. If, for example, the two photon widths are related to the mesons dipole moments, $(\vec{\epsilon})$, and those are similar for all nonet members, the SU(3) relation would look as for the 0^- nonet. Taking the covariant amplitude of the corresponding E_1 transition

$$T_{\mu\nu} \sim \vec{\epsilon} \left(g_{\mu\alpha} - \frac{q_{2\mu} q_{1\alpha}}{q_2 \cdot q_1} \right) \left(g_{\nu\beta} - \frac{q_{1\nu} q_{2\beta}}{q_1 \cdot q_2} \right) E^{\cdot\alpha\beta} \tag{2.4.15}$$

gives the sum rule

$$\begin{aligned} &\frac{\Gamma_{\gamma\gamma}(f, J_z = 2)}{M_f^3} / \frac{\Gamma_{\gamma\gamma}(A_2, Jz = 2)}{M_{A_2}^3} \cdot \frac{\Gamma_{\gamma\gamma}(f', Jz = 2)}{M_{f'}^3} = 25.9/2 \\ &\quad \textit{together with} \\ &\Gamma_{\gamma\gamma}(J_z = 0) = \frac{1}{6}\Gamma_{\gamma\gamma}(J_z = 2) \quad \textit{for all tensor mesons} \end{aligned} \tag{2.4.16}$$

In the framework of the quark model, there is a different class of calculations. Whereas the above E_1 transition can be interpreted as a two step process (i.e. the quarks are first put into an s - *orbital* by means of photon radiation and then annihilate), most published calculations attempt to calculate the radiative widths in a one step model. However, since the tensor mesons are regarded as p wave $q\bar{q}$ systems, one step annihilations can only occur due

[1] This result of purely formal considerations coincides with intuition. Two helicities one aligned give $J_z = 2$ and thus $J = 2$ without further L required. If, on the other hand, the helicities of the two photons annihilate - where but from an additional spatial angular momentum should the $J = 2$ come from?

to relativistic corrections involving the derivative of the wave function at the origin, $R'(r=0)$ (see for example ref [67]):

$$\Gamma_{\gamma\gamma}(f) = \frac{160}{9}\alpha^2\frac{R'(0)^2}{M^4} \qquad (2.4.17)$$

Since the derivatives of the wave functions have very different mass dependences in different models, $SU(3)_{Fl}$ cannot be used to test the basic model assumption, i.e. the assumption $q\bar{q}$ annihilation being responsible for the decay. However, it does provide a tool for fine tuning the shapes of the wave functions and thus the model parameters.

Experimental Status of $SU(3)_{Fl}$ for Tensor Mesons

Since there is only one statistically poor measurement of $\Gamma_{\gamma\gamma}(f')$, $SU(3)_{Fl}$ can only be "tested" (s.a.) together with the assumption of ideal mixing. Since the masses of the f and the A_2 only differ by 4%, the ways the masses enter the various $SU(3)_{Fl}$ relations in different dynamic approaches have only little influence on the experimental conclusions about the validity of $SU(3)_{Fl}$, in particular in view of the $\sim 20\%$ systematic errors quoted by most experimental groups.

From the tables of the measured radiative widths of the f and A_2, one can see that, in contrast to the [illegible]nonet, no serious deviations from $SU(3)_{Fl}$ have ever been observed. In fact, the most recent measurements point towards an exact fulfillment of this symmetry. We can thus be optimistic about the future, when more accurate measurements of $\Gamma_{\gamma\gamma}(f')$ may tell right from wrong concepts.

Comparison of the Radiative Widths with Models

A more direct access to the mechanism governing tensor meson formation in $\gamma\gamma$ collisions can be obtained by comparing the absolute values of the radiative widths with model calculations. An impressive amount of work has been dedicated to their calculation. The following table contains only the results published after 1972, since for older calculations, it is often hard to to find out to which extent the discrepancies between theory and experiment are due to a wrong Ansatz or the result of inaccurate data input.

$\Gamma_{\gamma\gamma}(f)$ /keV	$\Gamma_{\gamma\gamma}(A_2)$ /keV	$\Gamma_{\gamma\gamma}(f')$/keV	*Input*	*Ref.*
1.2 – 2.3	0.46 – 0.81	0.14 – 0.19	$VDM, h.o., q\bar{q}$	43
~ 2.1	–	–	*symmetries*	84
4.3 – 20	1.7 – 8	0.6 – 2.8	$VDM, SU(6), dipole$	64
~ 9.2	–	–	*sum rules*	85
2.6	0.83	0.012	$VDM.h.o., q\bar{q}$	46
0.92	0.33	0.08	$rel.q\bar{q}$, *pot.*	86
2.66 ± 0.45	0.9 ± 0.36	$0.144 \pm 0.4/B(K\bar{K})$	$SU(3), E_1$	87
3.61	1.44	0.063	$q\bar{q}\ pot + QCD$	47

Table 2.4.3: *Predictions for the radiative widths of tensor mesons*

Here, *h.o.* stands for harmonic oscillator. Notice that there is no "pure" VDM prediction. The reason is obvious: There are only little data on $T \to V\gamma$ and $T \to VV$ has no phase space. There is thus no obvious tool for normalisation. There is also no analogon of the PCAC quark parton prediction - again because there is no obvious normalisation procedure.

The predictions in the framework of dipole transitions of the type $T \to V\gamma \to \gamma\gamma$ using "heavy" ($m_q \simeq M/2$) quarks give a reasonnable description of the observed decay widths, whereas a calculation stressing relativistic effects and attempts to calculate radiative widths from symmetry considerations alone are less successful. It is very interesting to notice that the two calculations which are closest to the measured widths of the f and the A_2 ([46,87]) differ by about a factor of 10 for the radiative widths of the f'. The conclusion is thus similar as the conclusion of the $SU(3)_{Fl}$ discussion: A good measurement of the f' is needed.

Measurements of Tensor Meson Form Factors

The data on tagged tensor meson formation are quite poor. This can be understood as a consequence of a "lack of spin valley": in contrast to pseudoscalar formation, the lowest dimension $\gamma\gamma \to T$ coupling ($T^{TT2}_{\mu\nu}$) is structureless and thus, even in the absence of form factor effects the cross section for tensor mesons produced with helicity $J_z = 2$ falls, according to the flux factor, like $(1 - q_1^2/M^2)^{-1}$.

Only the f meson has been seen in single tag events. The TASSO collaboration [76] gives no quantitative result and simply states *"The data are not inconsistent with the model of Krasemann and Vermaseren [67] however, a lower width would be preferred."* The Mark II collaboration [81] shows "$\Gamma_{\gamma\gamma}(q^2)$" in three bins of q^2.

It is clear that due to the presence of three independent form factors for one real and one virtual photon, cross sections indegrated over a limited solid angle are difficult to interpret theoretically. Since in practice, acceptance functions for different helicity cross sections differ, the published measurements of tagged f meson production can mainly serve as upper limits for individual (transverse) amplitudes.

It is evident that a lot more statistics will be required until the helicity form factors can be measured individually. Notice though that in the special case where the final state is a pair of pions or kaons, one can reduce the number of parameters to two: recalling that $M_{J_z=1}(f \to \pi^+\pi^-) \sim sin\theta cos\theta$, it is evident that at 90°, the contribution from σ_{TL} vanishes. But, at least for moderate q^2, the detector acceptances have a maximum at 90°. A measurement of $\frac{d\sigma}{d\Omega}_{90°}$ which is a measurement of F_{TT2} and F_{TT0} alone, is thus feasible.

Predictions for Tensor Meson Form Factors

On purely dimensional grounds, the q^2 dependence of tensor meson formation is expected to go along with drastic changes in the helicity structure. The $J_z = 2$ cross section even falls with q^2 in the absence of form factor effects, whereas $T^{TT0}_{\mu\nu}$ ($T^{TL}_{\mu\nu}$) contain terms rising like q_1^4 (q_1^3) as $q_1^2 \to \infty$ with $q_2^2 = 0$. Eventually, the $J_z = 0$ amplitude will thus dominate. This was first noticed in ref. [17], where the dominance of the $J_z = \pm 0$ amplitude for $q_1^2 \to \infty$ was predicted in the framework of the quark model. The difficult question is: where and how does the take over of $M_{\pm\pm}$ take place?

There are only two papers making predictions for the q^2 dependence of tensor meson formation in the low q^2 region. Krasemann and Vermaseren [67] describe the tensor meson as a bound state of two massive quarks, carrying half of the meson's momentum each. Within this model, all $\gamma\gamma$ amplitudes are determined by a single unknown quantity, the derivative of the quark wave function at the origin. Adapting their result to our notation gives

$$\begin{aligned} M_{+-}(0,q_2^2) &= F_{TT2}(0,0)\frac{W^2}{2\sqrt{X}} \\ M_{++}(0,q_2^2) &= F_{TT2}(0,0)\frac{q_2^2}{2\sqrt{6X}} \\ M_{+0}(0,q_2^2) &= F_{TT2}(0,0)\sqrt{\frac{-q_2^2W^2}{8X}} \end{aligned} \tag{2.4.18}$$

Recently, Achasov and Kernakov [88] published an esthetically very pleasing extension of the VDM idea. They argue that not only the electric field vector (photon) acts like a vector meson, but also that a tensor meson might interact like the electromagnetic field tensor. The resulting amplitudes can be written as

$$\begin{aligned} M_{--}(q_1^2,q_2^2) &= F_{TT2}(0,0)R\frac{W^2-q_1^2-q_2^2}{W^2} \\ M_{++}(q_1^2,q_2^2) &= F_{TT2}(0,0)R\frac{1}{\sqrt{6}}\left(\left(\frac{q_1^2-q_2^2}{W^2}\right)^2-\frac{q_1^2+q_2^2}{W^2}\right) \\ M_{+0}(q_1^2,q_2^2) &= F_{TT2}(0,0)R\frac{\sqrt{-q_2^2}}{\sqrt{2}}\frac{W^2-q_1^2-q_2^2}{W^3} \\ M_{00}(q_1^2,q_2^2) &= F_{TT2}(0,0)R\sqrt{\frac{8}{3}}\frac{\sqrt{q_1^2q_2^2}}{W^2} \end{aligned} \tag{2.4.19}$$

where R is the product of two ρ^0 pole form factors: $R=(1-q_1^2/m_\rho^2)^{-1}(1-q_2^2/m_\rho^2)^{-1}$.

Notice that in both models, the helicity zero cross section vanishes for $q_1^2=q_2^2=0$. Suppose now that future experiments confirm the presence of a finite $J_z=0$ component (the published A_2 data give $\Gamma_{\gamma\gamma}(J_z=0)/\Gamma_\gamma(J_z=2)=0.32\pm0.18$). It would then not be very meaningful to test either of the two models with tagged data.

Given the excellent agreement between the calculation of Singer [87] with the measured widths, let us inspect the off shell behaviour of an E_1 transition. Since by means of eq.(2.4.15), the Lorentz structure, and thus the helicity amplitudes are fixed, the assumption of an E_1 transition reduces the number of free parameters to one: the form factor of the E_1 transition, $F_{E1}(q_1^2,q_2^2)$:

$$\begin{aligned} M_{+-}(q_1^2,q_2^2) &= F_{TT2}(0,0)F_{E1}(q_1^2,q_2^2) \\ M_{++}(q_1^2,q_2^2) &= \frac{1}{\sqrt{6}}F_{TT2}(0,0)F_{E1}(q_1^2,q_2^2) \\ M_{+0}(q_1^2,q_2^2) &= \frac{1}{\sqrt{2}}F_{TT2}(0,0)F_{E1}(q_1^2,q_2^2)\sqrt{-q_2^2}\left(\frac{q_1q_2-q_1^2}{Wq_1q_2}\right) \\ M_{00}(q_1^2,q_2^2) &= -\frac{2}{\sqrt{6}}F_{TT2}(0,0)F_{E1}(q_1^2,q_2^2)\sqrt{q_1^2q_2^2}\left(\frac{(q_1q_2+q_1^2)(q_1q_2-q_2^2)}{W^2(q_1q_2)^2}\right) \end{aligned} \tag{2.4.20}$$

There seems to be no way of determining $F_{E1}(q_1^2,q_2^2)$ from general principles. However, given that the helicity amplitudes for transversely polarised photons are indentical with the ones obtained in partial wave decomposition with $L=0$ (c.f. appendix D), qualitatively, one would expect $F_{E1}(q_1^2,q_2^2)$ to be a rather flat function, may be even constant at moderate values of q^2.

It is interesting to notice that in calculations assuming a direct photon quark coupling, a rapid take over of the $J_z=0$ amplitide is predicted, whereas in eq.(2.4.20), the ratio $\sigma_{\gamma\gamma}(J_z=0)/\sigma_{\gamma\gamma}(J_z=2)$ is constant if one of the photons is real. Therefore, the ratio of the helicity amplitudes provides an excellent measure of the dynamics. The "fall" of the $J_z=2$ amplitude may be interpreted as the take over of the pointlike photon coupling - if observed in an experiment.

Vector Meson Pair Production

Introduction

Vector meson pair production, and in particular $\rho^0\rho^0$ pair production is *the* most controversely discussed subject in two photon physics: *"The cross section for $\rho^0\rho^0$ production, first observed by the TASSO collaboration, shows a large enhancement near the $\rho^0\rho^0$ threshold. So far, this is the only effect observed in two photon experiments which had not been predicted, not even qualitatively."* [12]

"(...) $q^2\bar{q}^2$-resonance production can describe all features of the reactions $\gamma\gamma \to \rho^0\rho^0$ and $\gamma\gamma \to \rho^+\rho^-$ - both qualitatively and quantitatively." [89]

"The search for exotic explanations of $\gamma\gamma$ phenomena should be done above the background of conventional processes. In our judgement, factorisation can serve as a good estimate of this background." [90] Notice that this *background of conventional processes* refers to a cross section prediction which nearly interpolates the measured $\rho^0\rho^0$ cross section.(!)

If the same cross section leads to such vastly differing opinions, we can only hope for firm conclusions, once that the quantum mechanics of the processes (which is all but trivial) is followed down to all depths such that experiments can be analysed in an as model independent as possible manner. This will be attempted in the following sections.

Measurements of the Total $\rho^0\rho^0$ Cross Section

A $\rho^0\rho^0$ cross section can be derived using an acceptance calculation based on a four pion phase space Monte Carlo with a constant two photon cross section in which the events are weighted according to

$$M(\gamma\gamma \to 4\pi) \sim \left(\frac{p^*_{1,2} F_{\rho\pi\pi}(1,2)}{(W^2_{12} - m^2_\rho)^2 + i m_\rho \Gamma_\rho} \cdot \frac{p^*_{3,4} F_{\rho\pi\pi}(3,4)}{(W^2_{34} - m^2_\rho)^2 + i m_\rho \Gamma_\rho} + \frac{p^*_{1,4} F_{\rho\pi\pi}(1,4)}{(W^2_{14} - m^2_\rho)^2 + i m_\rho \Gamma_\rho} \cdot \frac{p^*_{2,3} F_{\rho\pi\pi}(2,3)}{(W^2_{23} - m^2_\rho)^2 + i m_\rho \Gamma_\rho} \right) \qquad (2.5.1)$$

Here, the pions have been labelled $\pi^+_1, \pi^-_2, \pi^+_3, \pi^-_4$ and $p^*_{i,j}$ is the three momentum of one of the pions i or j in the i,j centre of momentum system (c.f appendix-D). The coherent sum is necessary in order to account for the Bose symmetry of the outgoing like sign pions.[1] Of course, this procedure leads to a rather arbitrary spin parity composition in the event simulation. Nevertheless, the experiments agree that, at least in the central region, this Ansatz reproduces the angular distributions quite well (see below).

[1] If a four pion phase space Monte Carlo program is used, no additional phase space terms are needed. Such functions are useful if one seeks an analytic mapping of the type $d\sigma/dLips_{4\pi} \to d\sigma/(dm^2_{1,2} dm^2_{3,4})$. They are necessary if the final state is generated in a two step procedure: 1) $\gamma\gamma \to \rho\rho$ and 2) $\rho\rho \to 4\pi$. In this case, such factors account for the phase space correlations between the different systems. They are also necessary, if the width of the ρ^0 is put into the numerator of the ρ^0 Breit Wigner amplitude since in that case, the $\pi^+\pi^-$ phase space is implicitely inserted into the ρ^0 propagator.

Using this, or equivalent techniques, several experiments have arrived at similar cross sections [91,92,93]. A recent compilation by Erné [102] is shown in fig.(2.5.1). However, the published total cross sections are still subject to several non negligible uncertainties.

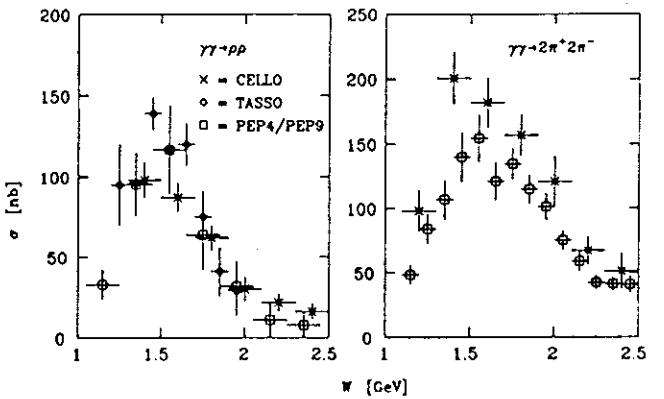

Figure 2.5.1: *Measurements of the total cross section for $\gamma\gamma \to 2\pi + 2\pi^-$, assuming a phase space like angular correlation between the pions. The graph on the left is the contribution from $\rho^0\rho^0$ alone.*

First of all, as can be seen in fig.(2.5.2), there is a rather large continuum cross section for $\gamma\gamma \to 4\pi$, as well as for $\gamma\gamma \to \rho^0\pi^+\pi^-$. The two continua together are produced about a frequently as ρ^0 pairs. Given the large width of the ρ^0 meson, the interference between the continua and the $\rho^0\rho^0$ pair production amplitude can be quite large. No collaboration has yet attempted to fit interference terms to the data. The absence of these fits in the literature can be explained by limited statistics, since in each bin of W, there may be up to three different phases between each pair of amplitudes.

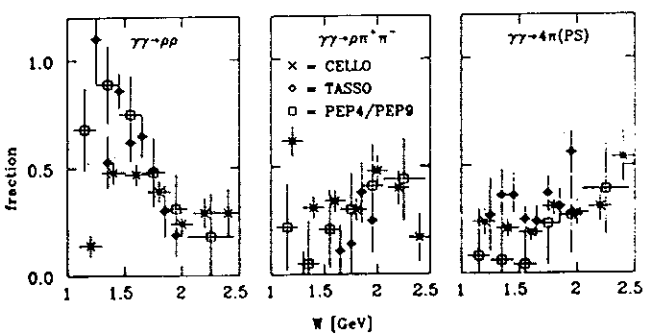

Figure 2.5.2: *Experimental decomposition of the $2\pi^+2\pi^-$ final state.*

The dynamics of the four pion continuum is to this day unknown. However, at $W = 1.5GeV$,

the pions are highly relativistic that there seems to be no reason, why they should be produced like phase space, as it has been repeatedly assumed in the experimental literature. Assume, for example, the four pion continuum was produced by quark fragmentation. Whatever the details of this mechanism may be, such process would lead to non trivial mass correlations which might even fake a ρ^0 signal. It would be very interesting to see, how the "measured" $\rho^0\rho^0$ cross section changed if, instead of a phase space Monte Carlo, a *Lund* Monte Carlo [116] was used for the simulation of the four pion continuum.

The parameterisation of the $\rho^0\pi^+\pi^-$ cross section is not trivial, as pointed out by Achasov et al [89]. The currently used amplitude, in which all particles but the two pions coming from the ρ^0 decay are produced isotropically in the $\gamma\gamma$ centre of momentum system, implicitely violates parity. The two pions not coming from the ρ^0 decay should be in an $L = 1$ state as well.

It may be that what has been observed as a $\rho^0\pi^+\pi^-$ cross section is to a large extent only the interference between the pair production amplitude and the continuum. As a simple check, one could use a simple phase space plus one phase model, i.e.

$$M(\gamma\gamma \to 4\pi) \sim F_1(W)e^{i\alpha}\left(\frac{p_{1,2}^{*}F_{\rho\pi\pi}(1,2)}{(W_{12}^2 - m_\rho^2)^2 - im_\rho\Gamma_\rho}\frac{p_{3,4}^{*}F_{\rho\pi\pi}(3,4)}{(W_{34}^2 - m_\rho^2)^2 - im_\rho\Gamma_\rho}\right.$$
$$\left. + \frac{p_{1,4}^{*}F_{\rho\pi\pi}(1,4)}{(W_{14}^2 - m_\rho^2)^2 + im_\rho\Gamma_\rho}\frac{p_{2,3}^{*}F_{\rho\pi\pi}(2,3)}{(W_{23}^2 - m_\rho^2)^2 - im_\rho\Gamma_\rho}\right) \qquad (2.5.2)$$
$$+ F_2(W)$$

where F_1, F_2 and α are real parameters and the four $W_{ik}'s$ are the invariant masses of the four neutral two pion combinations.

So far, the largest uncertainty can be attributed to the angular correlations between the pions coming from the ρ^0 decays. The TASSO collaboration [91] has shown that the measured $\rho^0\rho^0$ cross section is reduced by nearly a factor of 2 (!), if, instead of an isotropic production and decay Monte Carlo, a fit to the angular distributions is used for the calculation of the acceptance.

Right on and below the nominal production threshold, one reaches a principle limit of the interpretability of the data. The relativistic Breit Wigner amplitude is a numerical approximation to the Fourier transform of the radioactive decay of a *free*, i.e. *non interacting* particle. We shall see later that arround the $\rho^0\rho^0$ threshold, spin parity analyses suggest that the ρ mesons are in a state of relative orbital angular momentum $L = 0$. Their wave functions thus have a large overlap, and, because the ρ mesons hardly move, they "sit right on top of each other" for a long time compared to their life time. Because the ρ mesons are strongly interacting particles, the basic requirement for a decay according to a Breit Wigner amplitude is thus not fulfilled. It is thus *impossible* to make statements about the $\rho^0\rho^0$ cross section below threshold without making explicit assumptions about the way they interact with each other ("final state interactions"). In this light, the caution of the CELLO collaboration [92] gives the best parameterisation of the data. Below the nominal production threshold, only the total four pion cross section is shown.

Finally, with the exception of PEP49 (c.f. ref.[102]) the currently used detectors cannot sufficiently distinguishh between $\gamma\gamma \to 4\pi$ and $\gamma\gamma \to 4K$ to exclude a sizeable kaon cross

section experimentally. However, since the K meson is so much heavier than the π, neglecting kaon production may be reasonnable.

In conclusion, all measurements agree that the $\rho^0\rho^0$ cross section may be as large as $\simeq 120nb$, however, the experimental uncertainties still exceed a factor of two.

Conventional Interpretations of the $\rho^0\rho^0$ Cross Section

For a better understanding of the ongoing discussion of the $\rho^0\rho^0$ cross section, a historical remark to the meaning of the word *enhancement* seems necessary. The origin of this term in the context of $\rho^0\rho^0$ production is a discrepancy by a factor of ten between the first data [93,95] and a "VDM" prediction [12]. This "VDM" prediction is a simple one pomeron exchange amplitude and hence, the prediction is only valid in the limit $W \to \infty$. The large discrepancy on the other hand occurred right at the $\rho^0\rho^0$ threshold. The origin of the word *enhancement* can thus be traced back to a misunderstanding between theory and experiment.[1] Therefore the more neutral term "large cross section" seems more appropriate to the author.

One might suspect that direct channels are responsible for the large $\rho^0\rho^0$ cross section. However, in the $\rho^0\rho^0$ threshold region, there are only two known resonances having the right quantum numbers to be able to contribute to the reaction $\gamma\gamma \to \pi^+\pi^-\pi^+\pi^-$: the $f(1270)$ and the $\epsilon(1300)$. From the measured $\Gamma(f \to \pi^+\pi^-\pi^+\pi^-) = 5.0 \pm 0.8keV$ eq.(1.19) implies a cross section

$$\sigma_{peak}(\gamma\gamma \to f \to \pi^+\pi^-\pi^+\pi^-) \simeq 15nb$$

for a radiative width of $\Gamma_{\gamma\gamma}(f) = 3keV$. Only little is known about the $\epsilon(1300)$. Kolanoski [12] has argued that provided that the $\epsilon(1300)$ predominantly decays into pion pairs, VDM arguments together with the apparent absence of a large $\epsilon(1300)$ signal in the reaction $\gamma\gamma \to \pi^+\pi^-$ imply an upper limit of

$$\sigma_{peak}(\gamma\gamma \to \epsilon(1300) \to \pi^+\pi^-\pi^+\pi^-) \lesssim 5nb.$$

These numbers may be compared to a measured threshold cross section between 70 and 120 nb for $\gamma\gamma \to \rho^0\rho^0$. Thus, direct production of known resonances cannot account for the large $\rho^0\rho^0$ cross section.

The contributions from exchange diagrams may thus dominate. Before going into the details of particular models, it is useful to have a closer look at the internal kinematics of candidate theories. If the interaction takes place due to the exchange of a hadron[2], the matrix elements will always contain its propagators.

$$M(t\text{ - channel}) \sim \frac{1}{t - m_h^2} \qquad M(u\text{ - channel}) \sim \frac{1}{u - m_h^2}$$

whatever the dynamics at the vertices may be. As one moves to threshold, the accessible range of $t(u)$ gets smaller and smaller. Fig.(2.5.3) illustrates the implications: close to threshold,

[1] Notice that the one pomeron exchange assumption applied to the low energy $p\bar{p}$ or pp or πp or Kp total cross sections fits neither of these reactions. However, in these cases, the discrepancy has never been called enhancement.

[2] Sea gull terms are only necessary, if photons couple to currents of *charged* bosons.

the contributions from the exchange of heavy mesons are strongly suppressed. The light mesons are thus expected to dominate the threshold behaviour of the cross section. On the other hand, in the high energy region the propagator masses become less and less important. The interpretation of the threshold cross section may thus be quite different from the high energy one.

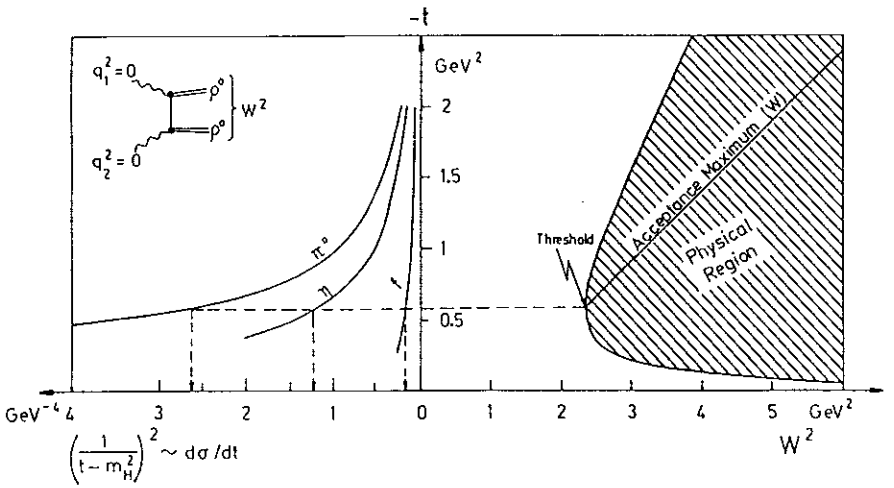

Figure 2.5.3: *t-channel propagator suppression for $\gamma\gamma \to \rho^0\rho^0$, examplified for π^0, η and f^0 exchange. The contour of the physical region assumes stable ρ^0 mesons. The finite width of the ρ^0 meson not only allows production below threshold, but also enlarges the accessible range in t at a given W.*

In view of these basic arguments, the calculation of Hatzis and Paschalis [94] appears to be a step into the right direction. The authors calculate the contributions from π^0, η and η' exchange. The pseudoscalar exchange diagrams have some promising features. First of all, the experimental knowledge of the decays $\omega \to \pi^0\gamma$, $\rho \to \pi\gamma$, $\phi \to \eta\gamma$, and $\eta' \to \rho^0\gamma$ provides an excellent tool for the normalisation of the coupling constants, i.e. only $SU(3)_{Fl}$, but *no* vector meson dominance assumption is required. Secondly, since there is only *one* VVP amplitude, the parameterisation of the vertices follows from first principles. Only two crucial points are subject to model assumptions: the $\eta - \eta'$ mixing angle and the t evolution of the amplitudes.

In ref [94] the mixing angle θ is taken to be -10° and the t evolution of the amplitudes is parameterised like[1] $F_{\rho\gamma\pi}(t) = F_{\rho\gamma\pi}(t = m_\pi^2)e^{1+(t-m_\pi^2)/c}$ where c is a constant parameter. Both assumptions do not fit very well into the picture laid out by the measurements of $\gamma\gamma \to 0^{-}$ and $\gamma\gamma \to \pi^+\pi^-$. The radiative widths of the pseudoscalar mesons are now in

[1] This parameterisation is very dangerous, as can be seen from the s channel contribution at resonance mass, f.ex: $F_{\rho\gamma\eta'}(s = m_{\eta'}^2) = F_{\rho\gamma\eta'}(s = m_{\eta'}^2)e^{1+0/c}$ which is contradictory.

conflict with $\theta = -10^0$, requiring $\theta = -18^\circ \pm 2^\circ$. The measurements of the η' form factor and the observed energy dependence of the reaction $\gamma\gamma \to \pi^+\pi^-$ suggest propagator modifications of the type $F(t) = (1 - \frac{t-m_{\rho,\omega}^2}{m_{\pi}^2})^{-1}$ for all pseudoscalar mesons.

In view of these discrepancies with the most recent developments of our understanding of the interactions of the pseudoscalars with photons, the agreement between the data and the pseudoscalar exchange calculations of ref.[94] is reasonnable. The overall amplitude is predicted correctly, but the W dependence appears to be steeper in the data than in the calculation. It seems possible that this discrepancy disappears once that our improved knowledge of the pseudoscalar interactions with photons is implemented into forthcoming calculations.

Given that in detail, the calculations carried out on the amplitude level are still subject to some uncertainties, it may be interesting to make a direct comparison between the the cross sections measured in photoproduction experiments and in two photon reactions.

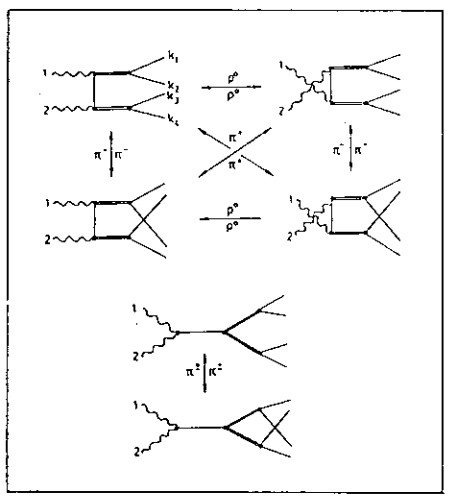

Figure 2.5.4: *Non resonant and resonant contributions to $\gamma\gamma \to \rho^0\rho^0$. By means of Bose symmetry, the four exchange amplitudes have to be equal in sign and magnitude. Only the top left matrix element has similarity with the process $\gamma p \to \rho^0 p$.*

There is a whole class of predictions which base their absolute normalisation on the measured photoproduction cross section $\sigma_{tot}(\gamma p \to \rho^0 p)$. In fact, if we only consider the t channel diagrams, there is a striking similarity between two photon physics and photoproduction. However, there is one subtilty in the internal kinematics of the two reactions, which makes it hard to find an unambiguous kinematic link between the two. The term threshold has a *dynamically* different meaning in photoproduction than in $\gamma\gamma$ physics. One reason is that in $\gamma\gamma$ reactions, two massive states have to be created, whereas in photoproduction, one only produces a single ρ^0. At threshold, one has $t_{thr} = -m_\rho^2$ for two photon reactions, whereas in photoproduction, $t_{thr} = -m_\rho^2 \frac{2m_{1,-}}{m_{1,+}+m_\rho}$. Since the values of the propagators drastically change their values near threshold, this slight difference can easily result in a factor of two in the cross section. Fig.(2.5.4) shows that for the u channel diagrams, the situation is even worse. In two photon physics, Boses Statistics requires each t channel diagram to be accompagnied by a u channel diagram of the *same strength*. In photoproduction, the situation is completely

different. Because of fermion number conservation at each vertex, the exchanged particles have to be *baryons*. The lightest baryon, the proton, is nearly an order of magnitude heavier than the pion. The u channel diagrams will thus have a small contribution to the threshold behaviour. A direct comparison between photoproduction and two photon data on the cross section level is thus subject to considerable uncertainty. Nevertheless, a recent calculation of Alexander et al [90] based on photoproduction data looks like an interpolation of the measured cross section.

In conclusion, the conventional approaches to the understanding of the $\rho^0\rho^0$ cross section are not inconsistent with the data. However, given the uncertainties inherent to the available calculations, and given the large systematic errors on the total cross section measurements, there is still room for exotic explanations for the rather large threshold cross section - but the *available data do not yet require* other than the known amplitudes.

Covariant Description of the $\rho^0\rho^0$ Spin Parity Amplitudes

The detailed understanding of the $\rho^0\rho^0$ production mechanisms needs analyses of the angular correlations. The experimental procedures for a determination of the spin parity composition of the $\rho^0\rho^0$ system are rather involved because the large widths of the ρ^0 meson, together with the requirements from Bose symmetry, leads to a large combinatorical background in all distributions.

A covariant formulation of the spin parity amplitudes offers the simplest way of describing the four pion system in an acceptance calculation. In such a parameterisation, neither Lorentz transformations, nor rotations into helicity frames are necessary. Furthermore, all Clebsch Gordan coefficients, sperical harmonics, spin barriere terms and all mass - momentum - phase space correlations are automatically inbeded into the amplitudes. The following explicit formulae might thus be helpful for future analyses.

States of specific total spin J can be projected out of the full amplitude by inserting the corresponding polarisation tensor $E^{\alpha_1\ldots\alpha_J}$ into the amplitude. The full $\gamma\gamma \to 4\pi$ amplitude is then the product

$$\begin{aligned} M(\gamma\gamma \to \pi_1^-\pi_2^-\pi_3^-\pi_4^-) &= \{M(\gamma\gamma \to J^P)\}\{M(J^P \to \rho_1^0\rho_2^0)\}\, BW(1,2) \\ &\quad \{M(\rho_1^0 \to \pi_1^+\pi_2^-)\}\, BW(3,4)\, \{M(\rho_2^0 \to \pi_3^+\pi_4^-)\} \\ &= \{M(\gamma\gamma \to J^P)\}\{E^{\alpha_1\ldots\alpha_J} T_{\alpha_1\ldots\alpha_J\beta\gamma}\epsilon^{*\beta}(\rho_1^0)\epsilon^{*\gamma}(\rho_2^0)\} \\ &\quad \{BW(1,2)\epsilon^{*}(\rho_1^0)(k_2-k_1)_\varepsilon\}\{BW(3,4)\epsilon^{*}(\rho_2^0)(k_4-k_3)_\varepsilon\} \end{aligned} \tag{2.5.3}$$

The first matrix element is identical to the one used for a description of single meson production, for example $M(\gamma\gamma \to 0^-) \sim \epsilon_1^\mu\epsilon_2^\nu e_{\mu\nu\alpha\beta}q_1^\alpha q_2^\beta$. The second matrix element is the object of interest. $T_{\alpha_1\ldots\alpha_J\beta\gamma}$ is the amplitude which links the state to the two ρ^0 mesons having polarisation vectors $\epsilon(\rho_1^0)$ and $\epsilon(\rho_2^0)$. The ρ mesons then propagate according to $BW(i,j) = ((k_i+k_j)^2 - m_\rho^2 + im_\rho\Gamma_\rho)^{-1}$, where k_i and k_j are the momenta of the pions coming from the ρ^0 decay. Since the pions have no spin they couple to the ρ^0 in no other way than through $\epsilon(k_j - k_i)$.

Because the pions have identical mass, the amplitudes can be drastically simplified due

to

$$\begin{aligned} \sum_{\alpha=helicities} \epsilon_\alpha^{*\alpha}\epsilon_\alpha^\beta(k_j-k_i)_\beta &= \left(-g^{\alpha\beta} - \frac{(k_j-k_i)^\alpha(k_j-k_i)^\beta}{(k_i+k_j)^2}\right)(k_j-k_i)_\beta \\ &= (k_i-k_j)^\alpha \end{aligned}$$

giving

$$\begin{aligned} \sum_\alpha M(\gamma\gamma \to \pi_1^+\pi_2^-\pi_3^+\pi_4^-) &= M(\gamma\gamma \to J^P)E^{\alpha_1\ldots\alpha_J}T_{\alpha_1\ldots\alpha_J\beta\gamma} \\ &\quad (k_2-k_1)^\beta(k_4-k_3)^\gamma BW(1,2)BW(3,4) \end{aligned} \tag{2.5.4}$$

Because the ρ mesons are identical bosons, the amplitudes T have to be symmetric:

$$T_{\alpha_1\ldots\alpha_J\beta\gamma}(k_1+k_2,k_3+k_4) = T_{\alpha_1\ldots\alpha_J\gamma\beta}(k_3+k_4,k_1+k_2) \tag{2.5.5}$$

Since the final state consists of 2x2 indistinguishable pions, the full amplitude has to be symmetrised:

$$M(\gamma\gamma \to 4\pi) = M(\gamma\gamma \to \pi_1^+\pi_2^-\pi_3^+\pi_4^-) + M(\gamma\gamma \to \pi_1^-\pi_4^+\pi_3^-\pi_2^+) \tag{2.5.6}$$

The construction of the $J^P \to \rho^0\rho^0$ amplitudes follows a slightly different path than the construction of the $\gamma\gamma \to J^P$ amplitudes. In the latter case, the form of the coupling tensors is largely predetermined by the principle of gauge invariance, whereas there is more freedom for the $\rho^0\rho^0$ amplitudes. Given that near threshold, it is very likely that the "true" amplitude is well approximated by a superposition of states with low orbital angular momenta L between the ρ^0 mesons, those amplitudes will be constructed, which describe states with specific low values of L. The tools for the construction of such amplitudes are given in the appendix.

In the following, all angles are defined such that in the hadronic centre of momentum system, any three vector $\vec{k}$ has the form $\vec{k} = \vec{k}\,(sin\theta cos\phi, sin\theta sin\phi, cos\theta)$. The index of an angle denotes its parent four vector, θ_{12-3} for example is the angle between the $\gamma\gamma$ axis and the vector $k_{12-3} \equiv k_3 + k_2 - k_1$.

Scalar (0^+) states can couple to ρ^0 mesons through an s-wave:

$$\begin{aligned} M(0^+ \to 4\pi)_{L=0} &\sim A^{\beta\gamma}(k_1-k_2)_\beta(k_3-k_4)_\gamma BW(1,2)BW(3,4) \\ &\quad + A^{\beta\gamma}(k_1-k_4)_\beta(k_3-k_2)_\gamma BW(1,4)BW(3,2) \\ \to M_{++} &\sim \left(k_{1-2}\cdot k_{3-4} - \frac{(k_{12}\cdot k_{3-4})(k_{34}\cdot k_{1-2})}{k_{12}\cdot k_{34}}\right)BW(1,2)BW(3,4) + (2 \to 4) \end{aligned} \tag{2.5.7}$$

But this is not the only amplitude connecting a scalar state to two ρ^0 mesons. The transition can also proceed through a d - *wave*:

$$\begin{aligned} M(0^+ \to 4\pi)_{L=2} &\sim k_{12-3-4}^\beta k_{12-3-4}^\gamma(k_1-k_2)_\beta(k_3-k_4)_\gamma BW(1,2)BW(3,4) \\ &\quad + (2 \to 4) \\ \to M_{++} &\sim (k_{12-3-4}\cdot k_{1-2})(k_{12-3-4}\cdot k_{3-4})BW(1,2)BW(3,4) \\ &\quad + (2 \to 4) \end{aligned} \tag{2.5.8}$$

Pseudoscalar states have no choice but a p-wave transition:

$$
\begin{aligned}
M(0^- \to 4\pi)_{L=1} &\sim e_{\beta\gamma\delta\epsilon}(k_1+k_2)^\beta(k_3+k_4)^\gamma(k_1-k_2)^\delta(k_3-k_4)^\epsilon \\
&\quad BW(1,2)BW(3,4) + (2 \to 4) \\
&\to M_{++} \sim \frac{1}{2}W(\vec{k}_4+\vec{k}_3-\vec{k}_2-\vec{k}_1)\cdot\left((\vec{k}_1-\vec{k}_2)\times(\vec{k}_3-\vec{k}_4)\right) \\
&\quad BW(1,2)BW(3,4) + (2 \to 4)
\end{aligned}
\tag{2.5.9}
$$

the three vectors are calculated in the hadronic centre of momentum system.

The description of states with spin $J = 2$ is complicated. There are in principle five independent tensors which contribute to the $2^+ \to 1^-1^-$ amplitude. One of them corresponds to an $L = 0$, three to an $L = 2$ and one to an $L = 4$ transition. Experimentally, there seems to be no hope to disentangle all of them. Therefore, we shall concentrate on two specific low angular momentum amplitudes. It must be emphasised though that, because the ρ^0 mesons are non relativistic near threshold, the assumption of coupling corresponding to a small angular momentum between the ρ^0 mesons is only justified on the "$\rho^0\rho^0$ side" of the matrix element. Such arguments do *not* apply to the "$\gamma\gamma$ side" of the matrix element. The ratio between the resulting helicity amplitudes for example, is predominantly determined by the coupling to the photons.

$$
\begin{aligned}
M(2^- \to 4\pi)_{L=0} &\sim E^{\alpha_1\alpha_2}A_{\alpha_1\beta}A_{\alpha_2\gamma}(k_1-k_2)^\beta(k_3-k_4)^\gamma \\
&\quad BW(1,2)BW(3,4) + (2 \to 4) \\
M_{--} &\sim \frac{1}{2}\left(|\vec{k}_{1-2}|sin\theta_{1-2}e^{i\phi_{1-2}} - Z(1,2)\,\vec{k}_{12}|sin\theta_{12}e^{i\phi_{12}}\right) \\
&\quad \cdot\left(|\vec{k}_{3-4}|sin\theta_{3-4}e^{i\phi_{3-4}} - Z(3,4)\,\vec{k}_{34}|sin\theta_{34}e^{i\phi_{34}}\right)BW(1,2)BW(3,4) \\
&\quad + (2 \to 1) \\
M_{--} &\sim \frac{1}{\sqrt{6}}\Big(\left\{\vec{k}_{1-2}\,sin\theta_{1-2}cos\phi_{1-2} - Z(1,2)\,\vec{k}_{12}|sin\theta_{12}cos\phi_{12}\right\} \\
&\quad \cdot\left\{\vec{k}_{3-4}\,sin\theta_{3-4}cos\phi_{3-4} - Z(3,4)\,\vec{k}_{34}|sin\theta_{34}cos\phi_{34}\right\} \\
&\quad - \left\{\vec{k}_{1-2}\,sin\theta_{1-2}sin\phi_{1-2} - Z(1,2)\,\vec{k}_{12}\,sin\theta_{12}sin\phi_{12}\right\} \\
&\quad \cdot\left\{\vec{k}_{3-4}\,sin\theta_{3-4}sin\phi_{3-4} - Z(3,4)\,\vec{k}_{34}|sin\theta_{34}sin\phi_{34}\right\} \\
&\quad - 2\left\{\vec{k}_{1-2}|cos\theta_{1-2} - Z(1,2)\vec{k}_{12}|cos\theta_{12}\right\} \\
&\quad \cdot\left\{|\vec{k}_{3-4}|cos\theta_{3-4} - Z(3,4)|\vec{k}_{34}|cos\theta_{34}\right\}\Big)BW(1,2)BW(3,4) \\
&\quad + (2 \to 4) \\
Z(i,k) &\equiv \frac{k_{1234}\cdot k_{i-k}}{k_{1234}\cdot k_{ik} - \sqrt{k_{1234}^2 k_{ik}^2}}
\end{aligned}
\tag{2.5.10}
$$

These amplitudes can thus only answer the question "given that a tensor state of certain helicity is produced, how will this tensor state desintegrate into ρ^0 mesons?" The ratio of the helicity amplitudes does *not* follow from general principles. Furthermore, these amplitudes, which are equivalent to expressions obtained in first order partial wave expansions, are not necessarily the appropriate ones. If it is assumed that the reaction $\gamma\gamma \to \rho^0\rho^0$ predominantly proceeds through the formation of a tensor *resonance*, then the above amplitude is the obvious choice. In case of a nonresonant production mechanism, the presence of t an u channel propagators would imply a sizeable contribution of $L = 2$ transitions and hence, beyond threshold, the following amplitude, which describes two ρ^0 mesons in a d wave, might have a much larger overlap with the "true" one:

$$
\begin{aligned}
M(2^+ \to 4\pi)_{L=2} &\sim E^{\alpha_1\alpha_2}(k_4+k_3-k_2-k_1)_{\alpha_1}(k_4+k_3-k_2-k_1)_{\alpha_2}A_{\beta\gamma} \\
&\quad (k_1-k_2)^\beta(k_3-k_4)^\gamma BW(1,2)BW(3,4) + (2 \to 4) \\
M_{--} &\sim \frac{1}{2}|\vec{k}_4+\vec{k}_3-\vec{k}_2-\vec{k}_1|^2 sin^2\theta_{43-2-1}e^{2i(\phi_{43-2-1})} \\
&\quad \cdot\left(k_{1-2}\cdot k_{3-4} - \frac{(k_{1-2}\cdot k_{34})(k_{3-4}\cdot k_{12})}{k_{12}\cdot k_{34} - \sqrt{k_{12}^2 k_{34}^2}}\right)BW(1,2)BW(3,4) \\
&\quad + (2 \to 4) \\
M_{--} &\sim \frac{1}{\sqrt{6}}|\vec{k}_4+\vec{k}_3-\vec{k}_2-\vec{k}_1|^2(3cos^2\theta_{43-2-1}-1) \\
&\quad \cdot\left(k_{1-2}\cdot k_{3-4} - \frac{(k_{1-2}\cdot k_{34})(k_{3-4}\cdot k_{12})}{k_{12}\cdot k_{34} - \sqrt{k_{12}^2 k_{34}^2}}\right)BW(1,2)BW(3,4) \\
&\quad + (2 \to 4)
\end{aligned}
\tag{2.5.11}
$$

It would be quite inspiring to see which of the two $J = 2$ amplitudes gives a better fit to the data, since the dynamic interpretations are so different.

States of $J^P = 2^-$ require p- or f-wave transitions. The p-wave amplitude can be written in the form

$$
\begin{aligned}
M(2^- \to 4\pi)_{L=1} &\sim E^{\alpha_1\alpha_2\alpha_3}(k_4+k_3-k_2-k_1)_{\alpha_1}(k_1+k_2+k_3+k_4)_\mu \\
&\quad (k_1-k_2)_\gamma(k_3-k_4)_\delta e_{\mu\alpha_2\gamma\delta}BW(1,2)BW(3,4) + (2 \to 4) \\
M_{--} &\sim \frac{W}{\sqrt{6}}|\vec{k}_4+\vec{k}_3-\vec{k}_2-\vec{k}_1|\,\vec{k}_2\cdot\vec{k}_4\,\vec{k}_3 \\
&\quad \Big(-2cos\theta_{43-2-1}sin\theta_{1-2}sin\theta_{3-4}(cos\phi_{1-2}sin\phi_{3-4} - sin\phi_{1-2}cos\phi_{3-4}) \\
&\quad - sin\theta_{43-2-1}(sin\theta_{1-2}cos\theta_{3-4}sin(\phi_{43-2-1}-\phi_{1-2}) \\
&\quad - cos\theta_{1-2}sin\theta_{3-4}sin(\phi_{43-2-1}-\phi_{3-4}))\Big) \\
&\quad BW(1,2)BW(3,4) + (2 \to 4)
\end{aligned}
\tag{2.5.12}
$$

Notice that the helicity two amplitude vanishes by means of Bose statistics. This is also true

for the f-wave transition

$$
\begin{aligned}
M(2^- \to 4\pi)_{L=3} \sim & E^{\alpha_1\alpha_2}(k_1+k_2-k_3-k_4)_{\alpha_1}(k_1+k_2-k_3-k_4)_{\alpha_2} \\
& (k_1+k_2)_\beta(k_3+k_4)_\gamma(k_2-k_1)_\delta(k_4-k_3)_\epsilon e_{\beta\gamma\delta\epsilon} \\
& BW(1,2)BW(3,4)+(2\to 4) \\
M_{++} \sim & \frac{W}{\sqrt{24}}|\vec{k}_4+\vec{k}_3-\vec{k}_2-\vec{k}_1|^2(3cos^2\theta_{43-2-1}-1) \\
& (\vec{k}_4+\vec{k}_3-\vec{k}_2-\vec{k}_1)\cdot\left\{(\vec{k}_2-\vec{k}_1)\times(\vec{k}_4-\vec{k}_3)\right\} \\
& BW(1,2)BW(3,4)+(2\to 4)
\end{aligned}
\qquad (2.5.13)
$$

In conclusion of this quantum mechanical exercise, it appears that a spin parity decomposition of the $\rho^0\rho^0$ final state in all generality requires a very large number of parameters. A completely model independent description of the process seems therefore hard to achieve. Nevertheless, the large number of parameters has also favourable implications. In fact, in the (how distant?) future, it might even provide the key to the understanding of the $\rho^0\rho^0$ production mechanism. The clue is that the possibility of different (L) amplitudes for states of identical spin parity (J^P) allows at least in principle a separation of the phases occurring in different states of spin parity, i.e. a fit of the form

$$M_{ab}(J^P) = e^{i\alpha}M_{ab}(J^P, L=L_{min}) + M_{ab}(J^P, L=L_{min}+2) \qquad (2.5.14)$$

tests the presence of a resonance of this particular J^P *irrespective of resonating structures in other* J^P *states*(!). In practise, however, this method not only requires a very homogenious detector acceptance, but also a very large statistics sample. For the time being, it may be more promising to search for certain characteristic features of particular processes.

An interesting aspect of the angular distributions which glances through the CELLO $\rho^0\rho^0$ analysis (see below), is to concentrate on particular corners of the phase space. Consider the production of a ρ^0 meson pair at zero degrees and assume that the amplitude is dominated by the exchange of spinless particles (e.g. pseudoscalars or pomeron). For both photons, this particular configuration corresponds to a *head on collision* with the propagating particle. Since such a collision involves neither a helicity transfer to the propagator, nor a change of the direction of momentum along each $\gamma - \rho^0$ line, helicity conservation at each vertex requires the helicities of the photons and the ρ^0 mesons to be (anti-)parallel in the $\gamma\gamma$ c.m.s. Since gauge invariance demands real photons to be transversely polarised, so have to be the ρ^0 mesons. Thus, if the amplitude is dominated by the exchange of scalar or pseudoscalar particles, ρ^0 mesons produced under 0° have to be transversely polarised.

Quite in contrast, if the amplitude is dominated by the presence of a resonant state, the resonance would have "forgotten" all about gauge invariance, and the longitudinal component would be of the order of the corresponding Clebsch Gordan coefficient.

Measurements of the $\rho^0\rho^0$ Spin Parity Amplitudes

In 1982, the TASSO Collaboration [91] showed the first spin parity analysis of the $\rho^0\rho^0$ final state. This analysis uses a large statistics data sample based on $49pb^{-1}$ taken at PETRA.

As an example of the decisivenes of the data, four projections of the angular correlations in the mass range from 1.4 to 1.6 GeV are shown (fig.(2.5.5)).

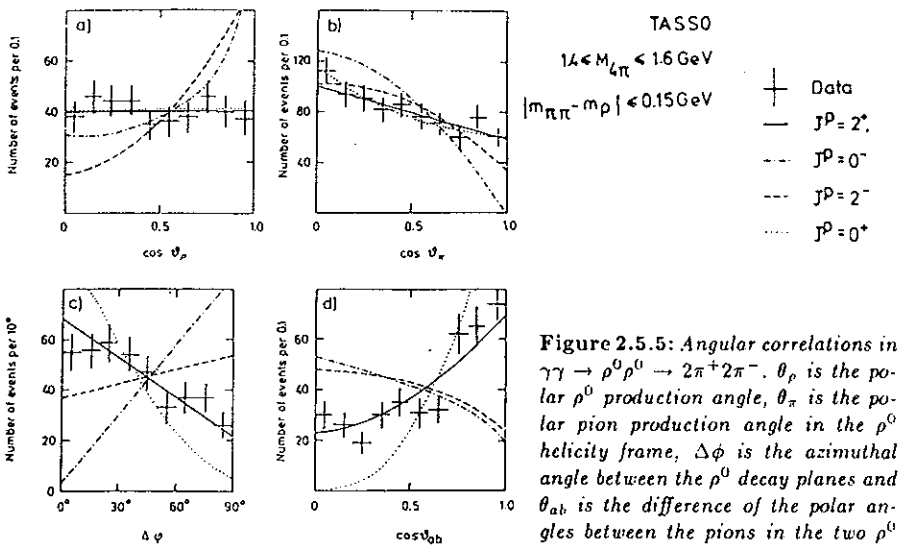

Figure 2.5.5: *Angular correlations in* $\gamma\gamma \to \rho^0\rho^0 \to 2\pi^+2\pi^-$. θ_ρ *is the polar* ρ^0 *production angle,* θ_π *is the polar pion production angle in the* ρ^0 *helicity frame,* $\Delta\phi$ *is the azimuthal angle between the* ρ^0 *decay planes and* θ_{ab} *is the difference of the polar angles between the pions in the two* ρ^0 *helicity frames.*

The distributions in the other mass bins are quoted to be similar. The gross features of the shown data are: 1)The ρ^0 mesons are produced isotropically. Because of helicity conservation, this confirms that states with $J > 2$ are not produced at a measurable level. 2)The decay angles of the ρ^0 mesons are positively correlated. This is the characteristic feature of those amplitudes, in which the spins of the ρ^0 mesons annihilate, i.e. $M_{L=0}(J^P = 0^+)$ and $M_{L=2}(J^P = 2^-)$. However, this is also compatible with a sizeable contribution from $M_{L=0}(J^P = 2^+)$. The strong positive correlation does *not* allow a sizeable contribution of states with negative parity.

A likelyhood fit including the various spin parity states for energies in the region $1.2 - 2.0GeV$ excludes large contributions from negative spin parity states throughout.[1] At threshold, the $J^P = 0^+$ amplitude dominates. With increasing energy, the 2^+ amplitude becomes more important.

In 1983, the CELLO Collaboration [92] published a moment analysis of the $\rho^0\rho^0$ angular correlations. Such an analysis is the most unbiassed way of determining the relative strengths of the partial wave amplitudes.[2] Whereas the formalism used by the TASSO Collaboration requires explicit assumptions about the relative phases of the different (L) amplitudes corresponding to specific J^P states, the CELLO analysis is free of such dynamical assumptions.

[1] The actual numbers from the fits have to be looked at with some caution, because some of the curves in fig.(2.5.5) are hard to interpret. The unisotropy of the ρ^0 production angle in the 0^- amplitude for example violates rotational invariance.

[2] The moment of a sperical harmonic is defined as the integral $\int Y_L^M N_{event} d\Omega$. Because of the orthogonality of the spherical harmonics, this integral vanishes, if the true amplitude contains no contribution from this Y_L^M.

The moments of the sperical harmonics corresponding to the relative orbital angular momenta show no significant structure for any $L \geq 1$. Therefore, amplitudes dominate in which the ρ^0 meson spins annihilate. Thus, the contribution from states with negative parity must be small.

The CELLO Collaboration also investigated the helicity composition of the ρ^0 mesons (c.f. fig(2.5.6). Motivated by the search for a peripheral component in the amplitude, the ρ^0 mesons produced at small angles were separated from the centrally produced ones. It was found that ρ^0 mesons produced under small angles have predominantly transverse polarisation. This is an indication that a non resonant amplitude dominates at least in the region of small production angles.

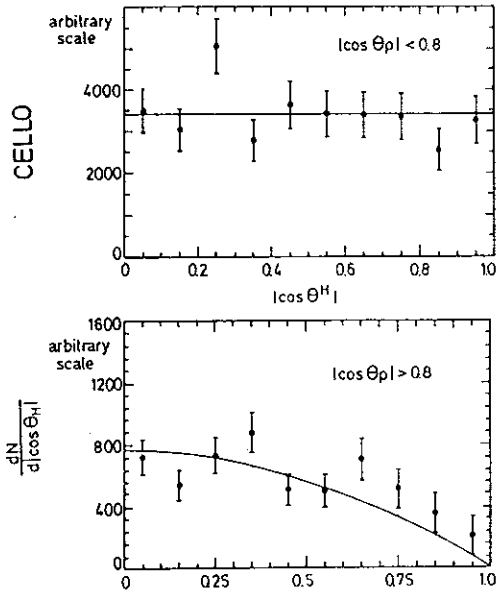

Figure 2.5.6: *The CELLO data indicate that ρ^0 mesons, produced under small angles, are transversly polarised.*

The conclusion of the experimental analyses of the angular correlations near threshold has to be more qualitative than quantitative because the large number of parameters involved. For more quantitative results, more data are needed. Nevertheless, the CELLO Collaboration finds evidence for a non resonant amplitude dominating the low angle ρ^0 production, and the TASSO analysis shows that there is no excess of events in this region. The two experiments together thus make a point for a non resonant amplitude dominating the *entire* $\rho^0\rho^0$ cross section. This interpretation also gives a natural explanation for the absence of states with negative parity, which is confirmed by both analyses.

The Off Shell Cross Section for $\gamma\gamma \to \rho^0\rho^0$

Because of the strong fall off of the photon flux, a measurement of the $\rho^0\rho^0$ cross section at non zero q^2 is much harder than the real photon cross section measurement. Only the

PEP49 [96] and the PLUTO [97] Collaborations have shown preliminary data on the q^2 evolution of $\sigma(\gamma\gamma \to \pi^+\pi^-\pi^+\pi^-)$. The limited statistics has not yet allowed to disentangle the different (i.e. $\rho^0\rho^0$, $\rho^0\pi^+\pi^-$ and $\pi^+\pi^-\pi^+\pi^-$) contributions in the tagged data. In fig.(2.5.7), the cross sections $\sigma \simeq \sigma_{TT} + \sigma_{TL}$ from the PEP49 detector are shown. Up to $|q^2| < 1.5GeV^2$, the evolution of the cross section seems to follow a simple ρ^0 pole.

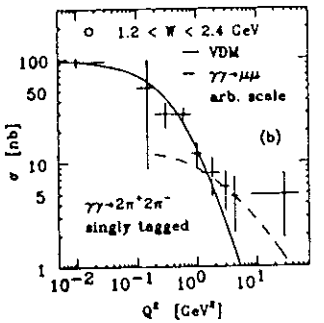

Figure 2.5.7: *Preliminary data from the PEP49 Collaboration show the off shell cross section for $\gamma\gamma \to 2\pi^+2\pi^-$*

It must be stressed though that by definition, what is measured is *not* a form factor. Only, if the $\rho^0\rho^0$ production amplitude is dominated by direct channels, the form factors directly enter the off shell cross sections, however together with flux and spin barriere terms. Thus, the observed q^2 evolution of the cross section has *not* an interpretation as simple as "the photons turn into vector mesons before they interact." In fact, for any model which is based on the VDM hypothesis, such a fall off can only be explained in three cases: 1)For exchange diagrams, the vertex dynamics must be such that it compensates the $1/\sqrt{X}$ flux factor in the cross section as well as the kinematically necessary decrease of the values of the propagators. The pseudoscalar exchange model is an obvious candidate for such a compensation since the antisymmetric form of the vertex couplings implies rising vertex amplitudes. 2)For direct channels, we have to distinguish between states of odd and even parity. For pseudoscalar or pseudotensor mesons, a ρ^0 pole fall off of the *cross section* is possible to the degree that an $L = 1$ spin valley cancels the $(1/\sqrt{X})$ flux factor, i.e. to within some 30 % in the $\rho^0\rho^0$ threshold region. For scalar or tensor resonances, the observed fall off of the cross section is in conflict with VDM, unless the longitudinal cross section is large ($\sigma_{TL} \geq \sigma_{TT}$). This point needs further experimental study. 3)It may be that many not yet understood things happen simultaneously and the net result happens to look like a ρ^0 pole.

An E_1 transition into a scalar or a tensor resonance would lead to a q^2 evolution of the transverse cross section which is softer the ρ^0 pole, however, not vastly different. Such a transition would imply a sizeable longitudinal-transverse cross section as well.

It is interesting to notice that beyond $|q^2| \simeq 1.5GeV^2$, the ρ^0 pole seems to underestimate the measured cross section. One is tempted to interpret this as a take over of the pointlike coupling of the photon ($\gamma\gamma \to q\bar{q}$). However, the data are also consistent with the assumption of a constant (i.e. q^2 independent) amplitude.

Exotic Models and a Measurement of $\gamma\gamma \to \rho^+\rho^-$

The JADE Collaboration [61] investigated the reaction $\gamma\gamma \to \pi^+\pi^-\gamma\gamma\gamma\gamma$ using an integrated luminosity of $77pb^{-1}$. In this analysis, π^0 mesons were identified as photon pairs with invariant masses between 60 and 220 MeV. Evidence was found for $\rho^\pm$ production, but there are no signs of a ρ^0.[1]

The preliminary measurement for $\gamma\gamma \to \rho^+\rho^-$ is shown in fig(2.5.8), together with the preliminary $\rho^0\rho^0$ cross section from the PEP49 detector [98]. The dissimilarity is striking. Experimentally, at least a factor of two in favour of the $\rho^0\rho^0$ cross section is required, however, it could also easily be a factor of 20.

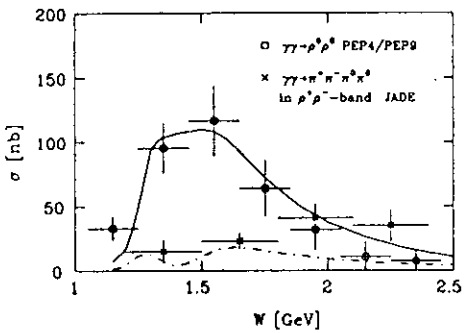

Figure 2.5.8: *Preliminary cross sections for $\rho^+\rho^-$ (JADE) and $\rho^0\rho^0$ (PEP49) production.*

The pseudoscalar exchange model alone has little chance of accounting for the large discrepancy between the $\rho^0\rho^0$ and the $\rho^+\rho^-$ cross section, since the kinematically favoured pion exchange has a larger contribution to $\rho^+\rho^-$ than to $\rho^0\rho^0$, the reason being that $<\rho^0|\rho^0\pi^0>$ is zero because of isospin. It is thus unlikely that a conventional hadronic argument can explain the difference between the cross sections. There must be some fundamental difference between the two processes. In the following, some possible explanations shall be discussed.

A simple isospin invariance argument points towards a possible interpretation of the observed ratio $\frac{\sigma(\gamma\gamma\to\rho^0\rho^0)}{\sigma(\gamma\gamma\to\rho^+\rho^-)} > 1$. Assume that both, the $\rho^0\rho^0$ and the $\rho^+\rho^-$ systems were predominantly produced through resonances. If such resonances are produced through a VDM amplitude and if in this amplitude, the ρ^0 meson dominates the incoming photons ($M(\gamma\gamma \to X) \sim M(\rho^0\rho^0 \to X)$) then, according to the Clebsch Gordan tables, one gets

$$\begin{aligned}
\sigma(\gamma\gamma \to "I=2" \to \rho^+\rho^-) &= \frac{1}{2}\sigma(\gamma\gamma \to "I=2" \to \rho^0\rho^0) \\
\sigma(\gamma\gamma \to "I=1" \to \rho^+\rho^-) &= \sigma(\gamma\gamma \to "I=1" \to \rho^0\rho^0) = 0 \\
\sigma(\gamma\gamma \to "I=0" \to \rho^+\rho^-) &= 2\sigma(\gamma\gamma \to "I=0" \to \rho^0\rho^0)
\end{aligned} \tag{2.5.15}$$

From this point of view, the large cross section ratio in favour of the ρ^0 mesons is quite naturally explained by the presence of $I = 2$, i.e.$q\bar{q}q\bar{q}$ states.

[1] The absence of the ρ^0 can be explained by isospin [12]. A four pion final state must have even isospin if it has positive charge conjugation. However, the ρ^0 has $I = 1$, requiring $I = 1$ for the $\pi^0\pi^0$ system as well which is impossible since the corresponding Clebsh Gordan coefficient is zero.

Two groups of theorists have followed this line of thought to the point of quantitative predictions. Both have come to the conclusion that the simultaneous occurrence of several resonances is necessary.

In the model of Li and Liu [99], there are three four quark tensor mesons populating the $\rho\rho$ threshold region. The authors calculate a $\rho^0\rho^0$ production cross section up to 94.4 nb and a $\rho^+\rho^-$ cross section being half as large. This calculation is not in conflict with the existing data however, it seems that the preliminary JADE measurement would prefer a substantially lower $\rho^-\rho$ cross section.

Wheres the calculation of Li and Liu makes very specific predictions for the cross sections for all vector meson pair production cross sections, Achasov et al [89] stick to more general spin parity / isospin considerations. In their model, the interference of four tensor mesons, the f plus three $q\bar{q}q\bar{q}$ states, of which only one has isospin $I = 2$, leads to the observed cross sections for $\gamma\gamma \to \rho^0\rho^0$ and $\gamma\gamma \to \rho^-\rho$. It must be mentionned though that this model has a number of free parameters which had only been ajusted after the JADE Collaboration had shown the first limits on ω production (see below). Conclusive statements about the validity of this model are thus not yet possible.

It appears to the author that before the observed cross sections are to be taken as evidence for the presence of exotic states, two basic phenomenological points need clarification by the "model builders".

1) The amplitudes for both reactions, $\gamma\gamma \to \rho^0\rho^0$ and $\rho^-\rho$ are bound to have some contributions from non resonant radiative matrix elements. The experimentally known radiative decay of the ρ meson ($\Gamma(\rho \to \pi\gamma) = 63 \pm 4keV$) for example requires a pion exchange contribution to the reaction $\gamma\gamma \to \rho^-\rho$. Only the strengths of this amplitude is subject to model assumptions - not its presence.

2) In contrast to the ρ^0 meson, the ρ^- meson has a direct coupling to the photon. The presence of a Born term like matrix element at some level is thus necessary. Given that pion and kaon pair production is well described by a simple modification of the Born amplitude, a substantial contribution for the production of ρ^- mesons might be expected.

Apart from direct channels, there are thus at least two more large amplitudes contributing to vector meson pair production. The presently published exotic models take neither of them into account. In terms of statistics, this means that there is no null hypothesis for the ratio $\frac{\sigma(\gamma\gamma\to\rho^0\rho^0)}{\sigma(\gamma\gamma\to\rho^-\rho)}$. Which number should be considered a *large* or *small* ratio is thus not yet defined.

Limits on ω Production

If the ρ^0 production cross section is large - why should there not be a sizeable ω signal in the data? The PLUTO [100] and the JADE [101] collaborations looked for such signals and did not find any evidence for ω production. There is not even a hint for single ω production accompagnied by pion pairs. The upper limits for $\sigma(\gamma\gamma \to \rho^0\omega)$ derived by the two groups are shown in fig.(2.5.9). The cross sections for $\gamma\gamma \to \rho^0\omega$ near threshold must be at least a factor two to three smaller than the $\rho^0\rho^0$ production cross section.

Notice that even with moderate detector resolution, an ω signal can be enhanced relative

to the $\pi^+\pi^-\pi^0$ continuum by requiring large angles between all the three pions in their common c.m.s. the reason being that the ω decay matrix element

$$M(\omega \to \pi^+\pi^-\pi^0) \doteq \epsilon^\alpha(\omega)k_a^\beta(\pi^+)k_b^\gamma(\pi^-)k_c^\delta(\pi^0)e_{\alpha\beta\gamma\delta} \tag{2.5.16}$$

leads to a sum of cross products between the pion momentum vectors.

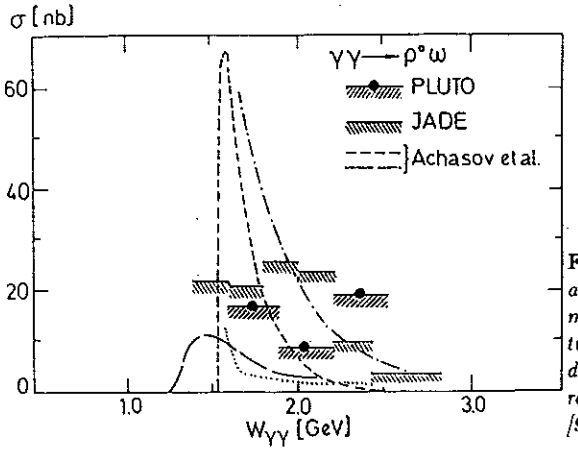

Figure 2.5.9: *Upper limits for the reaction $\gamma\gamma \to \rho^0\omega$ compared with the model of Achasov et al and two estimates based on photo production data. The dashed dotted line is from ref. [109], the dotted line is from ref. [90].*

The above matrix element could also be used for a spin parity analysis. The amplitudes for the different J^p states can be obtained from the corresponding $\rho^0\rho^0$ amplitudes by the replacement

$$\begin{aligned}
(k_1+k_2)^\alpha &\to P_1^\alpha \\
(k_3+k_4)^\alpha &\to P_2^\alpha \\
(k_1-k_2)^\alpha BW(1,2) &\to (-g^{\alpha\beta} + m_\omega^{-2}P_1^\alpha P_1^\beta)e_{\beta\gamma\delta\epsilon}k_a^\gamma k_b^\delta k_c^\epsilon BW(\omega_1) \\
(k_3-k_4)^\alpha BW(3,4) &\to (-g^{\alpha\beta} + m_\omega^{-2}P_2^\alpha P_2^\beta)e_{\beta\gamma\delta\epsilon}k_d^\gamma k_e^\delta k_f^\epsilon BW(\omega_2)
\end{aligned} \tag{2.5.17}$$

where P_1 is the four momentum of the ω meson decaying into the three pions having the momenta k_a, k_b, k_c and $BW(w_1)$ is the corresponding propagator.

The upper limits on the reaction $\gamma\gamma \to \omega\omega$ (c.f. fig.(2.5.10)) are consistent with the model of Li and Liu. They are also consistent with the most up to date version of an estimate by Alexenander et al using photo production data [90] The same conclusions hold for the limits on $\gamma\gamma \to \rho^0\omega$. This channel is also sensitive to the model of Achasov et al. However, since the model containes a number of free parameters, the validity of this model cannot yet be tested experimentally. In fig.(2.5.9), two extreme choices of parameters are shown.

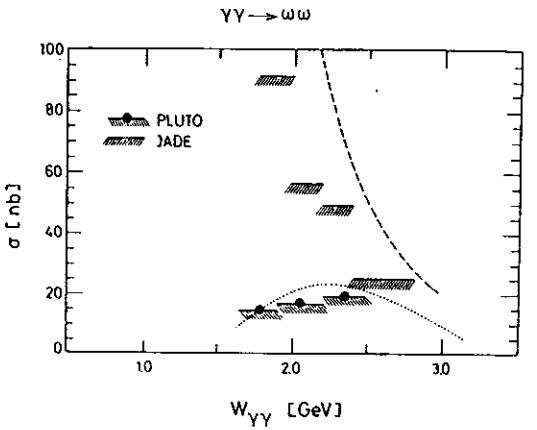

Figure 2.5.10: *Upper limits for the reaction $\gamma\gamma \to \omega\omega$ compared with two estimates based on photo production data. The dashed line is from ref. [109], the dotted line is from ref. [90].*

Observation of ϕ Production

The TASSO [102] and PEP49 [103] Collaborations found evidence for the reaction $\gamma\gamma \to K^+K^-\pi^+\pi^-$. In the TASSO detector, the kaons are found with help of the time of flight counters, while PEP49 uses ionisation measurements in the time projection chamber. The resulting cross sections for $\gamma\gamma \to K^+K^-\pi^+\pi^-$ are shown in fig.(2.5.11). It only reaches some 15nb, which is a factor of 5 to 10 smaller than the $\gamma\gamma \to \pi^+\pi^-\pi^+\pi^-$ cross section at the same energy. Both groups find small but significant ϕ signals in the data.

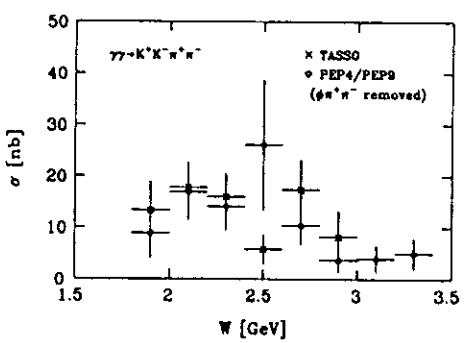

Figure 2.5.11: *Preliminary measurements of the cross section for $\gamma\gamma \to K^+K^-\pi^+\pi^-$.*

The PEP49 Collaboration attempted a resonance decomposition of $K^+K^-\pi^+\pi^-$ production. A survay of this final state shows that $\phi\rho^0$ production only occurs at a small rate. In the mass range from 1.7 to 3.7GeV, the average cross section is found to be less than 1.5

$nb(95\%cl.)$. Instead, the K^* seems to be more important for this channel:

state	*event fraction*	$\sigma Br/nb$
$K^+K^-\pi^+\pi^-$	$0.44 \pm 0.14 \pm 0.05$	$3.7 \pm 1.2 \pm 1.0$
$K^{0*}K^{\pm}\pi^{\mp}$	$0.42 \pm 0.13 \pm 0.05$	$3.5 \pm 1.1 \pm 1.0$
$K^{0*}\bar{K}^{0*}$	$0.09 \pm 0.06 \pm 0.04$	$0.8 \pm 0.5 \pm 0.4$
$\phi\pi^+\pi^-$	$0.05 \pm 0.01 \pm 0.01$	$0.6 \pm 0.2 \pm 0.2$

(PEP49)

Notice that neither TASSO nor PEP49 find any evidence for $\phi\phi$ production. Nevertheless, the data are neither in conflict with the model of Achasov et al, nor with the model of Li and Liu.

Baryon Pair Production

Introduction

The proton usually appears on the first few pages of high energy physics textbooks and there is no other particle which has been measured in so many reactions. One is thus temped to consider it "well understood". However, measurements of the process $\gamma\gamma \to p\bar{p}$ raise doubts about currently available calculations.

The question whether or not data from two photon experiments are sensitive to the structure of the proton, is answered by a comparison of the data with the QED Born term formula for fermion pairs. The corresponding matrix element can be written as

$$M_{a,b} = -e^2\bar{u}(k_1)\left\{\frac{\not{\epsilon}_{1a}(\not{k}_1 - \not{q}_1 + m)\not{\epsilon}_{2b}}{t-m^2} + \frac{\not{\epsilon}_{2b}(\not{k}_1 - \not{q}_2 + m)\not{\epsilon}_{1a}}{u-m^2}\right\}v(k_2) \qquad (2.6.1)$$

where k_1 is the momentum of the proton and the incoming photons have helicities a and b. If we allow one photon to be real (the complete QED helicity cross sections are given in Appendix C) three terms are sufficient to describe the process:

$$\begin{aligned}
\frac{d\sigma_{TT}}{d\Omega} &= \frac{\alpha^2\beta}{2\sqrt{X}}\left\{\frac{1-\beta^4}{(1-\beta^2cos^2\theta)^2}\right. \\
&\quad \left. + \beta^2 sin^2\theta\frac{q_1^2(2(1-\beta^2)W^2 + \beta^2(1+cos^2\theta)q_1^2) - W^4(2-\beta^2sin^2\theta)}{(1-\beta^2cos^2\theta)^2(W^2-q_1^2)^2}\right\} \\
\frac{d\tau_{TT}}{d\Omega} &= -\frac{\alpha^2\beta}{\sqrt{X}}\left\{\frac{(1-\beta^2)^2(W^2-q_1^2)^2}{(1-\beta^2cos^2\theta)^2(W^2-q_1^2)^2}\right. \\
&\quad \left. - \frac{2\beta^2sin^2\theta q_1^2(\beta^2sin^2\theta q_1^2 - 2(1-\beta^2)(W^2-q_1^2))}{(1-\beta^2cos^2\theta)^2(W^2-q_1^2)^2}\right\} \\
\frac{d\sigma_{LT}}{d\Omega} &= \frac{2\alpha^2\beta}{\sqrt{X}}\left\{\frac{\beta^2sin^2\theta(-q_1^2)W^2}{(1-\beta^2cos^2\theta)(W^2-q_1^2)^2}\right\}
\end{aligned} \qquad (2.6.2)$$

where β is the $\gamma\gamma$ c.m.s. velocity and θ is the c.m.s. angle between the fermion and the $\gamma\gamma$ axis.

Measurements of the $p\bar{p}$ Cross Section

The available data on proton pair creation are minute compared to the published meson pair data. The reason is simple: The proton is some seven times as heavy as the π meson, and thus, the photon flux at threshold is about a factor of 45 smaller than the flux at pion threshold. The implications are two fold: First of all, the statistics is limited, and secondly, a hadron pair produced at a given momentum will nearly always be a pion pair. Good particle identification is thus vital for $p\bar{p}$ measurements. This implies a major bottleneck for the comparison between data and calculations. Since the currently used techniques for particle identification (i.e. dE/dx and TOF) are based on measurements of the particle velocities, protons can only be identiefied up to momenta around 1.5 GeV, thus limiting

the measurement range to $W < 4$GeV. However, there is hope that inthe near future, the high point statistics dE/dx measurements in the PEP49 TPC might considerably extend this range of measurability.

The TASSO Collaboration [104] identified the proton antiproton pairs using the barrel time of flight system (fig(2.6.1)). An integrated luminosity of $74\,pb^{-1}$ yielded a sample of 71 events. The JADE collaboration [105] extracted a sample of 63 events[1] from an integrated luminosity of $84pb^{-1}$. In the JADE analysis, dE/dx information from the central drift chamber was used for particle identification in addition to *TOF*. The PEP49 collaboration has shown preliminary data on tagged $p\bar{p}$ production.

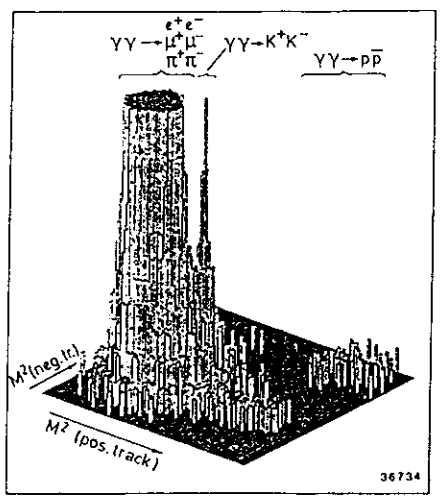

Figure 2.6.1: *The clean separaration of $p\bar{p}$ pairs by means of the TASSO time of flight system for tracks with momenta below 900 MeV enabeled the first measurement of $\gamma\gamma \to p\bar{p}$.*

The extracted cross sections $\int_{-0.6}^{0.6} \frac{d\sigma}{dcos\theta} dcos\theta$ from the interactions of real photons are shown in fig.(2.6.2). The QED Born term overestimates the cross section by about an order of magnitude (see also fig.(2.6.3)). The proton does *not* interact like a pointlike particle. The TASSO collaboration has also shown angular distributions of the $p\bar{p}$ pairs. Fig.(2.6.3) shows that the measured differential cross sections have no minimum at 90°. This would be the characteristic feature of a simple exchange amplitude. The full interpretation of the reaction $\gamma\gamma \to p\bar{p}$ is thus expected to be complicated.

[1] For the determination of the cross section, a sub-sample of 41 events obeying more restrictive trigger conditions was used.

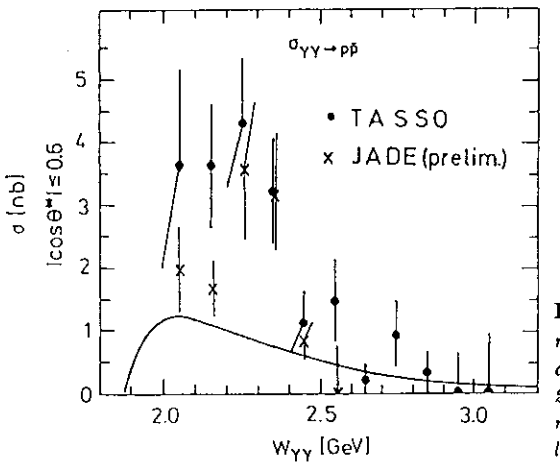

Figure 2.6.2: *The first two measurements of $\int_{-0.6}^{0.6} \frac{d\sigma(\gamma\gamma \to p\bar{p})}{dcos\theta} dcos\theta$ show a large cross section arround $W = 2900\,MeV$. At higher energies, the finite size model (solid line) interpolates the data .*

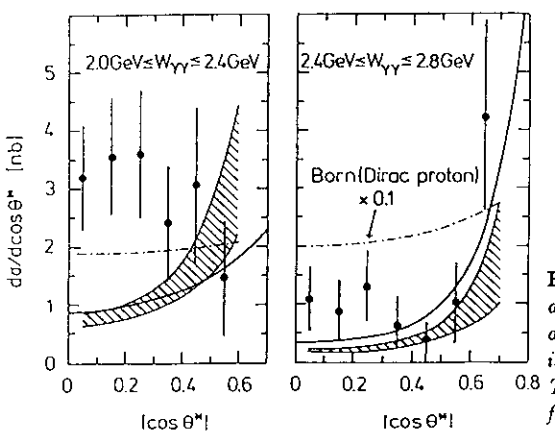

Figure 2.6.3: *A measurement of the angular distribution of $p\bar{p}$ pair production (TASSO). The shaded area is the QCD prediction of Damgaard. The solid line is the prediction of the finite size model.*

Finite Size Effects

A quantitative understanding of finite size effects is much harder to obtain than in the case of charged pions. Since the proton is a fermion, the coupling of a proton current to a photon involves in general two form factors. Since it is experimentally known that the proton has an anomalous magnetic moment, a simple analytic modification of the QED Born term (which only accounts for the γ^μ coupling) will implicitely contradict experimental facts. There is no straigh forward way of "implementing" the anomalous magnetic moment of the

proton into a pair production amplitude.[1]

However, for photons with moderate values of q^2, it may be a good approximation to simply neglect the anomalous magnetic moment of the proton. If we furthermore demand that finite size effects should be functions of the proton propagators alone[1] we get, similar to $\gamma\gamma \to \pi^+\pi^-$, for proton pairs

$$\frac{d\sigma(finite\,size)}{d\sigma(QED)} \simeq x_0^8(t+u-2m^2)^2\left(\frac{1}{(u-m^2)(x_0^2+m^2-u-q_1^2-q_2^2)^2} + \frac{1}{(t-m^2)(x_0^2+m^2-t-q_1^2-q_2^2)^2}\right)^2 \qquad (2.6.3)$$

where x_0 is the scale set by the electric form factor of the proton, i.e. $x_0^2 = 0.71\,GeV^2$. A striking, and to the author's knowledge unique feature of this calculation is that the 0^o production angle cross section *grows* with W, whereas the 90^o cross section rapidly falls.

Figs.(2.6.2/3) show that for invariant masses below 2.4 GeV, the finite size model underestimates the data by a factor of (roughly) three. This discrepancy can be traced back to an "excess" of protons produced at large angles. Above 2.4 GeV, the finite size model is consistent with the data, both in normalisation and shape.

QCD Calculations

Inspired by Brodsky's and Lepage's calculations on meson pair production, Damgaard published a first order QCD prediction for $\gamma\gamma \to p\bar{p}$ [106]. This process is much more difficult to calculate than $\gamma\gamma \to \pi^+\pi^-$. Since a leptonic proton decay has not been observed, there is no measured analogon to the pion decay constant, f_π, and thus no unambiguous normalisation of the parton distribution function $\Phi(x_i, \tilde{Q}_i)$. According to [106], the shape of this function evolves to

$$\Phi(x_i, \tilde{Q}_i) \to C x_1 x_2 x_3 (ln\frac{\tilde{Q}_i}{\Lambda^2})^{-2(33-2n_f)/3}$$

where $\tilde{Q}$ is the momentum transfer along the probed quark, x_i its fractional momentum. C is the (unknown) overall normalisation and $n_f = 2$. Again, the evolution of the distribution is logarithmic, and hence, Φ has to be considered unknown in the measured W range. It would be nice to normalise Φ through the clean and well measured reaction $e^-p \to e^-p$. However, for this process, the first order hard scattering amplitude T_H turns out to vanish (see for example [107]).[2] In ref.[106], the normalisation of the wave function is obtained by applying first order QCD to the decay $J/\Psi \to 3g \to p\bar{p}$.

The explicit form of the scattering amplitude must be very complicated, since it is not written down in any paper. Only curves for the final result are shown (c.f. fig.(2.6.3)). The QCD prediction of Damgaard compares with the data in a similar manner as the finite size model, may be slightly worse.

A calculation similar to the above one was carried out by Ferrar et al [107]. Using the same normalisation procedure as Damgaard, a cross section which is a factor 20 to 50 below Damgaards prediction is obtained and thus the prediction underestimates the true cross section by about one to two orders of magnitude. In ref.[107], it is claimed that, using the distribution function of Chernyak and Zhituitcky [108], a cross section of about 1 nb is obtained for $|cos\theta| < 0.6$.

Given that the predictions in the framework of QCD still oscillate within a factor of $\sim$ 50, measurements of $\gamma\gamma \to p\bar{p}$ can not yet be considered as QCD tests. Further suspicion about the applicability of the published calculations arise from the fact that so far, the mass of the proton has been disregarded. More precise calculations are urgently needed.

Direct Channels?

The TASSO data show that in the low energy region, the angular distribution has no minimum around 90^o. Preliminary data from PEP49 and JADE (not yet available) even seem to indicate a maximum of the differential cross section at $cos\theta = 0$. This "maximum" is due to events which populate an energy region, where the integrated cross section exceeds the cross section predicted by the finite size model. This may be a hint towards the presence of at least one resonance in this channel.

In the measured energy regime, there are many resonances seen in $p\bar{p}$ scattering experiments. However, only two of them have the right quantum numbers to be produced in $\gamma\gamma$ collisions:

state	$I^G J^P$	m_R/MeV	Γ_R/MeV	*modes seen*
$\epsilon(2150)$	$0^- 2^-$	2150 – 2190	~ 250	$\pi^+\pi^-$, $\pi^0\pi^0$, $n\bar{n}$
$\epsilon(2300)$	$0^- 4^+$	2300 – 2380	130 – 210	$\pi^+\pi^-$, $\pi^0\pi^0$, $n\bar{n}$

The $\epsilon(2150)$ seems to have a too small mass in order to account for the observed mass spectrum. Thus, only one known candidate remains.

At present, the data are not sufficiently accurate to confirm this hypothesis. Only more statistics can tell. If the data reveal signs of a $J^P = 4^+$ dominance, this would certainly stimulate the discussion between experiments at LEAR and e^+e^- machines.

[1] The anomalous magnetic moment of the proton is defined through a decomposition of the *squared* amplitude for $ep \to ep$. Therefore, it cannot be parameterised as a modification of the photon proton *vertex* and consequently, an implementation of the anomalous magnetic moment into cross section predictions for other processes can only proceed via explicit models of the proton which reproduce the observed $ep \to ep$ cross section.

[1] This requirement can be used to cancel the rather complicated numerators in eq.(2.6.1), the trick being the introduction of inversion operators $\hat{I}_1, \hat{I}_2$ which obey obey for example

$$\hat{I}_1 \cdot \{\bar{u}(k_1)\,\not{\epsilon}_{1a}(\not{k}_1 - \not{q}_1 + m)\,\not{\epsilon}_{2b}v(k_2)\} = 1$$

(c.f. eq.(2.5.1)). From here, one can proceed as in the case of $\pi^+\pi^-$ pair production, however with a different input form factor

[2] In this light, it seems inunderstandable that the electric form factor of the proton follows a $(1/q^2)^2$ fall off at large momentum transfer.

CONCLUSIONS

After a large number of exclusive two photon processes has been looked at in all detail, it appears that the attempt of describing two photon interactions in the resonance region within the framework of *one* dynamical model is -at least at present- overambitious. Two photon physics in the resonance region occurs in a kinematic regime, where the transition from observing hadrons as a whole to the production of quark pairs takes place. The available measurements of the reaction $\gamma\gamma \to \pi^+\pi^-$ illustrate this point most beautifully. Up to an invariant mass of $\sim \frac{1}{2}GeV$, little deviations from the QED Born term formula are visible in the data. At c.m.s. energies above $\sim 2GeV$, the data show the characteristic power law behaviour of a QCD $\gamma\gamma \to q\bar{q} + q\bar{q}$ "Born term". The energy region from $\frac{1}{2}$ to 2 GeV hosts most of the resonances seen in two photon experiments.

If we interpret measurements of the charged pion form factor as measurements of the charge distribution within the π^+ meson rather than a vector dominance effect, the energy scale at which the transition from mesons to quarks takes place comes out quite naturally -both qualitatively and quantitatively: the energy scale is then set by the inverse of the wavelengths of the photons which produce the state. Experimental two photon physics in the resonance region is thus *meson microscopy*.

For the sake of getting a conceptually simple picture in this dynamically difficult environment, let us assume that the light mesons all have a similar mean charge radius of approximately $\frac{1}{2}fm$ and let us consider two photon experiments as microscopes, whose wavelengths is chosen according to the mass of the hadronic state produced. In this simple framework, the following picture emerges:

At $W = m_\eta$, the wave length of the incident photons is approximately equal to the hadrons mean charge radius. From here on, the photons begin to probe the inside of mesons. Accordingly the production cross section of the η' is slightly smaller than the naive SU(3) relation predicts. The most recent and most precise measurements of the radiative width of the η' indicate such a deviation from SU(3). As the wavelengths is tuned to 0.16 fm, the f resonance appears. The f is not seen as an entire object any more. In fact, SU(6) predictions based on the interactions with pions and vector mesons fail. Model calculations which interpret the coupling of the f meson to two photons as an E_1 transition are successful. We do not see quarks yet, but we begin to see the charge distributions inside the mesons due to the motion of the quarks. The step from m_f to m_{A_2} is small. Accordingly, no deviations from SU(3) and ideal mixing are seen. Somewhere beyond $W = 1.5GeV$, quarks appear in the light of the two photons. We do not know yet, from which point onwards quarks are seen, simply because for the pair production amplitudes, first order perturbative QCD calculations give very similar results as the simplest possible finite size models of hadrons.

This simple picture can of course not replace a dynamical theory of the interactions between photons and hadrons. However, it does provide quite a natural link between phenomena which, at first sight, may seem to be quite disconnected:

High spin resonances never decay according to the simple Breit Wigner formula. The scale from which onwards the deviations become visible is just twice the mean charge radius of the π^+ meson. This scale is the one measured in form factor measurements. It is the same scale which also governes the $t - m^2$ evolution of pion and kaon pair production amplitudes. Last not least, this scale naturally explaines small deviations from SU(3). If the same number occurs in four completely different contexts, we may assume that this is more than a coincidence. The interpretation of two photon experiments as microscopes for mesons is thus meaningful.

The author noticed to his own surprise, how very simple estimates of finite size effects could explain features of the data, which in the literature are often attributed to VDM (photon-meson form factors), perturbative QCD ($\gamma\gamma \to \pi^+\pi^-, K^+K^-, p\bar{p}$), or even traces of gluonium admixtures (deviations from $SU(3)_{Fl}$ in $\Gamma_{\gamma\gamma}(0^-)$). These coincidences may be taken as a hint towards a synthesis: *Vector meson dominance parametrises photon quark interactions at the 1 fm scale.* We are still far away from formulating such a synthesis in a fully convincing, quantitative manner. However, qualitatively, it may help to explain why VDM and QPM give very similar predictions for $\Gamma_{\gamma\gamma}(\pi^0)$, why single current meson form factors follow simple vector meson poles without additional damping terms, and -last not least- why the form factors of the proton are *not* reproduced by vector meson dominance. A non trivial consequence of this point of view is that even at small values of q_1^2, q_2^2, two photon couplings should show no factorisation of the type $F(q_1^2, q_2^2) = f(q_1^2) \cdot f(q_2^2)$, as might be expected in a literal interpretation of vector meson dominance.

Exclusive two photon reactions remain a challenge for theory and experiment. It is hoped that by separating the basic constraints from specific model assumptions and by pointing out phenomenological differences between various dynamical approximations, this paper will help experimentalists to take up this challenge.

Good luck!

Acknowledgement

The author is very grateful to Prof. F. Gutbrod, Prof. V. Blobel, Dr. J.E. Olsson and Dr. K. Smith for checking the manuscript and making valuable suggestions in spite of heavy other commitments. He gratefully acknowledges the unusually large amount of scientific freedom and the many opportunities of outside research granted to him by the University of Hamburg through Prof. H. Spitzer. He thanks Prof. H. Joos for patiently explaining theory whenever asked. The author enjoyed the many fruitful discussions with his collegues from the PLUTO and CELLO collaborations, in particular with Prof. A. Skuja, Dr. G. Bella, Dr. J. Dainton, Dr. B. King, Dr. J. Thompson and M. Feindt. He thanks the DESY library staff for continuously friendly and efficient support and he is grateful to Dr. P.K. Schilling from the DESY Rechenzentrum for software support. He is also grateful to various members of the JADE and Crystal Ball collaborations for giving insight into ongoing analyses. Last, not least he thanks the DESY directorate for their hospitality and the provision of all the tools necessary.

Appendix-A Construction of the Two Photon Helicity Amplitudes

The amplitudes describing the coupling of a spin "n" particle to a system of two photons have the most general form

$$M_{a,b} = F\,\epsilon_1^{\mu}\epsilon_2^{\nu}T_{\mu\nu\alpha_1\ldots\alpha_n}E^{*\alpha_1\ldots\alpha_n}_{J_z=a-b} \tag{A-1}$$

where a, b and J_z denote the helicities of the photons and the meson respectively. E is the polarisation tensor of the prodced state. The form factors F are to be determined by experiments. In nearly all cases, the choice of form factors and thus the choice of amplitudes is not unique. Here, the particular choice follows from the demand that, to the possible extent, the form factors have a one to one correspondence with helicity matrix elements. The result of such a parameterisation is that in an experiment, the data can be parameterised with the smallest possible number of free parameters. Such a one to one correspondence can be achieved by expanding the amplitudes in terms of the following tensors:

$$\begin{aligned}
G_{\mu\nu} &= g_{\mu\nu} - \frac{1}{X}\left(-q_1q_2(q_{2\mu}q_{1\nu} + q_{1\mu}q_{2\nu}) + q_2^2q_{1\mu}q_{1\nu} + q_1^2q_{2\mu}q_{2\nu}\right)\\
Q_{1\mu} &= q_{1\mu} - \frac{q_1^2}{q_1q_2}q_{2\mu} \qquad Q_{2\nu} = q_{2\nu} - \frac{q_2^2}{q_1q_2}q_{1\nu}\\
L_{\mu\nu} &= \frac{q_1q_2}{X}Q_{1\mu}Q_{2\nu}\\
\tilde{G}_{\mu\nu} &= ie_{\mu\nu\alpha\beta}q_1^{\alpha}q_2^{\beta}\\
\tilde{P}_{1\mu\xi} &= iG_{\mu}^{\alpha}e_{\alpha\beta\gamma\xi}q_1^{\beta}q_2^{\gamma} \qquad \tilde{P}_{2\nu\xi} = iG_{\nu}^{\alpha}e_{\alpha\beta\gamma\xi}q_2^{\beta}q_1^{\gamma}\\
\tilde{S}_{\mu\nu\xi} &= iG_{\mu}^{\alpha}G_{\nu}^{\beta}(q_2 - q_1)^{\gamma}e_{\alpha\beta\gamma\xi}\\
\tilde{A}_{\mu\nu\xi} &= iG_{\mu}^{\alpha}G_{\nu}^{\beta}(q_2 + q_1)^{\gamma}e_{\alpha\beta\gamma\xi}
\end{aligned} \tag{A-2}$$

These tensors are all gauge invariant. Furthermore, $G_{\mu\nu}$ and $L_{\mu\nu}$ are orthonormal projection tensors:

$$\begin{aligned}
\epsilon_{1a}^{\mu}\epsilon_{2b}^{\nu}L_{\mu\nu} &= \epsilon_{1a}^{\mu}\epsilon_{2b}^{\nu}L_{\mu\alpha}g^{\alpha\beta}L_{\beta\nu} = \frac{\sqrt{q_1^2q_2^2}}{q_1q_2}\delta_a^b\delta_a^0\\
\epsilon_{1a}^{\mu}\epsilon_{2b}^{\nu}G_{\mu\nu} &= \epsilon_{1a}^{\mu}\epsilon_{2b}^{\nu}G_{\mu\alpha}g^{\alpha\beta}G_{\beta\nu} = \delta_a^b(\delta_a^+ + \delta_a^-)\\
G_{\mu\alpha}g^{\alpha\beta}L_{\beta\nu} &= G_{\mu\alpha}g^{\mu\beta}L_{\beta\nu} = G_{\mu\alpha}g^{\alpha\nu}L_{\beta\nu} = 0
\end{aligned} \tag{A-3}$$

They can thus be interpreted as filters for transversally and longitudinally polarised photons. Therefore, the helicity amplitudes which can be entirely expressed in terms of $G_{\mu\nu}$ and $L_{\mu\nu}$ represent a zeroth order estimate of the q^2 evolution of the helicity amplitudes. The two vectors $Q_{1\mu}$ and $Q_{2\nu}$ form a "Bose doublet", whereas $G_{\mu\nu}$ and $L_{\mu\nu}$ are invariant under the simultaneous transformations $\mu \leftrightarrow \nu$ and $q_1 \leftrightarrow q_2$. All two photon amplitudes for states with "normal" intrinsic parities ($J^P = 0^+, 1^-, 2^+, \ldots$) can be constructed from these tensors and simple outer products of the type $(q_2 - q_1)^{\alpha}(q_2 - q_1)^{\beta}\ldots$, which serve as "contractors" for remaining indices of the final state polarisation tensor. Amplitudes connecting two photons with a state of "abnormal" intrinsic parity ($J^P = 0^-, 1^+, 2^-, \ldots$) must contain the antisymmetric tensor once. It can easily be shown that in such amplitudes, the antisymmetric tensor

has to contract at least one of the photon helicities. Therefore, it is not possible to construct projection tensors for such states. Nevertheless, the tilded tensors in eq(A-2) *select* certain helicity configurations:

$$\begin{aligned}
\epsilon^{\mu}_{1a}\epsilon^{\nu}_{2b}\widetilde{G}_{\mu\nu} &= \sqrt{X}\delta^{b}_{a}(\delta^{+}_{a}-\delta^{-}_{a}) \\
\epsilon^{\mu}_{1a}\widetilde{P}_{1\mu\delta}\epsilon^{*\delta}_{c} &= -\sqrt{X}\delta^{c}_{a}(\delta^{+}_{a}-\delta^{-}_{a}) \\
\epsilon^{\nu}_{2b}\widetilde{P}_{2\nu\delta}\epsilon^{*\delta}_{c} &= -\sqrt{X}\delta^{c}_{b}(\delta^{+}_{b}-\delta^{-}_{b}) \\
\epsilon^{\mu}_{1a}\epsilon^{\nu}_{2b}\widetilde{S}_{\mu\nu\delta}\epsilon^{*\delta}_{c} &= \frac{q_1^2-q_2^2}{W}\delta^{b}_{a}\delta^{0}_{c}(\delta^{+}_{a}-\delta^{-}_{a}) \\
\epsilon^{\mu}_{1a}\epsilon^{\nu}_{2b}\widetilde{A}_{\mu\nu\delta}\epsilon^{*\delta}_{c} &= -W\delta^{b}_{a}\delta^{0}_{c}(\delta^{+}_{a}-\delta^{-}_{a})
\end{aligned} \tag{A-4}$$

Whereas $\widetilde{G}_{\mu\nu\delta}$ and $\widetilde{S}_{\mu\nu\delta}$ are invariant under a Bose transformation, $\widetilde{A}_{\mu\nu\delta}$ changes sign and $\widetilde{P}_{1\mu\delta}$ and $\widetilde{P}_{2\nu\delta}$ are interchanged.

Having constructed suitable sub-tensors, we can proceed to write down the amplitudes. The following equations also define the helicity form factors F.

0^+ *states*
$$\begin{aligned}
T^{TT0}_{\mu\nu} &= F_{TT0}G_{\mu\nu} \\
T^{LL}_{\mu\nu} &= F_{LL}L_{\mu\nu}
\end{aligned}$$

1^- *states*
$$\begin{aligned}
T^{TT0}_{\mu\nu} &= F_{TT0}(q_2^2-q_1^2)G_{\mu\nu}(q_2-q_1)_{\alpha}\epsilon^{*\alpha} \\
T^{LL}_{\mu\nu} &= F_{LL}(q_2^2-q_1^2)L_{\mu\nu}(q_2-q_1)_{\alpha}\epsilon^{*\alpha} \\
T^{TL}_{\mu\nu} &= F_{TL}\left\{G_{\mu\alpha}Q_{2\nu}+Q_{1\mu}G_{\nu\alpha}\right\}\epsilon^{*\alpha} \\
T^{TL\prime}_{\mu\nu} &= F'_{TL}(q_2^2-q_1^2)\left\{G_{\mu\alpha}Q_{2\nu}-Q_{1\mu}G_{\nu\alpha}\right\}\epsilon^{*\alpha}
\end{aligned}$$

2^+ *states*
$$\begin{aligned}
T^{TT0}_{\mu\nu} &= F_{TT0}G_{\mu\nu}(q_2-q_1)_{\alpha}(q_2-q_1)_{\beta}E^{*\alpha\beta} \\
T^{TT2}_{\mu\nu} &= F_{TT2}G_{\mu\alpha}G_{\nu\beta}E^{*\alpha\beta} \\
T^{LL}_{\mu\nu} &= F_{LL}L_{\mu\nu}(q_2-q_1)_{\alpha}(q_2-q_1)_{\beta}E^{*\alpha\beta} \\
T^{TL}_{\mu\nu} &= F_{TL}\left\{G_{\mu\alpha}Q_{2\nu}-Q_{1\mu}G_{\nu\alpha}\right\}(q_2-q_1)_{\alpha}E^{*\alpha\beta} \\
T^{TL\prime}_{\mu\nu} &= F'_{TL}(q_2^2-q_1^2)\left\{G_{\mu\alpha}Q_{2\nu}+Q_{1\mu}G_{\nu\alpha}\right\}(q_2-q_1)_{\alpha}E^{*\alpha\beta}
\end{aligned}$$

3^- *states*
$$\begin{aligned}
T^{TT0}_{\mu\nu} &= F_{TT0}(q_2^2-q_1^2)G_{\mu\nu}(q_2-q_1)_{\alpha}(q_2-q_1)_{\beta}(q_2-q_1)_{\gamma}E^{*\alpha\beta\gamma} \\
T^{TT2}_{\mu\nu} &= F_{TT2}(q_2^2-q_1^2)G_{\mu\alpha}G_{\nu\beta}(q_2-q_1)_{\gamma}E^{*\alpha\beta\gamma} \\
T^{LL}_{\mu\nu} &= F_{LL}(q_2^2-q_1^2)L_{\mu\nu}(q_2-q_1)_{\alpha}(q_2-q_1)_{\beta}(q_2-q_1)_{\gamma}E^{*\alpha\beta\gamma} \\
T^{TL}_{\mu\nu} &= F_{TL}\left\{G_{\mu\alpha}Q_{2\nu}+Q_{1\mu}G_{\nu\alpha}\right\}(q_2-q_1)_{\beta}(q_2-q_1)_{\gamma}E^{*\alpha\beta\gamma} \\
T^{TL\prime}_{\mu\nu} &= F'_{TL}(q_2^2-q_1^2)\left\{G_{\mu\alpha}Q_{2\nu}-Q_{1\mu}G_{\nu\alpha}\right\}(q_2-q_1)_{\beta}(q_2-q_1)_{\gamma}E^{*\alpha\beta\gamma}
\end{aligned}$$

0^- *states*
$$T^{TT0}_{\mu\nu} = F_{TT0}\widetilde{G}_{\mu\nu}$$

1^+ *states*
$$\begin{aligned}
T^{TT0}_{\mu\nu} &= F_{TT0}\widetilde{S}_{\mu\nu\alpha}\epsilon^{*\alpha} \\
T^{TL}_{\mu\nu} &= F_{TL}\left\{\widetilde{P}_{1\mu\alpha}Q_{2\nu}+Q_{1\mu}\widetilde{P}_{2\nu\alpha}\right\}\epsilon^{*\alpha} \\
T^{TL\prime}_{\mu\nu} &= F'_{TL}(q_2^2-q_1^2)\left\{\widetilde{P}_{1\mu\alpha}Q_{2\nu}-Q_{1\mu}\widetilde{P}_{2\nu\alpha}\right\}\epsilon^{*\alpha}
\end{aligned}$$

2^- *states*
$$\begin{aligned}
T^{TT0}_{\mu\nu} &= F_{TT0}\widetilde{A}_{\mu\nu\alpha}(q_2-q_1)_{\alpha}E^{*\alpha\beta} \\
T^{TT2}_{\mu\nu} &= F_{TT2}(q_2^2-q_1^2)\left\{G_{\mu\alpha}\widetilde{P}_{2\nu\beta}-\widetilde{P}_{1\mu\alpha}G_{\nu\beta}\right\}E^{*\alpha\beta} \\
T^{TL}_{\mu\nu} &= F_{TL}\left\{\widetilde{P}_{1\mu\alpha}Q_{2\nu}-Q_{1\mu}\widetilde{P}_{2\nu\alpha}\right\}(q_2-q_1)_{\beta}E^{*\alpha\beta} \\
T^{TL\prime}_{\mu\nu} &= F'_{TL}(q_2^2-q_1^2)\left\{\widetilde{P}_{1\mu\alpha}Q_{2\nu}+Q_{1\mu}\widetilde{P}_{2\nu\alpha}\right\}(q_2-q_1)_{\beta}E^{*\alpha\beta}
\end{aligned}$$

3^+ *states*
$$\begin{aligned}
T^{TT0}_{\mu\nu} &= F_{TT0}\widetilde{S}_{\mu\nu\alpha}(q_2-q_1)_{\beta}(q_2-q_1)_{\gamma}E^{*\alpha\beta\gamma} \\
T^{TT2}_{\mu\nu} &= F_{TT2}(q_2^2-q_1^2)\left\{G_{\mu\alpha}\widetilde{P}_{2\nu\beta}+\widetilde{P}_{1\mu\alpha}G_{\nu\beta}\right\}(q_2-q_1)_{\gamma}E^{*\alpha\beta\gamma} \\
T^{TL}_{\mu\nu} &= F_{TL}\left\{\widetilde{P}_{1\mu\alpha}Q_{2\nu}+Q_{1\mu}\widetilde{P}_{2\nu\alpha}\right\}(q_2-q_1)_{\beta}(q_2-q_1)_{\gamma}E^{*\alpha\beta\gamma} \\
T^{TL\prime}_{\mu\nu} &= F'_{TL}(q_2^2-q_1^2)\left\{\widetilde{P}_{1\mu\alpha}Q_{2\nu}-Q_{1\mu}\widetilde{P}_{2\nu\alpha}\right\}(q_2-q_1)_{\beta}(q_2-q_1)_{\gamma}E^{*\alpha\beta\gamma}
\end{aligned}$$

Since all of these amplitude are explicitely invariant under exchange of photon vectors and polarisations, so are the corresponding form factors, i.e. $F(q_1^2,q_2^2) = F(q_2^2,q_1^2)$. This set of amplitudes represents *all possible* couplings of two photons to systems up to spin $J = 3$. Moreover, since for $J \geq 2$, one can write without loss of generality

$$T_{\mu\nu\alpha_1\ldots\alpha_{J+2}} \sim T_{\mu\nu\alpha_1\ldots\alpha_J}(q_2-q_1)_{\alpha_{J-1}}(q_2-q_1)_{\alpha_{J+2}} \tag{A-6}$$

the form of the helicity amplitudes for higher spin states is given by the form of given ones:

$$M_{a,b}(\{J+2\}^P) \sim M_{a,b}(J^P)\frac{4X}{W^2} \tag{A-7}$$

The explicite forms of the amplitudes for the low spin states are given in the following table. In this table, we abbreviate $D = (q_2^2 - q_1^2)$.

J^P	M_{++}/F_{TT0}	M_{+-}/F_{TT2}	$M_{0+}/(F_{TL}-(q_2^2-q_1^2)F'_{TL})$	M_{00}/F_{LL}
0^+	1	0	0	$\frac{\sqrt{q_1^2q_2^2}}{q_1q_2}$
1^-	$2D\frac{\sqrt{X}}{W}$	0	$\frac{\sqrt{-q_1^2}}{q_1q_2}$	$2D\frac{\sqrt{q_1^2q_2^2}}{q_1q_2}\frac{\sqrt{X}}{W}$
2^+	$\frac{8}{\sqrt{6}}\frac{X}{W^2}$	1	$-\sqrt{2}\frac{\sqrt{-q_1^2}}{q_1q_2}\frac{X}{W}$	$\frac{8}{\sqrt{6}}\frac{\sqrt{q_1^2q_2^2}}{q_1q_2}\frac{X}{W^2}$
3^-	$\frac{8}{\sqrt{10}}D\frac{X^{3/2}}{W^3}$	$\frac{2}{\sqrt{3}}D\frac{\sqrt{X}}{W}$	$\frac{4}{\sqrt{15}}\frac{\sqrt{-q_1^2}}{q_1q_2}\frac{X^{3/2}}{W^2}$	$\frac{8}{\sqrt{10}}D\frac{\sqrt{q_1^2q_2^2}}{q_1q_2}\frac{X^{3/2}}{W^3}$
0^-	$\sqrt{X}$	0	0	0
1^+	$-\frac{D}{W}$	0	$-\frac{\sqrt{-q_1^2}}{q_1q_2}\sqrt{X}$	0
2^-	$-\frac{4}{\sqrt{6}}\sqrt{X}$	$2D\sqrt{X}$	$\sqrt{2}\frac{\sqrt{-q_1^2}}{q_1q_2}\frac{\sqrt{X}}{W}$	0
3^+	$-\frac{8}{\sqrt{10}}D\frac{X}{W^3}$	$\frac{4}{\sqrt{3}}\frac{X}{W}$	$-\frac{8}{\sqrt{15}}\frac{\sqrt{-q_1^2}}{q_1q_2}\frac{X^{3/2}}{W^2}$	0

From this table, we can deduce the experimental interpretations of the form factors, since their indices define the configuration they describe, F_{TT0} for example, is a measure of the collision of two transversally polarised photons, forming a state with polarisation $J_z = 0$.

If one calculates the remaining helicity amplitudes, one finds that the following symmetries are always fulfilled:

$$\begin{aligned} M_{a,b}(q_1^2,q_2^2) &= M_{-a,-b}(q_1^2,q_2^2) && for \quad J^P = 0^+,1^-,2^+,... \\ M_{a,b}(q_1^2,q_2^2) &= -M_{-a,-b}(q_1^2,q_2^2) && for \quad J^P = 0^-,1^+,2^-,... \\ M_{a,b}(q_1^2,q_2^2) &= (-1)^{(J-a+b)}M_{b,a}(q_2^2,q_1^2) && for \quad all \quad J^P \end{aligned} \tag{A-9}$$

Thus, for example, the $+0$ matrix element for tensor meson production is given by $M_{+0}(\gamma\gamma \to 2^+) = +\sqrt{2}\frac{\sqrt{-q_2^2}}{q_1 q_2}\frac{X}{W}(F_{TL}(\gamma\gamma \to 2^+) - (q_1^2 - q_2^2)F'_{TL}(\gamma\gamma \to 2^+))$. From this set of equations, most selection rules can be obtained. The form factors are chosen such that for single particle production amplitudes, they are real at $W^2 \simeq M_R^2$.

Appendix-B Non Peripheral Contributions to $e^+e^- \to e^+e^-X$

The $\gamma\gamma$ fusion amplitudes dominate the $e^+e^- \to e^+e^-X$ cross section. The second largest contribution comes from the Bremsstrahlungs graphs. According to ref.[19], the cross section for this process is

$$\begin{aligned} d\sigma &= \frac{1}{(2\pi)^5 2s}(A_1 + A_2 + A_3) f(W_{\mu\mu}^2)\delta^4(p_1 + p_2 - p_1' - p_2' - K)\frac{d^3p_1'}{2E_1'}\frac{d^3p_2'}{2E_2'}\frac{d^3K}{2E_{\mu\mu}}dW_{\mu\mu}^2 \\ &= \frac{1}{(4\pi)^5\sqrt{ss}}(A_1 + A_2 + A_3) f(W_{\mu\mu}^2) dW_{ee}^2 dW_{\mu\mu}^2 d\phi_\gamma d\Omega_2' dE_2' \end{aligned} \tag{B-1}$$

where Ω_2' and E_2' describe the motion of the outgoing e^- and ϕ_γ is the azimuthal angle of the $\mu^+\mu^-$ pair around the e^-. W_{ee}^2 and $W_{\mu\mu}^2$ are the invariant masses squared of the final state lepton pairs. The distribution function $f(W_{\mu\mu}^2)$ originates in an integration over the polar angle of the μ^+ around the timelike photon and describes its conversion into a $\mu^+\mu^-$ pair:

$$f(W_{\mu\mu}^2) = \frac{\alpha}{6\pi}\frac{\beta(3-\beta^2)}{W_{\mu\mu}^2} \tag{B-2}$$

Here, β is the velocity of the muons in their common center of momentum frame. The squared amplitudes A_1, A_2 and A_3 are given by

$$\begin{aligned} A_1 = \frac{4e^6}{q_2^4}\Bigg\{ & -\frac{W_{\mu\mu}^2}{(W_{\mu\mu}^2 - 2p_1K)^2}g(p_1 - K, p_1') - \frac{W_{\mu\mu}^2}{(W_{\mu\mu}^2 + 2p_1'K)^2}g(p_1, p_1' + K) \\ & + \frac{1}{(W_{\mu\mu}^2 - 2p_1K)(W_{\mu\mu}^2 + 2p_1'K)}\Big(q_2^2\{g(p_1 - K, p_1') + g(p_1, p_1' + K)\} \\ & + \{W_{\mu\mu}^2 + 2p_1'K\}g(p_1, p_1 - p_1' - K) - \{W_{\mu\mu}^2 - 2p_1K\}g(p_1 - p_1' - K, p_1') \\ & - W_{\mu\mu}^2\{g(p_1', p_1' + K) - g(p_1 - K, p_1) + 8(p_1p_1')(q^2 + d^2)\}\Big)\Bigg\} \end{aligned} \tag{B-3}$$

where K is the four momentum of the $\mu\mu$ system and the function g is defined by $g(a,b) = 8(ad)(bd) - (ab)(2q^2 + 4d^2)$ with $d_\nu = (E_2p_{2\nu}' - E_2'p_{2\nu})/(E_2 - E_2')$. The second amplitude can be obtained from the first one by interchanging two four momenta:

$$A_2(p_1, p_1', p_2, p_2') = A_1(-p_2', -p_2, -p_1', -p_1) \tag{B-4}$$

leaving

$$\begin{aligned} A_3 = \frac{4e^6}{q_1^2q_2^2}\Bigg\{ & (s^2 + W_{ee}^2 + (p_1 - p_2')^4 + (p_2 - p_1')^4)\Big(\frac{s - W_{\mu\mu}^2}{(W_{\mu\mu}^2 - 2p_1K)(W_{\mu\mu}^2 - 2p_2K)} \\ & + \frac{W_{ee}^2 - W_{\mu\mu}^2}{(W_{\mu\mu}^2 + 2p_1'K)(W_{\mu\mu}^2 + 2p_2'K)} - \frac{(p_1 - p_2')^2 - W_{\mu\mu}^2}{(W_{\mu\mu}^2 - 2p_1K)(W_{\mu\mu}^2 + 2p_2'K)} \\ & - \frac{(p_2 - p_1')^2 - W_{\mu\mu}^2}{(W_{\mu\mu}^2 - p_2K)(W_{\mu\mu}^2 + 2p_2'K)}\Big) \\ & - \frac{2W_{\mu\mu}^2q_1^2q_2^2[(s - W_{ee}^2 - ((p_1 - p_2')^2 - (p_2 - p_1')^2)^2]}{(W_{\mu\mu}^2 - 2p_1K)(W_{\mu\mu}^2 + 2p_1'K)(W_{\mu\mu}^2 - 2p_2K)(W_{\mu\mu}^2 + 2p_2'K)}\Bigg\} \end{aligned} \tag{B-5}$$

The total cross section for this process is about two orders of magnitude smaller than the cross section of the $\gamma\gamma$ fusion mechanism.

Appendix-C The QED Helicity Cross Sections for Fermion Pairs

The matrix element for the creation of a pair of pointlike Fermions can be written as

$$M_{a,b} = -e^2\bar{u}(k_1)\left\{\frac{\not\epsilon_{1a}(\not k_1 - \not q_1 + m)\not\epsilon_{2b}}{t-m^2} + \frac{\not\epsilon_{2b}(\not k_1 - \not q_2 + m)\not\epsilon_{1a}}{u-m^2}\right\}v(k_2) \qquad \text{(C-1)}$$

where k_1 is the momentum of the fermion and the incoming photons have helicities a and b. Using the Dirac equation, $\bar{u}(k_1)(\not k_1 - m) = 0$, the Lorentz gauge condition and summing over the fermion spins gives

$$\begin{aligned} M_{a,b}M^{\dagger}_{c,d} =& e^4 Sp\left\{\left(\frac{2(\epsilon_{1a}k_1)\not\epsilon_{2b} + \not q_1\not\epsilon_{1a}\not\epsilon_{2b}}{t-m^2} + \frac{2(\epsilon_{2b}k_1)\not\epsilon_{1a} + \not q_2\not\epsilon_{2b}\not\epsilon_{1a}}{u-m^2}\right)(\not k_2 - m)\right. \\ & \left.\left(\frac{2(\epsilon^*_{1c}k_1)\not\epsilon^*_{2d} + \not\epsilon^*_{2d}\not\epsilon^*_{1c}\not q_1}{t-m^2} + \frac{2(\epsilon^*_{2d}k_1)\not\epsilon^*_{1c} + \not\epsilon^*_{1c}\not\epsilon^*_{2d}\not q_2}{u-m^2}\right)(\not k_1 + m)\right\} \end{aligned} \qquad \text{(C-2)}$$

It is convenient to introduce

$$\begin{aligned} \kappa =& 8(t-m^2)^2(u-m^2)^2/(\alpha^2\beta d\Omega) \\ =& \frac{1}{2\alpha^2\beta d\Omega}\Big((1-\beta^2cos^2\theta)^2(W^2-q_1^2-q_2^2)^4 \\ & - 8\beta^2cos^2\theta q_1^2q_2^2\{(1-\beta^2cos^2\theta)(W^2-q_1^2-q_2^2)^2 + 2\beta^2cos^2\theta q_1^2q_2^2\}\Big) \end{aligned} \qquad \text{(C-3)}$$

so that the $REDUCE$ results of the above traces can be written as

$$\begin{aligned} \kappa\, dW_{++++} =& (1-\beta^4)(W^2-q_1^2-q_2^2)^4 - 4q_1^2q_2^2(W^2-q_1^2-q_2^2)^2 \\ & + 2sin^2\theta\beta^2(W^2-q_1^2-q_2^2)^2\left((1-\beta^2)W^2(q_1^2+q_2^2) + \beta^2(q_1^2+q_2^2)^2\right) \\ & + 4\beta^2cos^2\theta q_1^2q_2^2\left(4q_1^2q_2^2 - (1-2\beta^2)(W^2-q_1^2-q_2^2)^2\right) \\ & - \beta^4\left(sin^2\theta(q_1^2+q_2^2)(W^2-q_1^2-q_2^2) - 4cos^2\theta q_1^2q_2^2\right)^2 \\ \kappa\, dW_{+-+-} =& \beta^2sin^2\theta W^4(2-\beta^2sin^2\theta)(W^2-q_1^2-q_2^2)^2 \\ \kappa\, dW_{++--} =& -(1-\beta^2)^2(W^2-q_1^2-q_2^2)^4 + 4q_1^2q_2^2(W^2-q_1^2-q_2^2)^2 \\ & + 2\beta^2(1-\beta^2)sin^2\theta(q_1^2+q_2^2)(W^2-q_1^2-q_2^2)^3 \\ & + 4\beta^2cos^2\theta q_1^2q_2^2\left(4q_1^2q_2^2 - (3-2\beta^2)(W^2-q_1^2-q_2^2)^2\right) \\ & - \beta^4\left(sin^2\theta(q_1^2+q_2^2)(W^2-q_1^2-q_2^2) - 4cos^2\theta q_1^2q_2^2\right)^2 \\ \kappa\, dW_{0000} =& 16\beta^2cos^2\theta W^4q_1^2q_2^2(1-\beta^2cos^2\theta) \\ \kappa\, dW_{0+0+} =& 2\beta^2(-q_1^2)W^2\{sin^2\theta(w^2-q_1^2-q_2^2)^2 + 8cos^2\theta q_2^4 \\ & - \beta^2cos^2\theta sin^2\theta(W^2+q_2^2-q_1^2)^2\} \\ \kappa\, dW_{0+-0} =& 2\beta^2\sqrt{q_1^2q_2^2}W^2\{sin^2\theta\left(\beta^2cos^2\theta(W^4-(q_1^2-q_2^2)^2) - (W^2-q_1^2-q_2^2)^2\right) \\ & - 8cos^2\theta q_1^2q_2^2\} \\ \kappa\, dW_{++00} =& 4\beta^2cos^2\theta\sqrt{q_1^2q_2^2}W^2\{-(1-\beta^2cos^2\theta)\left(W^2(q_1^2+q_2^2) - (q_1^2-q_2^2)^2\right) \\ & + (1-\beta^2)W^2(W^2-q_1^2-q_2^2)\} \end{aligned} \qquad \text{(C-4)}$$

Appendix-D Covariant Formulation of Meson Decays

There are two ways of describing the decays of mesons. Most experimental physicists prefer to express their results in terms of partial waves, whereas most theoretical physicists prefer a representation of their results in terms of covariant tensors. We can combine the advantages of the two approaches by expressing transitions of particular angular momentum in terms of covariant tensors.

In general, we can write the transition matrix element of a decay $P(E) \to P_1(E_1)\,P(E_2)$ as

$$M = E^{\alpha_1\alpha_2\cdots}T_{\alpha_1\ldots\beta_1\ldots\gamma_1\ldots}E_1^{\beta_1\cdots}E_2^{\gamma_1\cdots} \qquad \text{(D-1)}$$

where the $E's$ are the polarisation tensors associated with the particles. They can be constructed from the corresponding polarisation vectors which, in the helicity system of the final state , i.e. $P_1 = (E_1, 0, 0, p)$ and $P_2 = (E_2, 0, 0, -p)$ can be taken to be of the form

$$\begin{aligned} &\epsilon_+ = \frac{1}{\sqrt{2}}(0,-1,-i,0),\ \epsilon_- = \frac{1}{\sqrt{2}}(0,+1,-i,0),\ \epsilon_0 = (0,0,0,1) \\ &\epsilon_{1+} = \frac{1}{\sqrt{2}}(0,-1,-i,0),\ \epsilon_{1-} = \frac{1}{\sqrt{2}}(0,+1,-i,0),\ \epsilon_{10} = \frac{1}{m_1}(p,0,0,E_1) \\ &\epsilon_{2+} = \frac{1}{\sqrt{2}}(0,+1,-i,0),\ \epsilon_{2-} = \frac{1}{\sqrt{2}}(0,-1,-i,0),\ \epsilon_{20} = \frac{1}{m_2}(p,0,0,-E_2) \end{aligned} \qquad \text{(D-2)}$$

Polarisation tensors of higher spin states can be constructed from these vectors:

$$E^{\alpha_1\alpha_2\cdots}(J_z) = \sum_i a_i\epsilon_a^{\alpha_1}\epsilon_b^{\alpha_2}\ldots \qquad for\ all \quad a+b+\ldots = J_z \qquad \text{(D-3)}$$

with the coefficients a_i such that for all J, J_z

$$\begin{aligned} E^{\alpha_1\alpha_2\cdots}(J_z = A)E^*_{\alpha_1\alpha_2\ldots}(J_z = B) &= (-1)^J\delta^B_A \quad orthonormal \\ E^{\ldots\alpha_l\ldots\alpha_m\ldots}(J_z) &= E^{\ldots\alpha_m\ldots\alpha_l\ldots}(J_z) \quad symmetric \\ E^{\ldots\alpha_l\ldots\alpha_m\ldots}(J_z)g_{\alpha_l\alpha_m} &= 0 \quad traceless \end{aligned} \qquad \text{(D-4)}$$

A spin two meson for example is characterised by

$$\begin{aligned} E_{\mu\nu}(J_z = \pm 2) &= \epsilon_\mu(\pm 1)\epsilon_\nu(\pm 1) \\ E_{\mu\nu}(J_z = \pm 1) &= \frac{1}{\sqrt{2}}\left(\epsilon_\mu(\pm 1)\epsilon_\nu(0) + \epsilon_\mu(0)\epsilon_\nu(\pm 1)\right) \\ E_{\mu\nu}(J_z = 0) &= \frac{1}{\sqrt{6}}\left(2\epsilon_\mu(0)\epsilon_\nu(0) + \epsilon_\mu(+1)\epsilon_\nu(-1) + \epsilon_\mu(-1)\epsilon_\nu(+1)\right) \end{aligned} \qquad \text{(D-5)}$$

The covariant amplitudes are most suitably constructed from the following objects:

$$\begin{aligned} & e_{\mu\nu\alpha\beta}P_1^\mu P_2^\nu \\ & \Delta_\beta = (P_2 - P_1)_\beta \\ & A_{\alpha\beta}(P_i, P_k) = g_{\alpha\beta} - \frac{P_{k\alpha}P_{i\beta}}{P_i\cdot P_k - \sqrt{P_i^2P_k^2}} \end{aligned} \qquad \text{(D-6)}$$

The antisymmetric tensor $e_{\mu\nu\alpha\beta}$ is only needed if the intrinsic parities don't "match" the spins involved, i.e. if

$$(-1)^{sum\ of\ intrinsic\ spins} \cdot \prod_{i=1}^{3}(p_i = intrinsic\ parities) = -1 \qquad \text{(D-7)}$$

The vector Δ puts the particles having momenta P_1 and P_2 into an $L = 1$ state whose orientation is given by the polarisation vector it is multiplied with.

The *helicity annihilation tensor* $A_{\alpha\beta}(P_1, P_2)$ compensates helicities in a structureless (i.e. $L = 0$) manner if P_1 and P_2 are both in the final (or initial) state. If P_1 is in the initial state and P_2 is in the final state, $A_{\alpha\beta}$ transfers the helicity of the parent to the final state particle.

With the help of these tensors, we can readily write down many of the lowest possible angular momentum decays. Apart from the corresponding form factors F, they are

$J^p(init)$	$\rightarrow$	$J_1^p(final)$	$J_2^p(final)$	$T(L_{min})/F$	L_{min}
0^+		$0^\pm$	$0^\pm$	1	0
0^+		$0^\pm$	$0^\mp$	*forbidden*	–
0^+		$1^\pm$	$1^\pm$	$A_{\beta\gamma}$	0
0^+		$1^\pm$	$1^\mp$	$e_{\mu\nu\beta\gamma}P_1^\mu P_2^\nu$	1
0^+		$1^\pm$	$0^\pm$	*forbidden*	–
0^+		$1^\pm$	$0^\mp$	Δ_β	1
0^+		$2^\pm$	$2^\pm$	$A_{\beta_1\gamma_1}A_{\beta_2\gamma_2}$	0
0^+		$2^\pm$	$2^\mp$	$A_{\beta_1\gamma_1}e_{\mu\nu\beta_2\gamma_2}P_1^\mu P_2^\nu$	1
0^+		$2^\pm$	$1^\pm$	$e_{\mu\nu\alpha\beta_1}P_1^\mu P_2^\nu \Delta_{\beta_2}$	2
0^+		$2^\pm$	$1^\mp$	$A_{\beta_1\gamma}\Delta_{\beta 2}$	1
0^+		$2^\pm$	$0^\pm$	$\Delta_{\beta_1}\Delta_{\beta 2}$	2
0^+		$2^\pm$	$0^\mp$	*forbidden*	–
1^+		$1^\pm$	$1^\pm$	$e_{\mu\alpha\beta\gamma}P^\mu$	0
1^+		$1^\pm$	$1^\mp$	$A_{\alpha\beta}\Delta_\gamma$	1
				$\Delta_\alpha A_{\beta\gamma}$	1
				$\Delta_\beta A_{\alpha\gamma}$	1
1^+		$2^\pm$	$2^\pm$	$e_{\mu\alpha\beta_1\gamma_1}P_\mu A_{\beta_2\gamma_2}$	0
1^+		$2^\pm$	$2^\mp$	$\Delta_\alpha A_{\beta_1\gamma_1}A_{\beta_2\gamma_2}$	1
				$A_{\alpha\gamma_1}A_{\beta_1\gamma_2}\Delta_{\beta_2}$	1
				$A_{\alpha\beta_1}A_{\beta_2\gamma_1}\Delta_{\gamma_2}$	1
1^+		$2^\pm$	$1^\pm$	$A_{\alpha\beta_1}A_{\beta_2\gamma}$	0
1^+		$2^\pm$	$1^\mp$	$e_{\mu\alpha\beta_1\gamma}P^\mu\Delta_{\beta 2}$	1
2^+		$2^\pm$	$2^\pm$	$A_{\alpha_1\beta_1}A_{\beta_2\gamma_1}A_{\alpha_2\gamma_2}$	0
2^+		$2^\pm$	$2^\mp$	$A_{\alpha_1\beta_1}e_{\mu\alpha_2\beta_2\gamma_1}P^\mu\Delta_{\gamma 2}$	1
				$A_{\alpha_1\gamma_1}e_{\mu\alpha_2\beta_1\gamma_2}P^\mu\Delta_{\beta_2}$	1
				$e_{\mu\nu\beta_1\gamma_1}P_1^\mu P_2^\nu A_{\alpha_1\beta_2}A_{\alpha_2\gamma_2}$	1

(D-8)

In this table, α_i are the Lorentz indices contracting the polarisation tensor of the initial state, e.t.c. The indeces of Δ and the spin annihilation tensor A define the four vectors it is made

of:

$$\begin{array}{lll} A_{\alpha\beta} \equiv A_{\alpha\beta}(P, P_1) & A_{\beta\gamma} \equiv A_{\beta\gamma}(P_1, P_2) & A_{\alpha\gamma} \equiv A_{\alpha\gamma}(P, P_2) \\ \Delta_\alpha \equiv (P_1 - P_2)_\alpha & \Delta_\beta \equiv (P - P_2)_\beta & \Delta_\gamma \equiv (P - P_1)_\gamma \end{array}$$

Further amplitudes follow because of

$$\begin{array}{c} |T(J^+ \rightarrow J_1^a\, J_2^b)| = |T(J^- \rightarrow J_1^{-a}\, J_2^b)| = |T(J^- \rightarrow J_1^a\, J_2^{-b})| \\ |T(J^a \rightarrow J_1^b\, J_2^c)| = |T(J_1^b \rightarrow J^a\, J_2^c)| \quad with \quad P \leftrightarrow P_1 \\ T_{\alpha_1\ldots\alpha_{(J+1)}\alpha_{(J+2)}}((J+2)^a \rightarrow J_1^b\, J_2^c) = T_{\alpha_1\ldots\alpha_J}(J^a \rightarrow J_1^b\, J_2^c)\Delta_{\alpha_{(J+1)}}\Delta_{\alpha_{(J+2)}} \\ for \quad J \geq J_1, J_2 \end{array} \qquad \text{(D-9)}$$

For the cases where several amplitudes are given, additional dynamical assumptions have to be made to decide which of the amplitudes, or which linear combination applies.

There are only few data on the decay form factors. However, neglecting the momentum dependence of the couplings completely cannot be appropriate, since for large ($L > 2$) angular momentum transitions, the covariant amplitudes themselves contain momentum factors which lead to a finite cross section, even if $W_R^2/M_R^2 \rightarrow \infty$, which is clearly meaningless. Following Blatt and Weisskopf [48], who consider an interaction potential which is constant within a sphere of radius r, the shapes of the form factors depend on the spatial orbital angular momentum of the final state in the following manner:

$$\begin{aligned} F^2(L=0) &\sim \xi \\ F^2(L=1) &\sim \frac{\xi}{k^{*2}}\,\frac{(k^*r)^2}{1+(k^*r)^2} \\ F^2(L=2) &\sim \frac{\xi}{k^{*4}}\,\frac{(k^*r)^4}{9+3(k^*r)^2+(k^*r)^4} \\ k^{*2} &= \frac{(P_1\cdot P_2)^2 - P_1^2P_2^2}{(P_1+P_2)^2} \quad (= c.m.s.\ momentum^2) \end{aligned} \qquad \text{(D-10)}$$

The factor ξ is M_R^2/W^2 for amplitudes containing the antisymmetric tensor and unity in all other cases[1]. For the few measurements we have on decay form factors, a value of $r \simeq 1fm$ fits the data reasonably well.

Notice that in eq(D-8), restrictions other than parity and four momentum conservation have *not* been incorporated. If, for example, the final state consists of identical mesons, some amplitudes differ from the lowest possible order ones:

$J^p(init)$	$\rightarrow$	$J_1^p(final)$	$J_2^p(final)$	T/F
1^-		$0^\pm$	$0^\pm$	*forbidden*
1^+		$1^\pm$	$1^\pm$	$e_{\mu\alpha\beta\gamma}(P_1 - P_2)^\mu$
1^-		$1^\pm$	$1^\mp$	$A_{\alpha\gamma}P_{2\beta} + A_{\alpha\beta}P_{1\gamma}$
2^-		$1^\pm$	$1^\pm$	$e_{\mu\alpha 1\beta\gamma}P^\mu\Delta_{\alpha 2}$
1^+		$2^\pm$	$2^\pm$	$e_{\mu\alpha\beta_1\gamma_1}(P_2 - P_1)^\mu A_{\beta_2\gamma_2}$
2^-		$2^\pm$	$2^\pm$	$e_{\mu\nu\beta_1\gamma_1}P_1^\mu P_2^\nu A_{\alpha_1\beta 2}A_{\alpha 2\gamma 2}$

(D-11)

[1] This factor is cannot be found in the literature, since it is not necessary if the amplitudes are constructed in a non Lorentz covariant manner. However, since the totally antisymmetric tensor is the only object which reduces to a cross product in the c.m.s, we have to introduce the artificial mass dependences of the type $\epsilon_{\mu\alpha\beta\gamma}P^\mu \sim W$ and correct for it afterwards.

Chain Decays

For a large variety of processes, we are now in the position of formulating chain decays such that all mass corelations come out correctly.

The partial width of a decay of the type

$$I \to F + R, \quad R \to F_1, F_2$$

where F, F_1 and F_2 are stable spinless particles and R is a resonance with nominal mass M_R, can be written as

$$\frac{1}{2M_I(2J_I+1)} \int \Big| \sum_{J_z(R)} \frac{M_{J_z}(I \to R\,F) M_{J_z}(R \to F_1 F_2)}{(P_R^2 - M_R^2) + iM_R\Gamma_R} \Big|^2 dLips_{F,F_1,F_2} \qquad \text{(D-12)}$$

If R has a non zero spin, this expression contains terms of the type

$$\sum_{J_z(R)} E^{\beta_1\beta_2\cdots}_{J_z} E^{*\gamma_1\gamma_2\cdots}_{J_z}$$

This summation can be expressed in a covariant manner[1]. Following J.Koerner et al [120], we get

$$\begin{aligned} J_R = 0 &\to 1 \\ J_R = 1 &\to s^{\beta\gamma} \equiv -g^{\beta\gamma} + \frac{P_R^\beta P_R^\gamma}{P_R^2} \\ J_R = 2 &\to \frac{1}{2}\left(s^{\beta_1\gamma_1} s^{\beta_2\gamma_2} + s^{\beta_1\gamma_2} s^{\beta_2\gamma_1}\right) - \frac{1}{3} s^{\beta_1\beta_2} s^{\gamma_1\gamma_2} \end{aligned} \qquad \text{(D-13)}$$

The entire chain is thus expressed in terms of covariant amplitudes alone. Anybody who has ever written a Monte Carlo simulation program will appreciate this fact since neither Lorentz transformations, nor rotations into helicity frames are necessary.

The energy dependent widths in eq.(D-12) can be the source of serious headaches. In contrast to the numerator of this equation, the denominator contains the energy dependence of *all* decay modes. Thus, in principle, one should write

$$\Gamma_R(W_R) = \Gamma_1(W_R) B(R \to X_1)_{W_R = M_R} + \Gamma_2(W_R) B(R \to X_2)_{W_R = M_R} + \ldots.$$

However, in nearly all practical cases, the energy dependences are quite similar. If the final state X consists of stable particles, we can write for the energy dependence of the width $\Gamma_R(W_R) \sim |M|^2 k^* / W_R$. If the final state of a particular decay contains a resonance as well, the energy dependence of the width can be obtained in a "back to front" procedure. First, the propagator of the "last" resonance is calculated for various invariant masses W_R. Then, this propagator is used to determine the energy dependence of the last but one resonance, and so on. Notice though, that in practice, a simple $\Gamma(W_R) = \Gamma(M_R)\left(\frac{k^*(W_R)}{k^*(M_R)}\right)^{(2L+1)}$ is nearly always a good approximation, in particular in those most frequent cases, where high W_R "tails" of the Breit Wigner amplitudes are damped by the limited phase space.

[1] Instead of the $1/P_R^2$ factor the literature often gives a $1/M_R^2$ which is identical for narrow resonances, but leads to wrong admixtures of longitudinal polarisation for wide resonances.

[1] see for example
S.L.Wu *DESY 84-028* (1984)

[2] J.J.Sakurai *Ann.Phys.11* (1960)

[3] Donnachie, Shaw *Plenum Press,New York* (1978) 169

[4] M.Gell-Mann, D.Sharp, W.G.Wagner *Phys.Rev.Lett.8* (1969) 261

[5] I.Ginzburg, V.Serbo *Phys.Lett.109B* (1982) 231

[6] U.Maor, E.Gotsman *Phys.Rev.D28* (1983) 2149
G.Alexander, U.Maor, C.Milstone *Phys.Lett.131B* (1983) 224

[7] For an introduction, see for example
F.Close *Academic Press, London* (1979)

[8] The complete list of Brodsky and Lepage's predictions is in
S.Brodsky, P.Lepage *Phys.Rev.D24* (1981) 1808

[9] V.M.Budnev et al *Phys.Rep.15 No.4* (1974) 181

[10] P.Kessler *Il Nuovo Cim.17* (1960) 809

[11] W.Wagner *Habilitationsschrift, RTWH Aachen* (1981)

[12] H.Kolanoski *Springer tracts in Mod.Phys.105* (1984)

[13] J.Field *LPNHE-84-04,Paris* (1984)

[14] H.Terezawa *Rev.Mod.Phys.45* (1973) 615

[15] G.Bonneau, M.Gourdin, F.Martin *Nucl.Phys.B54* (1973) 573

[16] C.N.Yang *Phys.Rev.77* (1950) 242

[17] G.Koepp, P.Zerwas, T.Walsh *Nucl.Phys.B70* (1974) 461

[18] The EPA was introduced by
K.F.von Weizsaecker *Z.Physik* (1934) 612
E.Willams *Kgl.Danske Vidensk.Selskab.Mat.-Fiz.Med No.13* (1935)

[19] F.A.Behrends, P.H.Daverfeldt, R.Kleiss *Z.Phys.22* (1984) 239
For details and a descirption of the Monte Carlo Generator, see also
P.H. Daverveldt *Ph.D.-Thesis, Rijksuniversiteit te Leiden* (1985)

[20] S.Kavabata *KEK 85-26* (1985)

[21] P.Jenni et al *Phys.Rev.D27* (1983) 1031

[22] W.Bartel et al *Phys.Lett.113B* (1982) 190

[23] H.J.Behrend et al *Phys.Lett.114B* (1982) 378

and Erratum *Phys.Lett.125B* (1983) 518

[24] Ch.Berger et al *Phys.Lett.142B* (1984) 125

[25] M.Althoff et al *Phys.Lett.147B* (1984) 487

[26] G.Gidal in Int.Workshop on Two Photon Collisons, Lake Tahoe, Ca.
Ed. R.Lander *World Scientific Pub.Co.,Singapore* (1985)

[27] J.Sens *SLAC-Pub.3754* (1985)

[28] J.D.Jackson *Il Nuov.Cim.34* (1964) 1644

[29] A.Weinstein et al *Phys.Rev.D28* (1983) 2896

[30] W.Bartel et al *Phys.Lett.158B* (1985) 511

[31] C.Bemporad et al *Phys.Lett.25B* (1967) 380

[32] A.Browman et al *Phys.Rev.Lett.32* (1974) 1067

[33] F.E.Low *Phys.Rev.120* (1960) 582

[34] D.A.Williams in Int.Workshop on Two Photon Collisons, Lake Tahoe, Ca.
Ed. R.Lander *World Scientific Pub.Co.,Singapore* (1985)

[35] H.Atherton et al *Phys.Lett.158B* (1985) 81

[36] R.van Royen, V.F.Weisskopf *Il Nuo.Cim LA* (1967) 617

[37] S.Okubo *Prog.Theor.Phys.(Kyoto)27* (1967) 949

[38] M.Channowitz *"public communication"* (1984)

[39] S.Adler *Phys.Rev.177* (1969) 2426

[40] J.Bell, R.Jackiw *Il Nuovo Cim.60* (1969) 47

[41] S.Matsuda, S.Oneda *Phys.Rev.187* (1969) 2107

[42] H.Suura, T.Walsh, B.Young *Lett.Nuovo Cim.4* (1972) 505

[43] S.B.Berger, B.T.Feld *Phys.Rev.D8* (1973) 3875

[44] A.Bramon, M.Greco *Phys.Lett.48B* (1974) 137

[45] E.Etim, M.Greco *Il Nuovo Cim.42* (1977) 124

[46] V.M.Budnev, A.E.Kaloshin *Phys.Lett.86B* (1979) 351

[47] S.Godfrey, N.Isgur *Phys.Rev.D32* (1985) 189

[48] J.M.Blatt, V.Weisskopf *John Wiley & sons, NY* (1952)
The author has used the formulation given by
H.Pilkuhn *North Holland Pub.Co., Amsterdam* (1967)

[49] C.Quigg, J.L.Rosner *Phys.Rep.56 No.4* (1979) 167

[50] A.T.Philippov *Sov.J.Nucl.Phys.29* (1979) 534

[51] Ch.Berger et al *Z.Phys.C26* (1984) 199

[52] Ch.Berger et al *DESY 85-???* (1985)

[53] see for example
A.E.Kaloshin, V.V.Serebryakov *Novosibirsk TPh-125* (1981)
K.Sundereyer *Ph.D.Thesis,Universitaet Hamburg,DESY 74-17* (1974)

[54] G.Mennessier *Z.Phys.C16* (1983) 241

[55] The most recent measurement references all previous ones:
S.R.Amendolia et al *Phys.Lett.146B* (1984) 116

[56] Ch.Berger et al *Phys.Lett.137B* (1984) 267

[57] Mark II Coll. contributed paper, Int.Workshop on Two Photon Collisons,
Lake Tahoe, Ca. Ed. R.Lander *World Scientific Pub.Co.,Singapore* (1985)

[58] E.B.Dally et al *Phys.Rev.Lett.45* (1980) 232

[59] D.Morgan *Phys.Lett.51B* (1974) 71

[60] C.Edwards et al *Phys.Lett.110B* (1982) 82

[61] J.Olsson *DESY 83-076* (1983)

[62] D.Antreasyan et al *DESY 85-97* (1985)

[63] A.Bramon, M.Greco *Lett.Nuovo Cim.2* (1971) 522

[64] J.Babcock, J.L.Rosner *Phys.Rev.D14* (1976) 1286

[65] G.K.Greenhut, G.W.Intermann *Phys.Rev.D18* (1978) 231

[66] see for example
J.Weinstein, N.Isgur *Phys.Rev.Lett.48* (1982) 659 or
R.L.Jaffe *Phys.Rev.D17* (1982) 1444

[67] H.Krasemann, J.Vermaseren *Nucl.Phys.B184* (1981) 269

[69] H.D.I.Arbabanel, M.Goldberger *Phys.Rev.175* (1968) 1594

[70] B.& O.Schrempp, T.F.Walsh *Phys.Lett.36B* (1971) 463

[71] C.Edwards et al *Phys.Lett.110B* (1982) 82

[72] J.H.Behrend et al *Phys.Lett.114B* (1982) 378

[73] Ch.Berger et al *Phys.Lett.149B* (1984) 427

[74] Ch.Berger et al *Phys.Lett.94B* (1980) 254

[75] A.Roussary et al *Phys.Lett.105B* (1981) 304

[76] R.Brandelik et al *Z.Phys.C10* (1981) 117

[77] H.J.Behrend et al *Z.Phys.C23* (1984) 223

[78] K.M.Watson *Phys.Rev.88* (1952) 1163

[79] A.Courau et al *Phys.Lett.174B* (1984) 227

[80] K.Wong in Int.Workshop on Two Photon Collisons,
Lake Tahoe, Ca. Ed. R.Lander *World Scientific Pub.Co.,Singapore* (1985)

[81] J.R.Smith et al *Phys.Rev.D30* (1984) 851

[82] M.Althoff et al *Phys.Lett.149B* (1984) 427

[83] D.Faiman, H.J.Lipkin, H.R.Rubinstein *Phys.Lett.59B* (1975) 269
and references therein

[84] P.Grassberger, R.Kogerler *Nucl.Phys.B106* (1976) 451

[85] M.Greco, Y.Srivastava *Il Nuovo Cim.43A* (1978) 88

[86] L.Bergstroem et al *Z.Phys.C16* (1983) 263

[87] P.Singer *Phys.Rev.Lett.124B* (1983) 531

[88] N.N.Achasov, V.A.Karnakov *Novosibirsk TF 14-147* (1985)

[89] N.N.Achasov, S.A.Devyanin, G.N.Shestakov *Z.Phys.C27* (1985) 99

[90] G.Alexander, A.Levy, U.Maor *DESY 85-079* (1985)

[91] M.Althoff et al *Z.Phys.C16* (1982) 13

[92] J.H.Behrend et al *Z.phys.C21* (1984) 205

[93] D.L.Burke et al *Phys.Lett.100B* (1981) 153

[94] M.Hatzis, J.Paschalis *Lett.Nuovo Cim.40* (1984) 362

[95] R.Brandelik et al *Phys.Lett.97B* (1980) 448

[96] PEP49 Coll. Contributed paper to the Int. Conf. on
High Energy Physics, Leipzig (1984)

[97] H.Mueller in Verhandlungen der Deutschen Physikalischen
Gesellschaft,Muenchen (1985)

[98] compilation by A.Cordier, Int.Workshop on Two Photon Collisons,
Lake Tahoe, Ca. Ed. R.Lander *World Scientific Pub.Co.,Singapore* (1985)

[99] B.A.Li, K.F.Liu *Phys.Rev.D30* (1984) 631

[100] Ch.Berger et al *DESY 85-080* (1985)

[101] J.Olsson in Proceedings of the European Conf. on
High Energy Physics *Brighton* (1983)

[102] compilation by J.Erné, Int.Workshop on Two Photon Collisons,
Lake Tahoe, Ca. Ed. R.Lander *World Scientific Pub.Co.,Singapore* (1985)

[103] H.Ahaira et al *UCR-TPC-85-08* (1985)

[104] R.Brandelik et al *Phys.Lett.130B* (1983) 449

[105] J.A. Skard, Int.Workshop on Two Photon Collisons,
Lake Tahoe, Ca. Ed. R.Lander *World Scientific Pub.Co.,Singapore* (1985)

[106] P.H.Damgaard, Nucl.Phys.B211 *1983* (434)

[107] G.R.Farrar, E.Maina, F.Neri *RU 85-08* (1985)

[108] V.L.Chernyak, I.R.Zhitnisky *Nucl.Phys.B246* (1984) 52

[109] G.Alexander et al *Phys.Rev.D26* (1982) 1198

[110] An extensive discussion of glueball speculations including references is in
J.H.Field *DESY-85-110* (1985)

[111] The latest measurement references all previous ones
Ch. Berger et al *Z.Phys.C27* (1985) 249

[112] K.Wacker in Proc. EPS Int. Europhys. Conf.
Bari *(to be published)* (1985)

[113] J.Olssson, Proc. of the Fifth Int. Coll. on $\gamma\gamma$ Interactions, Aachen
Ed. Ch.Berger *Springer Lecture Notes in Physics Vol.191* (1983)

[114] M.Althoff et al *DESY-85-089* (1985)

[115] A.L.Spadafora *Illinois-UI-HEPG-84/03* (1984)

[116] see for example
B.Anderson et al *Phys.Rep.97* (1983) 31

[117] J.Steinberger *Phys.Rev.76* (1949) 1180

[118] H.Kück, Int.Workshop on Two Photon Collisons,
Lake Tahoe, Ca. Ed. R.Lander *World Scientific Pub.Co.,Singapore* (1985)

[119] V.A.Novikov et al *Nucl.Phys.B97* (1984) 525

[120] J.Körner et al *Nucl.Phys.B229* (1983) 115